

Synthesis of Plantwide Control Strategies using Mixed Integer Optimization

Dissertation

zur Erlangung des akademischen Grades

**Doktoringenieurin / Doktoringenieur
(Dr.-Ing.)**

von M.Tech. Ganesh Paramasivan

geb. am 06-07-1982 in Tirunelveli, India

genehmigt durch die Fakultät für Elektrotechnik und Informationstechnik

der Otto-von-Guericke Universität Magdeburg

Gutachter:

Prof. Dr.-Ing. Achim Kienle

Prof. Dr.-Ing. Günter Wozny

Promotionskolloquium am 26-01-2012

Acknowledgements

This thesis originated during my doctoral program at the International Max Planck Research School in Magdeburg.

I want first to thank my supervisor Prof. Achim Kienle for all the hope he has put on me. He has always encouraged me to live intensively, even when I was thinking about doing something else. He has enlightened me through his wide knowledge of chemical process control and his deep intuitions about where it should go and what is necessary to get there. Throughout, he has found a proper balance between setting the right direction and still allowing a great amount of 'scientific freedom'.

I would like to express my gratitude to all of my group members for their kind cooperation. Here, Michael Mangold, Ilknur Disli Kienle, Malte Kaspereit and Sommer are worth mentioning for their readiness to sort out many of my initial queries in DIVA and controller implementation. Among other group members, I want to thank Rene Schenkendorf for his valuable guidance in the proof-reading of some of the chapters in this thesis.

I would like to thank the IMPRS coordinator Barbara Witter for the support provided. Without her constant cooperation, my stay in Magdeburg would not have been very pleasant. A special thanks to the group secretary Carolyn Mangold for her prompt response to my queries. I would also like to express my gratitude to IT staff members for always sorting out my IT related problems so efficiently and quickly. A special thanks to our library staff members for their prompt response to my literature needs. I am also thankful to the secretary Annett Bartels for helping me out in the administrative works.

In addition, I want to thank for the financial funds I received from the , "Interna-

tional Max Planck Research School (IMPRS) for Analysis, Design and Optimization in Chemical and Biochemical Process Engineering”, Otto-von-Guericke-Universität, Magdeburg for this PhD program.

I am also very grateful to all my friends who made life in the institute and Magdeburg in general a pleasurable experience. Finally, I would like to thank my parents for giving me the much needed love and moral support. A special thanks to my wife Sudha for enduring me during all these years of hard work. Her support, tolerance and patience towards me has been amazing.

To my parents

Contents

Acknowledgements	ii
Dedication	iv
List of Figures	vii
List of Tables	x
Notation	xii
German Abstract	xv
Abstract	xvii
Chapter	
1. Introduction	1
1.1 State of the art and objectives	2
1.2 Outline of the thesis	4
2. Decentralized control system design	6
2.1 Mathematical formulation	6
2.2 Controller formulation	7
2.2.1 Decentralized controller	7
2.2.2 Multivariable PI controller	8
2.3 Objective function	9
2.3.1 Formulation I	9
2.3.2 Formulation II	9
2.4 Solution approach for MIDO problem	10
2.5 Case studies	13
2.5.1 Case study 1: Ideal reactive distillation	14

2.5.2	Case study 2: Methyl acetate system	21
2.6	Summary	26
3.	Decentralized control system design under uncertainty	28
3.1	Mathematical formulation	29
3.2	Objective function	30
3.3	Sigma-point method	31
3.4	Case study : Ideal reactive distillation - Quaternary system .	33
3.5	Summary	44
4.	Control of a ternary reactive distillation with inert	46
4.1	Introduction	46
4.2	Benchmark problem: Ternary RD column with inert	47
4.3	Control system design : Deterministic MIDO approach	52
4.4	Control system design: Stochastic MIDO approach	56
4.4.1	Case 1	56
4.4.2	Case 2	58
4.4.3	Case 3	61
4.5	Summary	64
5.	Application to plantwide control problem	65
5.1	DMC process	65
5.2	Process modeling	66
5.3	Control strategy - Heuristic method	68
5.3.1	Remarks on the control strategy by heuristic method	70
5.4	Optimal control strategy - MIDO formulation	74
5.4.1	Complexity of the plantwide control problem	74
5.4.2	MIDO formulation	76
5.5	Optimal control strategy under uncertainty	81
5.5.1	MIDO problem under uncertainty	83
5.6	Summary	85
6.	Conclusions	86
Appendices	89
A.1	VLE model for dimethyl carbonate (DMC) process	89
Bibliography	91

List of Figures

Figure

2.1	Ideal reactive distillation column	16
2.2	Steady state composition and temperature profile of ideal reactive distillation	16
2.3	Closed loop response for a $\pm 10\%$ change in the vapor boil up VB, Formulation I (Ideal reactive distillation)	18
2.4	Closed loop response for a $\pm 10\%$ change in the vapor boil up VB - Ideal reactive distillation	20
2.5	Closed loop response for a $\pm 10\%$ change in the vapor boil up VB, Formulation II - Multivariable controller (Ideal reactive distillation)	21
2.6	Methyl acetate reactive distillation column	23
2.7	Steady state composition and temperature profile of Methyl acetate system	24
2.8	Closed loop response for a $\pm 10\%$ change in MeOH feed rate - Methyl acetate system	25
3.1	Expected value of the performance index: MC samples vs Sigma Point method - Case 1	36
3.2	Location of the sigma points and random samples for calculating the mean and variance of the performance index - Case 2	39
3.3	Expected value of the performance index: random samples vs sigma point method - case 2	39

3.4	Closed loop response of the optimal decentralized control system - case 2 (stochastic approach)	40
3.5	Closed loop response of the decentralized control system (nominal case)	41
3.6	Closed loop response of the decentralized control system (heuristic method)	42
3.7	Expected value of the performance index: random samples vs sigma point method - case 3	44
4.1	Flowsheet for a ternary reactive distillation column with inerts . . .	48
4.2	Steady state composition and temperature profile	48
4.3	Closed loop response for a +20% change in the vapor boil up V_s - Heuristic method	50
4.4	Closed loop response for a -20% change in the vapor boil up V_s - Heuristic method	51
4.5	Closed loop response for a +20% step change of the vapor boil up V_s - Deterministic MIDO approach	53
4.6	Closed loop response for a -20% step change of the vapor boil up V_s - Deterministic MIDO approach	54
4.7	Closed loop response for a $\pm 10\%$ step change of the inert concentration $Z_{0A(I)}$ in the feed F_{0A} - Deterministic MIDO approach (solid line, $Z_{0A(I)} = 0.55$; dashed line, $Z_{0A(I)} = 0.45$)	55
4.8	Closed loop response for a $\pm 20\%$ step change of the feed F_{0B} - Stochastic MIDO approach (case 2) (solid line, -20%; dashed line, +20%)	59
4.9	Closed loop response for a $\pm 10\%$ step change of the inert concentration $Z_{0A(I)}$ in the feed F_{0A} - Stochastic MIDO approach (case 2) (solid line, $Z_{0A(I)} = 0.55$; dashed line, $Z_{0A(I)} = 0.45$)	60
4.10	Closed loop response for a $\pm 20\%$ step change of the feed F_{0B} - Stochastic MIDO approach (case 3) (solid line, -20%; dashed line, +20%)	62

4.11	Closed loop response for a $\pm 10\%$ step change of the inert concentration $Z_{0A(I)}$ in the feed F_{0A} - Stochastic MIDO approach (case 3) (solid line, $Z_{0A(I)} = 0.55$; dashed line, $Z_{0A(I)} = 0.45$)	63
5.1	Flowsheet of the complete process for Dimethyl Carbonate (DMC) synthesis [35]	67
5.2	Overall control strategy - Heuristic method [35]	71
5.3	Closed loop results with $\pm 20\%$ change in F_{EC} - Heuristic method (solid line, $+20\%$ of F_{EC} ; dashed line, -20% of F_{EC})	72
5.4	Closed loop response for change in MeOH feed composition (heuristic method) (solid line, $Z_{MeOH} = 0.95$, $Z_{DMC} = 0.05$; dashed line, $Z_{MeOH} = 0.98$, $Z_{DMC} = 0.02$)	73
5.5	“Sign reversal” in steady state gain	76
5.6	Optimal control strategy - Formulation II	79
5.7	Closed loop results with $\pm 20\%$ change in F_{EC} - Optimal solution (Formulation II) (solid line, $+20\%$ of F_{EC} ; dashed line, -20% of F_{EC})	80
5.8	First order sensitivity indices of the output variables	83
5.9	Closed loop response for change in MeOH feed composition (Stochastic approach) (solid line, $Z_{MeOH} = 0.95$, $Z_{DMC} = 0.05$; dashed line, $Z_{MeOH} = 0.98$, $Z_{DMC} = 0.02$)	84

List of Tables

Table

2.1	Physical data for the ideal reactive distillation	15
2.2	The optimal control structure and PI controller parameters - Ideal reactive distillation	17
2.3	Control structure and PI controller parameters - Methyl acetate system	24
3.1	Comparison of the sigma point method with other integration methods	31
3.2	Sigma point method	32
3.3	Uncertainty model - Ideal reactive distillation	34
3.4	The expectation and the variance of the performance index for the optimal decentralized control system for case 1	35
3.5	Decentralized control structure and controller parameters	35
3.6	Performance comparison of different control system for case 1	36
3.7	The expectation and the variance of the performance index for the optimal decentralized control system for case 2	38
3.8	Performance comparison of different control system for case 2	38
3.9	The expectation and the variance of the performance index for the optimal decentralized control system for case 3	43
3.10	Performance comparison of different control system for case 3	44
4.1	Control structure and PI controller parameters - nominal case	49

4.2	Control structure and PI controller parameters - Stochastic MIDO approach	57
5.1	Measurements and control loops requirement for DMC process	77
5.2	Optimal control loops and PI controller parameters for DMC process	81
5.3	Uncertainty model for the DMC process	82
5.4	Optimal control loops and PI controller parameters under disturbance uncertainty	85

Notation

Abbreviations

Symbols	Meaning
DMC	Dimethyl Carbonate
EC	Ethylene Carbonate
ED	Extractive Distillation
EG	Ethylene Glycol
ER	Entrainer Recovery column
GAMS	General Algebraic Modelling System
GBD	Generalized Benders Decomposition
HOAc	Acetic Acid
LBD	Lower bound for objective function
MILP	Mixed-Integer Linear Programming
MINLP	Mixed-Integer Non-Linear Programming
MIDO	Mixed-Integer Dynamic Optimization
MeAC	Methyl Acetate
MeOH	Methanol
NLP	Non-Linear Programming
OA	Outer Approximation
RD	Reactive Distillation
SQP	Sequential Quadratic Programming
UBD	Upper bound for objective function

Arabic Symbols

Symbols	Meaning	SI Units
a	activity of component	
B	bottoms flow rate	[mol/sec]
D	distillate flow rate	[mol/sec]
e_i	error between setpoints and output variable i	
E	expectation of performance index	
F_{HOAc}	fresh Acetic acid flow rate	[kmol/hr]
F_{MeOH}	fresh Methanol flow rate	[kmol/hr]
F_{EC}	fresh Ethylene carbonate flow rate	[kmol/hr]
F_{0A}	fresh reactant A flow rate	[mol/sec]
F_{0B}	fresh reactant B flow rate	[mol/sec]
J	objective function	
k_f	specific forward reaction rate constant	[hr ⁻¹]
K_{eq}	reaction equilibrium constant	
K_u	ultimate gain	
N_{cp}	number of collocation points	
N_{fe}	number of finite elements	
N_u	number of potential manipulated variables	
N_y	number of potential controlled variables	
p	vector of controller parameters	
P_u	ultimate period	[min]
Q	weighting matrix	
R	weighting matrix	
RR	Reflux Ratio	
r	reaction rate	[kmol/hr]
t_{set}	settling time	[hour]
$u(t)$	vector of manipulated variables	
$v(t)$	vector of disturbances	
V	variance of performance index	
VB	vapor boil up rate	[kmol/hr]
V_s	vapor boil up rate	[mol/sec]
$x(t)$	vector of differential variables	
$x_a(t)$	vector of algebraic variables	
$X_{B,D}$	bottoms composition : component D	[mole fraction]
$X_{D,C}$	distillate composition : component C	[mole fraction]

Arabic Symbols - Continued ...,

Symbols	Meaning	SI Units
$y(t)$	vector of output variables	
y_{ov}	overshoot	
y_{sp}	setpoint for output variables	
Z_{0j}	fresh feed mole fraction of component j	

Greek Symbols

Symbols	Meaning
δ	vector of binary variables
τ_I	integral reset time
τ_D	derivative time
θ	uncertain parameters
α	relative volatility
λ	parameter in sigma-point method
κ	parameter in sigma-point method
β	parameter in sigma-point method
Ω_q	Legendre's polynomial
λ_p^T	set of Lagrange multipliers for the point constraints
ω^T	set of Lagrange multipliers for the time invariant equality constraints
ξ^T	set of Lagrange multipliers for the time invariant inequality constraints
η_B	objective function in the MILP master problem
μ	mean value of uncertain disturbances
Σ	covariance matrix
φ	objective function of an infeasibility minimization problem
ω	weighting function in the statistical objective function

Subscripts

Symbols	Meaning
i	index for output variables
j	index for input variables
k	index for NLP subproblems
$feas$	feasible NLP subproblems
$infeas$	infeasible NLP subproblems

German Abstract

Bei der Regelung verfahrenstechnischer Prozesse werden oft dezentrale lineare Regler wegen ihrer einfachen Implementierung und ihrer praktischen Bedienerfreundlichkeit verwendet. Der Aufbau eines solchen Regelungskonzeptes beinhaltet eine Auswahl geeigneter Regelungsstrukturen und Reglerparameter. Normalerweise geht man sequentiell vor, indem man zuerst die Regelungsstruktur festlegt und danach die Reglerparameter unter Inanspruchnahme heuristischer Methoden bestimmt. Dieser Ansatz ist einfach und intuitiv, führt aber oft zu suboptimalen Lösungen. Außerdem können Nebenbedingungen für die Prozessdynamik nicht berücksichtigt werden.

Die vorliegende Arbeit konzentriert sich auf einen algorithmischen Ansatz, um diese Einschränkungen zu überwinden. Im algorithmischen Ansatz wird eine gemischt ganzzahlige Optimierung benutzt, um die optimale Regelung und die Regelungsparameter gleichzeitig zu bestimmen. Die Prozessdynamik wird explizit in die Nebenbedingungen unter Nutzung rigoroser nichtlinearer Prozessmodelle einbezogen. Dies führt zu einem gemischt ganzzahligen dynamischen Optimierungsproblem. In der aktuellen Arbeit werden verschiedene Ansätze vorgeschlagen und mit etablierten heuristischen Entwurfsmethoden verglichen. Unterschiedliche Problemformulierungen führen (1) zu einer Minimierung des Aufwandes, um eine vorgegebene Performance zu erzielen und (2) zur Maximierung der Gesamtperformance. Beide Problemformulierungen wurden für nominale Störszenarien mit Hilfe deterministischer Optimierung gelöst. Die zweite Fragestellung wurde auch mit einem erweiterten stochastischen Ansatz gelöst, um die Robustheit zu berücksichtigen. Beim stochastischen Ansatz werden Störungen mittels mehrdimensionaler Wahrscheinlichkeitsverteilungen modelliert. Ein analoger Ansatz kann auf parametrische Modellunsicherheiten angewandt werden. Die daraus resultierende Zielfunktion ist eine gewichtete Summe des Erwartungswertes und der Varianz der Prozessperformance. Es wurde gezeigt, dass mit Hilfe der Sigma-Punkt-Methode, welche stochastische Optimierungsprobleme in deterministische umrechnet,

Erwartungswert und Varianz akkurat und effektiv evaluiert werden können. Des Weiteren hat sich gezeigt, dass die resultierenden deterministischen gemischt ganzzahligen dynamischen Optimierungsprobleme mit einem sequentiellen Ansatz und unter Verwendung der verallgemeinerten Bender-Zerlegung effektiv gelöst werden können.

Als Anwendungsbeispiel wurde die Regelung von Reaktivdestillationskolonnen als anspruchsvolles Problem untersucht, das in der aktuellen Fachliteratur große Aufmerksamkeit erlangte. Die Prozessbeispiele reichen von etablierten idealisierten Benchmark-Problemen aus der Literatur hin zu hochgradig nicht-idealen Prozessen wie die Methyl-Azetat-Produktion als reales Anwendungsbeispiel. Weiterhin wurde eine komplexe Mehrkolonnen-Anlage für die Produktion von Dimethyl-Karbonat als Beispiel eines großtechnischen Prozesses betrachtet. In allen Fällen wurden im Vergleich zu bestehenden heuristischen Regelungsstrukturen signifikante Verbesserungen nachgewiesen. Im Fall einer ternären Reaktivdestillationskolonne mit Inert-Komponente wurde mit unserem systematischen Ansatz eine zulässige Lösung gefunden, obwohl in der Literatur behauptet wird, dass Inferential Control für diesen Prozesstyp nicht anwendbar ist.

Abstract

In chemical process control, frequently decentralized linear controllers are used, because of their ease of implementation and handling in practice. The design of such a control system involves the selection of a suitable control structure and controller parameters. This is usually done sequentially by first fixing the control structure and then tuning the controller parameters using some heuristic methods. This approach is simple and intuitive, but often leads to suboptimal solutions. Further, hard constraints on the process dynamics cannot be taken into account.

The present work focuses on an algorithmic approach to overcome these limitations. In the algorithmic approach, mixed integer optimization is used to determine the optimal control structure and controller parameters simultaneously. Process dynamics is included explicitly into the constraints using rigorous nonlinear dynamic process models, which leads to mixed-integer dynamic optimization (MIDO) problems. In the present work, different problem formulations are proposed and compared with each other and with established heuristic design methods. Different problem formulations comprise (1) minimizing the effort to achieve a specified performance; (2) maximizing the overall performance. Both formulations were solved for nominal disturbance scenarios using deterministic optimization. The second formulation was also solved with an extended stochastic approach to account for robustness. In the stochastic approach, disturbances are modeled by multivariate probability distributions. An analogous approach can be applied for parametric model uncertainty. The resulting objective function is a weighted sum of the expectation and the variance of process performance. It was shown, that expectation and variance can be evaluated accurately and efficiently by means of the sigma point method, which converts the stochastic optimization problem into a deterministic one. Further, it was shown that the resulting deterministic MIDO problems can be solved efficiently with a sequential approach using Generalized Benders decomposition.

On the application side, first, inferential control of reactive distillation columns was studied as a challenging class of problems, which has received a lot of attention in recent literature. Process examples range from established idealized benchmark problems taken from the literature to highly nonideal methyl acetate production in a reactive distillation column as a real world application example. Finally, also a complex multi column plant for the production of Dimethyl carbonate was considered as a large scale application example. In all cases, significant improvement over existing heuristic control structures were found. In one case, a ternary reactive distillation column with inert, a feasible solution was found with our systematic approach, although, it was stated in the literature, that inferential control is not feasible for this type of process.

Chapter 1

Introduction

In recent years, complexity of chemical plants has increased significantly due to process integration. On the flowsheet level material and energy is recycled as much as possible to minimize waste and energy requirements. On the process unit level, different functionalities such as reaction and separation can be combined into a single device to improve yield and selectivity while simultaneously reducing material and energy requirements. A typical example, which has been studied extensively during the past two decades is the integration of reaction and distillation in a reactive distillation column [1, 2].

Although economically attractive, process integration provides significant challenges to smooth dynamic plant operation due to complex dynamic behavior. Typical examples are: input and output multiplicities, inverse responses and self sustained oscillations in reactive distillation columns (see e.g. Chapter 10 in Sundmacher and Kienle [1] and references therein); steady state sensitivity (popularly known as snowball effect [3]), back propagation of disturbances and stability problems in multi unit plants with recycles [4].

Therefore, designing a suitable control system is of fundamental importance. Traditionally, focus in the process industries is on decentralized linear controllers because of their ease of implementation and handling in practice. The design of such a control system involves the selection of a suitable control structure and suitable controller parameters.

1.1 State of the art and objectives

Several methods for plantwide control design have been developed resulting in the availability of a wealth of literature. A thorough classification and evaluation of all approaches is beyond the scope of this thesis, and the reader is referred to some of the reviews devoted to the topic [5, 6, 7]. Instead, only a brief summary is given here. Buckley presented a first study on plantwide control in 1964 [8], however, plantwide control has been actively studied mainly in the past 15 years. These methods can be best captured in the labels [6] “**heuristic methods**“ and “**algorithmic approach**”.

In the **heuristic methods**, some guidelines based on experience are given as part of the plantwide control methodology that helps the designer to make control decisions at each stage of the control system development [10, 11]. The most popular heuristic guidelines were proposed by Luyben and coworkers [10]. This is the first complete procedure that generates an effective plantwide control structure for an entire process flowsheet and not just for individual units. However, there are several heuristic based design procedures that have been appeared in the literature [12, 13] apart from the work of Luyben and coworkers. In the heuristic approaches, control system design is often done sequentially by first fixing the control structure and then tuning controller parameters. Control structures are often selected using the heuristic rules [10] or some simplified interaction measures like Relative Gain Array [14], Singular Value Decomposition (SVD) etc.,. Controllers for the selected control loops are often designed using some SISO tuning rules in combination with detuning strategies to account for the interaction between the different control loops [15] or sequential relay feedback testing [16]. These heuristic methods are simple and intuitive. However, a major drawback of these procedures is that they often lead suboptimal solutions. Further, hard constraints on the nonlinear process dynamics can not be taken into account.

In the **algorithmic approach**, mixed integer optimization can be used to determine the optimal control structure and controller parameters simultaneously. Depending on how the performance of the control system is measured, this leads to a mixed integer linear program (MILP) or a mixed integer nonlinear program (MINLP) or a mixed integer dynamic optimization (MIDO) problem if the nonlinear process dynamics is explicitly taken into account. Perkins and co-workers [17, 18, 19, 20] were among the first to discuss plantwide control synthesis based on mixed integer op-

timization. In their first work, the objective function involves the maximization of profit during the disturbance rejection by the control system and a linear dynamic model for the process, which was performed using an MILP technique [17]. In a later work [21], they extended the method to nonlinear dynamic models aiming to identify input-output pairings using an MINLP techniques. Some authors [22, 23, 24] suggested the solution to a very broad problem of simultaneous design and control of the process by formulating the problem as a MIDO. Although, simultaneously optimizing the process design and control strategy is a very active research area in the academic world [25], many researchers have adopted the approach of control system design only after the process design for improving the controllability characteristics of plant-wide processes (e.g. the review paper by Yuan et al., [26]).

Apart from the above cited methodologies for plantwide control, an important example of a combination between an algorithmic approach and heuristic methods is presented by Skogestad [27, 28]. In this work, focus is on the selection of the controlled variables that keeping them constant, the process is maintained close to the optimum (i.e., steady state optimization) when disturbances and control errors are present. This approach is therefore called “*self-optimizing control*”.

So far, main focus has been on the heuristic approach. This is due to the fact that the algorithmic approach depends on the availability of suitable optimization methods to solve the resulting complex optimization problems. However, the last decade has been witnessing a steady growth of optimization algorithms for the solution of a large-scale mixed-integer and dynamic optimization (e.g. the review papers by Biegler et al., [29] and Sakizlis et al., [25]). This allows a more rigorous and systematic approach accounting explicitly for nonlinear process dynamics, which is urgently required for highly nonlinear integrated processes.

And this is where to a thesis sets in. The following **objectives** are articulated in order to contribute better insight into the algorithmic approach of plantwide control problems:

- To find suitable problem formulations in order to include explicitly the nonlinear process dynamics into the constraints of the optimization problem and find some suitable measures for control system performance.
- Since the resulting optimization problem involves the presence of continuous and discrete variables, it leads to a complex MIDO problem; the solution of

which can be a formidable task. Therefore suitable solution strategies have to be provided to achieve optimality of the control structure and controller parameters.

- Due to nonlinearity the optimal control structure and the optimal controller parameters will differ for different disturbance scenarios. Therefore, robustness with respect to various disturbances arising in practice has to be studied.
- Finally, the feasibility of the proposed approach has to be illustrated for some challenging benchmark problems with the typical characteristics discussed in the introduction section.

1.2 Outline of the thesis

In order to achieve the objectives of the thesis and contribute to a better understanding, the thesis follows a structured strategy as shown below.

Chapter 2

This chapter gives a detailed description of the MIDO framework for control system design. In the MIDO framework, two different formulations based on the closed loop response characteristics are presented: (1) minimizing the effort to achieve a specified performance (2) maximizing the overall performance. Afterwards suitable solution strategies are discussed. Application is demonstrated for highly integrated and highly nonlinear reactive distillation columns, which have received a lot of attention in the recent literature [1, 30, 31, 32, 33]. Finally, the results are compared with heuristic methods to illustrate the advantages of the proposed MIDO framework.

Chapter 3

In this chapter, the proposed MIDO framework is further extended to account for various disturbance scenarios. The sigma point method is introduced in order to solve the MIDO problem under uncertainty. Furthermore, an ideal reactive distillation which was considered in the previous chapter is investigated under disturbance uncertainty.

Chapter 4

In this chapter, a ternary reactive distillation column with inert is considered as a very interesting example. Based on a heuristic design method it was claimed in the literature [34] that an inferential control scheme does not work for this system. However, it is demonstrated that the complex ternary system with inert can be controlled by an inferential control scheme by choosing a suitable control structure using the proposed MIDO framework.

Chapter 5

The potential application of the MIDO framework in terms of a complete chemical plant can be seen by considering a large integrated plant with recycle i.e., dimethyl carbonate (DMC) synthesis process via reactive and extractive distillation [35, 36]. It starts with the process description. Combinatorial complexity of the resulting optimization problem is discussed. Further, a few guidelines are provided in this chapter to handle the complexity of the problem.

Chapter 6

This chapter concludes the thesis and presents the summary along with the potential areas for the future work.

Chapter 2

Decentralized control system design

In this chapter, the algorithmic approach for decentralized control system design is presented. As it has been already pointed out in the introduction chapter, mixed integer optimization can be used to determine the optimal control structure and controller parameters simultaneously. Two different formulations are proposed based on the closed loop response characteristics: (1) minimizing the effort to achieve a specified performance (2) maximizing the overall performance. In both formulations, the nonlinear plant dynamics is included explicitly into the constraints. This will lead to a complex mixed-integer dynamic optimization (MIDO) problem. First, the mathematical formulation of the MIDO problem for control system design and the solution techniques are presented. Subsequently, application of the proposed formulations is demonstrated for a class of challenging control problems, which has received a lot of attention in the recent literature, i.e. reactive distillation column control [1, 2].

2.1 Mathematical formulation

The following mathematical formulation of the control system design is used:

$$\min_{p, \delta} J(x(t), x_a(t), u(t), y(t), v(t), p, t) \quad (2.1)$$

s.t.,

$$h_d(\dot{x}(t), x(t), x_a(t), u(t), y(t), v(t), p) = 0, \quad \forall t \in [t_0, t_f] \quad (2.2)$$

$$h_a(x(t), x_a(t), u(t), y(t), v(t), p) = 0, \quad \forall t \in [t_0, t_f] \quad (2.3)$$

$$g_p(x(t_n), x_a(t_n), u(t_n), y(t_n), v(t_n), p, t_n) \leq 0, \quad \forall t_n \in [t_0, t_f] \quad (2.4)$$

$$h_c(\dot{x}(t), x(t), u(t), y(t), v(t), p) = 0, \quad \forall t \in [t_0, t_f] \quad (2.5)$$

$$h_\delta(p, \delta) = 0 \quad (2.6)$$

$$g_\delta(p, \delta) \leq 0 \quad (2.7)$$

$$\delta \in \{0, 1\} \quad (2.8)$$

where $h_d(\cdot) = 0$ and $h_a(\cdot) = 0$ in Eqs. (2.2) and (2.3) represent a system of differential-algebraic equations (DAEs) modeling the nonlinear process dynamics; $g_p \leq 0$ in Eq. (2.4) represents a set of inequality point constraints, that must be satisfied at specific time instances; h_c represents the dynamic equations for the controllers; $h_\delta = 0$ and $g_\delta \leq 0$ are the time-invariant equality and inequality constraints for the controller parameters and the control structure; $x(t)$ and $x_a(t)$ are the vectors of differential state and algebraic variables respectively; $u(t)$ is the vector of manipulated variables, $v(t)$ is the vector of disturbances acting on the plant; $y(t)$ is the vector of output variables which are measured and have to be controlled at their setpoint; p is the vector of time-invariant continuous controller parameters and δ is the vector of time-invariant binary variables which defines the structure of the decentralized control system. The objective function J is an integral over time which is minimized subject to the dynamic process model and operating constraints. Because of the presence of continuous and discrete variables, the present optimization problem represents a mixed-integer dynamic optimization problem.

2.2 Controller formulation

Two types of controller formulations are considered, starting from the decentralized control system to multivariable, i.e., centralized controllers. Although, the decentralized control system is mostly considered in the present thesis, the multivariable control structure is also presented here in order to show that the proposed MIDO formulation can be easily extended to other control structures.

2.2.1 Decentralized controller

First, decentralized linear controllers are considered. The controller dynamics together with controller parameters are given by,

$$u_j(t) = \sum_{i=1}^{N_y} kp_{i,j} \left(e_i(t) + \frac{1}{\tau_{I,j}} \int_0^t e_i(t) dt + \tau_{D,j} \frac{de_i}{dt} \right), \quad \forall j = 1, \dots, N_u \quad (2.9)$$

$$e_i(t) = y_{sp,i} - y_i(t), \quad \forall i = 1, \dots, N_y \quad (2.10)$$

where $kp_{i,j}$ are the elements of the unknown controller gain matrix, i is an index over the set of potential controlled variables ($i = 1, \dots, N_y$) and j is an index over the set of potential manipulated variables ($j = 1, \dots, N_u$), and $\tau_{I,j}, \tau_{D,j}$ are the integral and derivative time; Eqs. (2.9) and (2.10) provide the continuous form of the PID controller relationships between inputs and outputs which can be easily recast into the form given by Eq. (2.5). Binary variables δ are introduced in the bounds of the controller gain in Eq. (2.11) in order to restrict the values of the elements of the gain matrix used in the selected pairs and at the same time ensure that the gains of the loops not selected become zero [21].

$$kp_{i,j}^L \delta_{i,j} \leq kp_{i,j} \leq \delta_{i,j} kp_{i,j}^U \quad (2.11)$$

$$\tau_{I,j}^L \leq \tau_{I,j} \leq \tau_{I,j}^U \quad (2.12)$$

$$\tau_{D,j}^L \leq \tau_{D,j} \leq \tau_{D,j}^U \quad (2.13)$$

$$\sum_{i=1}^{N_y} \delta_{i,j} \leq 1 \quad \forall j = 1, \dots, N_u \quad (2.14)$$

$$\sum_{j=1}^{N_u} \delta_{i,j} \leq 1 \quad \forall i = 1, \dots, N_y \quad (2.15)$$

Eqs.(2.14) and (2.15) are used to enforce the requirements of a decentralized control structure. Note that, we restrict ourselves here to PI control, i.e., $\tau_{D,j} = 0$. However, extension for $\tau_{D,j} \neq 0$ is straightforward. But it was found to give only little improvement in terms of the objective function in our case studies and is therefore omitted in the following.

2.2.2 Multivariable PI controller

The mathematical formulation of multivariable, i.e. centralized, controllers is obtained by eliminating the constraints that enforce the requirement of a decentralized control structure, i.e. Eqs.(2.14) and (2.15). However, in the formulation of a centralized control law [20], the requirement of a square control structure may be imposed. The following constraints on the binary variables are used:

$$\sum_{i=1}^{N_y} \delta_{i,j} \leq N \quad \forall j = 1, \dots, N_u \quad (2.16)$$

$$\sum_{j=1}^{N_u} \delta_{i,j} \leq N \quad \forall i = 1, \dots, N_y \quad (2.17)$$

Where $N = \min \{N_u, N_y\}$. In summary, the MIDO formulation of a multivariable PI controller is obtained by adding Eqs.(2.16) and (2.17) to the original MIDO formulation. Again, we restrict ourselves here to PI control.

2.3 Objective function

This section considers two different formulations to measure the performance of the decentralized control system on the basis of the closed loop response characteristics.

2.3.1 Formulation I

In this formulation, the objective function is a measure of how much effort (manipulated variables movement from the steady state u_{ss}) is required in order to achieve a specified performance on the outputs. The objective function is given as,

$$J = \int_0^{t_f} (u_{ss} - u)^T R (u_{ss} - u) dt \quad (2.18)$$

The performance specifications are given in terms of overshoot and settling time by means of inequality path constraints as follows,

$$y_i(t) - y_{sp,i} \leq y_{ov,i}, \quad \forall t \in [0, t_{set}] \quad (2.19)$$

$$0.95y_{sp,i} \leq y_i(t) \leq 1.05y_{sp,i}, \quad \forall t > t_{set} \quad (2.20)$$

In the above constraints, Eq. (2.19) defines the specified overshoot $y_{ov,i}$, the maximum value by which the output variables are allowed to proceed beyond the set point. Eq. (2.20) defines the desired performance in terms of settling time t_{set} . This is the time in which the control variables have entered and remained within a specified ε band around the desired set point. In this study, a value of ε of $\pm 5\%$ is chosen.

2.3.2 Formulation II

In this formulation, the objective function minimizes a weighted sum of the quadratic control error and quadratic control action. The objective function is given

as,

$$J = \int_0^{t_f} [(y_{sp} - y)^T Q (y_{sp} - y) + (u_{ss} - u)^T R (u_{ss} - u)] dt \quad (2.21)$$

Q and R are positive definite weighting matrices. The solution of the MIDO problem with formulation II is subject to the selection of suitable Q and R matrices in the objective function Eq. (2.21). In the present work, the weighting matrices are diagonal matrices, in which each diagonal entry is the inverse of the square of the steady state values. Alternatively, guidelines given by Bryson and Ho [37] can also be adopted for calculating the Q and R matrices. In this approach, the maximum allowable deviations in the measured output variables $y_{i,U}$ and manipulated variables $u_{j,U}$ are calculated from the steady state sensitivities. Then, the Q and R matrices can be selected as:

$$Q = \text{diag} \{q_i\} = \text{diag} \left\{ \frac{1}{(y_{i,U})^2} \right\} \quad (2.22)$$

$$R = \text{diag} \{r_i\} = \text{diag} \left\{ \frac{1}{(u_{j,U})^2} \right\} \quad (2.23)$$

The suitable choice of the Q and R matrices from these two approaches will be discussed subsequently in the application section.

2.4 Solution approach for MIDO problem

The inclusion of structural (binary variables) decisions in the control system design leads to a very challenging mixed-integer dynamic optimization problem; the solution of which can be a formidable task. In general, two different solution strategies [25] are possible, i.e., the simultaneous approach and the sequential approach. In the simultaneous approach [29, 38, 22], the underlying process dynamics described by a system of differential-algebraic equations is discretized in a first step leading to a large-scale MINLP problem. In stead, a sequential solution approach [39, 40, 41] is considered to solve the MIDO problems in the present work.

In the sequential solution approach, the MIDO problem is decomposed into a series of dynamic NLP sub problems where binary variables are fixed and MILP master problems which determine a new binary configuration for the next NLP sub problem. The dynamic NLP problem is solved with the dynamic flowsheet simulator DIVA [42] using the DAE integrator DDASAC [43] and the SQP algorithm E04UCF [44] from the NAG library. The NLP sub problem gives an upper bound (UBD) on the final

solution. The master problem can be constructed using the approaches such as the Generalized Benders Decomposition (GBD) [45] or the Outer Approximation (OA) algorithm [46]. In both the cases, the NLP sub problem of dynamic optimization is identical and the master problem will differ. Further, it is worth noting that similar results are obtained in the benchmark problems using the GBD and OA methods. Therefore, only the GBD based sequential approach is considered here. The OA based method can be found in the paper by Schweiger et al. [41].

For fixed control structure ($\delta = \delta^k$), the k^{th} NLP sub problem has the following form:

$$\min_p J(x(t_f), x_a(t_f), y(t_f), u(t_f), v(t_f), p, t_f) \quad (2.24)$$

s.t.,

$$h_d(\dot{x}(t), x(t), x_a(t), u(t), y(t), v(t), p) = 0, \quad \forall t \in [t_0, t_f] \quad (2.25)$$

$$h_a(x(t), x_a(t), u(t), y(t), v(t), p) = 0, \quad \forall t \in [t_0, t_f] \quad (2.26)$$

$$g_p(x(t_n), x_a(t_n), u(t_n), y(t_n), v(t_n), p, t_n) \leq 0, \quad \forall t_n \in [t_0, t_f] \quad (2.27)$$

$$h_c(\dot{x}(t), x(t), u(t), y(t), v(t), p) = 0, \quad \forall t \in [t_0, t_f] \quad (2.28)$$

$$h_\delta(p, \delta^k) = 0 \quad (2.29)$$

$$g_\delta(p, \delta^k) \leq 0 \quad (2.30)$$

The solution of the k^{th} NLP sub problem is denoted as $u^k(t)$, $x^k(t)$, $y^k(t)$ and p^k .

The master problem based on the Generalized Benders Decomposition [45] is formulated using dual information and the solution of the NLP sub problem. However, since the binary variables δ do not participate in the DAEs for the decentralized control system design, a simplified master problem which does not use the adjoint problem [41] can be used. The Lagrange multipliers for the point constraints and other constraints are used in order to construct the master problem. For this situation, the master problem has the following form:

$$\min_{\delta, \eta_B} \eta_B \quad (2.31)$$

s.t.,

$$\begin{aligned} \eta_B \geq & J(x^k(t_f), x_a^k(t_f), u^k(t_f), y^k(t_f), v(t_f), p^k, t_f) \\ & + \lambda_p^T g_p(x^k(t_n), x_a^k(t_n), u^k(t_n), y^k(t_n), v(t_n), p^k, t_n) \\ & + \omega^T h_\delta(p^k, \delta) + \xi^T g_\delta(p^k, \delta) \quad k \in K_{feas} \end{aligned} \quad (2.32)$$

$$\begin{aligned} 0 \geq & J(x^k(t_f), x_a^k(t_f), u^k(t_f), y^k(t_f), v(t_f), p^k, t_f) \\ & + \lambda_p^T g_p(x^k(t_n), x_a^k(t_n), u^k(t_n), y^k(t_n), v(t_n), p^k, t_n) \\ & + \omega^T h_\delta(p^k, \delta) + \xi^T g_\delta(p^k, \delta) \quad k \in K_{infeas} \end{aligned} \quad (2.33)$$

$$\sum_{i=1}^{N_y} \delta_{i,j} \leq 1 \quad (2.34)$$

$$\sum_{j=1}^{N_u} \delta_{i,j} \leq 1 \quad (2.35)$$

$$\delta \in \{0, 1\} \quad (2.36)$$

where K_{feas} is the set of all feasible NLP problems and K_{infeas} is the set of all infeasible NLP sub problems solved up to the iterations under consideration. λ_p^T , ω^T and ξ^T are the set of Lagrangian multipliers associated with the point constraints, the time invariant equality and inequality constraints respectively. These are calculated from the first order optimality conditions of the NLP sub problem. Pure binary constraints of the original system are also included as indicated in Eqs. (2.34) and (2.35). Note that integer cuts [39] are introduced along with the above equations in the master problem in order to exclude previous integer solutions. The above master problem is an MILP, which is solved using GAMS/CPLEX [47] and this gives the lower bound (LBD) to the original problem. The MIDO algorithm based on the GBD terminates when the difference between the least upper bound from the NLP sub problems and the lower bound from the master problem is less than a specified tolerance, or if there is an infeasible master problem. The solution to the MIDO problem then corresponds to the solution of the NLP sub problem with the least upper bound.

Note that if a particular set of values of binary variables (δ^k) renders the NLP sub-problem infeasible, then an infeasibility minimization problem is solved instead. This can involve, for example, minimizing the L_1 or L_∞ sum of constraint violations [48].

The infeasibility minimization problem is then solved to obtain multipliers in order to construct the master problem. The formulation corresponding to minimizing the L_∞ sum of violations is shown below:

$$\min_{p, \varphi} \varphi \quad (2.37)$$

s.t.,

$$h_d(\dot{x}(t), x(t), x_a(t), u(t), y(t), v(t), p) = 0, \quad \forall t \in [t_0, t_f] \quad (2.38)$$

$$h_a(x(t), x_a(t), u(t), y(t), v(t), p) = 0, \quad \forall t \in [t_0, t_f] \quad (2.39)$$

$$g_p(x(t_n), x_a(t_n), u(t_n), y(t_n), v(t_n), p, t_n) \leq \varphi \epsilon, \quad \forall t_n \in [t_0, t_f] \quad (2.40)$$

$$h_c(\dot{x}(t), x(t), u(t), y(t), v(t), p) = 0, \quad \forall t \in [t_0, t_f] \quad (2.41)$$

$$h_\delta(p, \delta^k) = 0 \quad (2.42)$$

$$g_\delta(p, \delta^k) \leq 0 \quad (2.43)$$

$$\varphi \geq 0 \quad (2.44)$$

Where φ is a positive scalar quantity and ϵ is a vector whose elements are all equal to one. Throughout this work, all computations were performed on a Linux workstation with Intel Pentium D CPU 3.0 GHz processor.

2.5 Case studies

Reactive distillation (RD) combines reaction and separation in a single unit that provides substantial economic incentives for some chemical processes. The books by Sundmacher and Kienle [1], Luyben and Yu [2] give an updated summary of modeling, simulation and control of reactive distillation. Due to close interaction of reaction and distillation in the same unit reactive distillation columns can show intricate non-linear dynamic behavior including input and output multiplicities, inverse responses and self sustained oscillations (see e.g. Chapter 10 by Kienle and Marquardt and references therein [1]). Hence, reactive distillation column control is an interesting and challenging field of application, which has received a lot of attention in the recent literature.

In the control of RD column, a “control structure” refers to the number of control loops and the specific input-output pairing used in the decentralized PI control loops.

Potential input variables are the reflux rate, reflux ratio, reboiler duty, reboiler ratio, distillate rate, bottoms rate, and the fresh feeds. Potential output variables to be controlled are product compositions. However, since online composition measurement is often difficult and expensive, some sensitive tray temperatures are used instead leading to inferential control schemes to be considered subsequently. The combination of suitable input variables with possible tray temperatures leads to thousands of possible control structures even though the RD column is considered as a single-unit chemical plant [33].

Roat et al., [49] were among the first to propose a decentralized two-temperature PI control structure for an industrial column, in which two fresh feeds are manipulated by two tray temperatures (inferential control structure). Several different control structures based on two-temperature control have been investigated for RD columns by Luyben and coworkers [2]. In the recent literature, most of the control structures investigated for RD columns are obtained with heuristic methods in which, the non-linear process dynamics is not explicitly taken into account in the control system design. Therefore, application of the proposed framework to RD columns is very well suited to demonstrate the advantages of the present approach.

Furthermore, the appropriate control structure depends on the flowsheet and on the type of reactions occurring in the column [2]. Therefore, two different types of RD columns are considered to confirm the usefulness of the proposed methodology:

1. Ideal reactive distillation with two reactants and two products
2. Non-ideal system of methyl acetate synthesis

Each flowsheet has different characteristics and a different level of complexity. These will be discussed subsequently.

2.5.1 Case study 1: Ideal reactive distillation

An ideal reactive distillation column with two products and two feeds presented by Al-Arfaj and Luyben [30] is considered as the first case study and is illustrated in Fig 2.1. The reversible reaction occurring on the reactive trays is given by,



The reactants A and B are intermediate boiling between the products. The fresh feed stream F_{0A} containing reactant A is fed at the bottom of the reactive zone, and the fresh feed stream F_{0B} containing reactant B is fed at the top of the reactive zone. The

Table 2.1: Physical data for the ideal reactive distillation

activation energy of the reaction	cal/mol	
forward		30 000
reverse		40 000
specific reaction rate at 366 K	kmol/(s kmol)	
forward		0.008
reverse		0.004
average heat of reaction	cal/mol	-10 000
average heat of vaporization	cal/mol	6944
ideal gas constant	cal/(mol K)	1.987
relative volatilities		
α_A		4
α_B		2
α_C		8
α_D		1
vapor-pressure constants		
$\ln P_j^s = A_{VP,j} - \frac{B_{VP,j}}{T}$ with T in K		
A	$A_{VP,j} = 12.34$	$B_{VP,j} = 3862$
B	$A_{VP,j} = 11.65$	$B_{VP,j} = 3862$
C	$A_{VP,j} = 13.04$	$B_{VP,j} = 3862$
D	$A_{VP,j} = 10.96$	$B_{VP,j} = 3862$

reactive section contains N_{RX} trays. The rectifying section above the reactive section contains N_R trays, and the stripping section below the reactive section contains N_S trays. The detailed mathematical modeling of the reactive distillation column can be found in the paper by Al-Arfaj and Luyben [30]. Chemical kinetics, physical properties and column design parameters are taken from Kaymak and Luyben [31] which are given in Table 2.1. The two fresh feed flow rates are each 12.6 mol/s of pure reactants. Fig 2.2 gives the steady-state composition and temperature profiles. Note that reactants A and B have fairly high concentrations in the reactive zone but are prevented from leaving the top or bottom of the column by means of separation in the nonreactive rectifying and stripping section and recycling into the reaction zone. The principal impurity in the bottom is B, and that in the top is A.

2.5.1.1 Inferential control system

Since, focus is on inferential control, i.e., tray temperatures are used instead of composition measurement for product composition control, the selection of trays for temperature control loops is the key issue. Kaymak and Luyben [31, 32] presented the use of steady state gain and singular value decomposition (SVD) analysis to choose

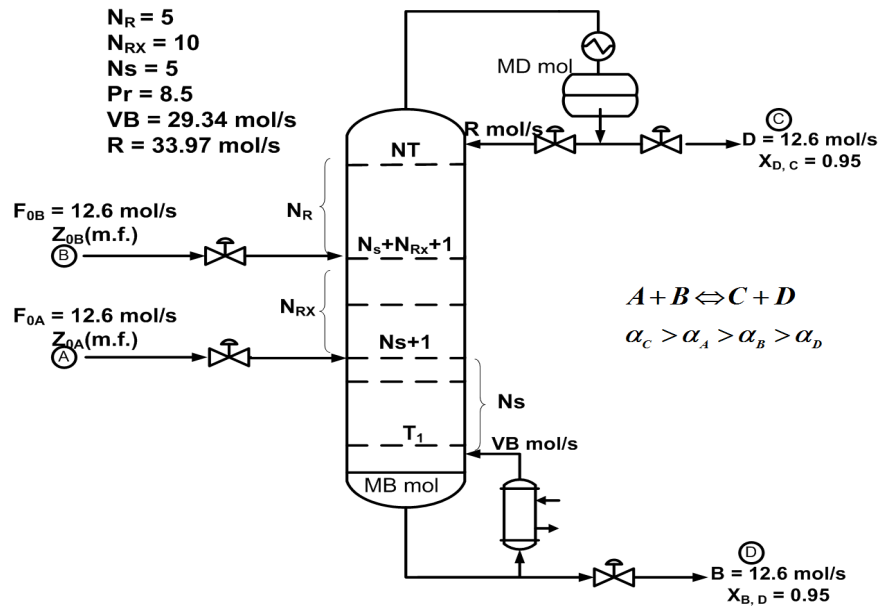


Figure 2.1: Ideal reactive distillation column

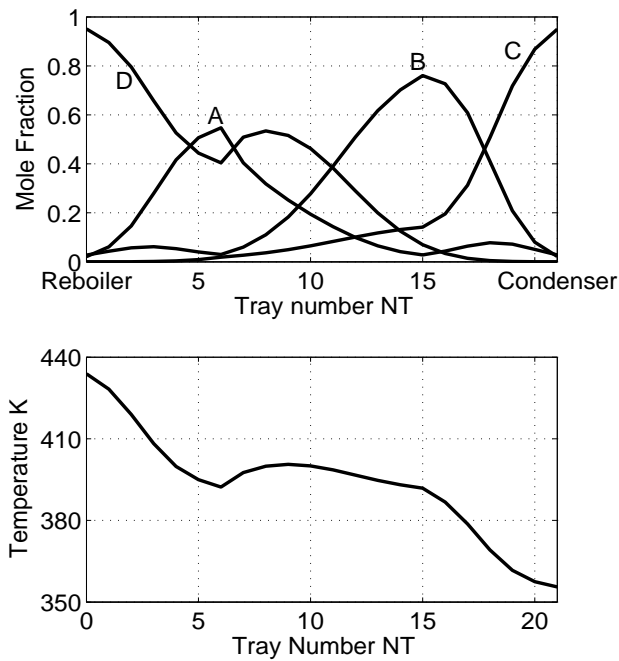


Figure 2.2: Steady state composition and temperature profile of ideal reactive distillation

the trays for temperature control. In order to compare the results with earlier studies, pressure and level control loops are assumed to be the same as given by Kaymak and Luyben [31]. Further, PI controllers are considered for the temperature control loops in order to compare the results with the previous studies. Furthermore, the same test scenario is considered, i.e. a $\pm 10\%$ step change in the vapor boil up VB. The selection of two-temperature control loops from 20 tray measurements and then combination with 2 manipulated variables yields 380 possible combinations. Due to the underlying assumptions, the problem has still moderate complexity but manual enumeration is not feasible. For both formulations I and II, the nonlinear DAE model of the reactive distillation is implemented in the dynamic flowsheet simulator DIVA [42] and NLP subproblems are solved using SQP algorithm in DIVA. Further, the master problems based on the GBD methods are implemented in GAMS and solved using an MILP solver CPLEX [50].

Table 2.2: The optimal control structure and PI controller parameters - Ideal reactive distillation

	Control structure	kp	τ_I (min)	CPU time
Formulation I	$F_{0A} - T_3$	0.4	14.0	20 min
	$F_{0B} - T_{13}$	2.6	15.0	(6 iterations)
Formulation II	$F_{0A} - T_3$	0.6	10.6	5 min
	$F_{0B} - T_{12}$	4.5	14.0	(4 iterations)

2.5.1.2 Decentralized PI controller design using Formulation I

In order to solve the decentralized PI controller design problem with formulation I, the performance constraints in terms of the overshoot and settling time are specified for the top and bottom purities. An overshoot of 1% of the set-points and a settling time of 1 hour are considered as the performance specifications. The solution algorithm which was explained in the previous section is applied to solve the resulting MIDO problem. Using a termination tolerance $UBD-LBD < 0$, the sequential algorithm based on the GBD has converged after 6 iterations. The optimal control structure and PI controller parameters are reported in Table 2.2. It should be noted that the problem becomes infeasible if the performance specifications are chosen too tight. The closed loop performance of the optimal control structure is shown in Fig 2.3 for a $\pm 10\%$ change in vapor boil up VB. These performance constraints such as

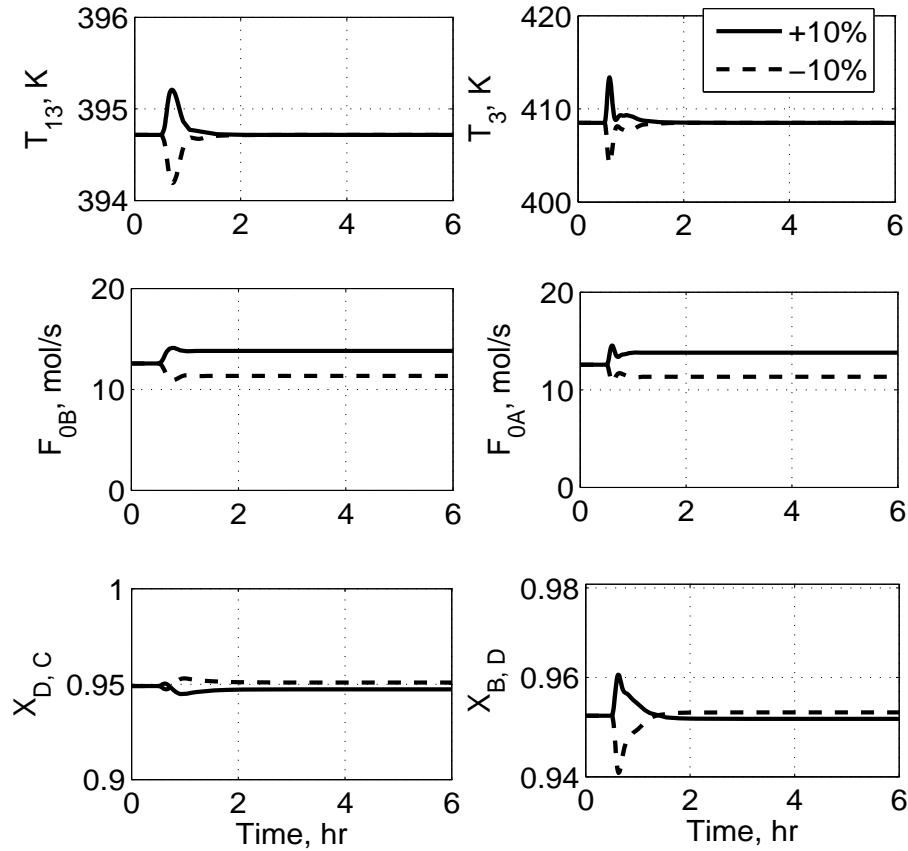


Figure 2.3: Closed loop response for a $\pm 10\%$ change in the vapor boil up VB, Formulation I (Ideal reactive distillation)

the overshoot and settling time provided in the algorithm act as active constraints and the closed loop response is lying within these constraints. Further, it is worthwhile to mention particularly about the GBD approach of solving the problem with formulation I. If a particular set of fixed binary variables renders the NLP sub problem infeasible, then an infeasibility minimization problem is solved instead. This can involve, for example, minimizing an L_∞ sum of constraint violations in order to obtain dual information with a feasible point for the construction of the master problem. The performance constraints in this formulation relatively often lead to solution of an infeasibility minimization problem (Eqs. (2.37) - (2.44)). Hence, the problem demands 20 minutes of computational effort to achieve the optimal solution.

2.5.1.3 Decentralized PI controller design using Formulation II

In formulation II, the weighting matrices Q and R are diagonal matrices, in which each diagonal entry is the inverse of the square of the steady state values. Alternatively, steady state sensitivities can be used for the weighting matrices Q and R . In the present case, however this leads to very similar results. Further, it is worthwhile to mention that the control error in the distillate and bottoms purities from their desired specifications is also included in the objective function along with the tray temperatures as the output variables. Like formulation I, the solution algorithm based on the GBD is considered to solve the resulting MIDO problem. The optimal control structure and PI controller parameters are reported in Table 2.2. Using a termination tolerance $UBD - LBD < 0$, the GBD method is converged after 4 iterations which demands 5 minutes of computational effort. The closed loop performance of the optimal control structure is shown in Fig 2.4(b) for a $\pm 10\%$ change in vapor boil up VB. The overall response is well behaved and both temperature loops are fast, less oscillatory and achieved their set-points less than an hour compared to the earlier studies by Kaymak and Luyben [31]. The closed loop performance of the control structure which is designed based on the heuristic method is shown in Fig 2.4(a). While comparing the optimal control loop performance in Fig 2.4(b) with Fig 2.4(a), it is clearly shown that the performance is better than the heuristic method. It is worth mentioning that formulation II is applied to this process to design multivariable PI controllers. However, only little improvement was observed compared to the decentralized controllers. The closed loop performance of multivariable controllers is shown in Fig 2.5

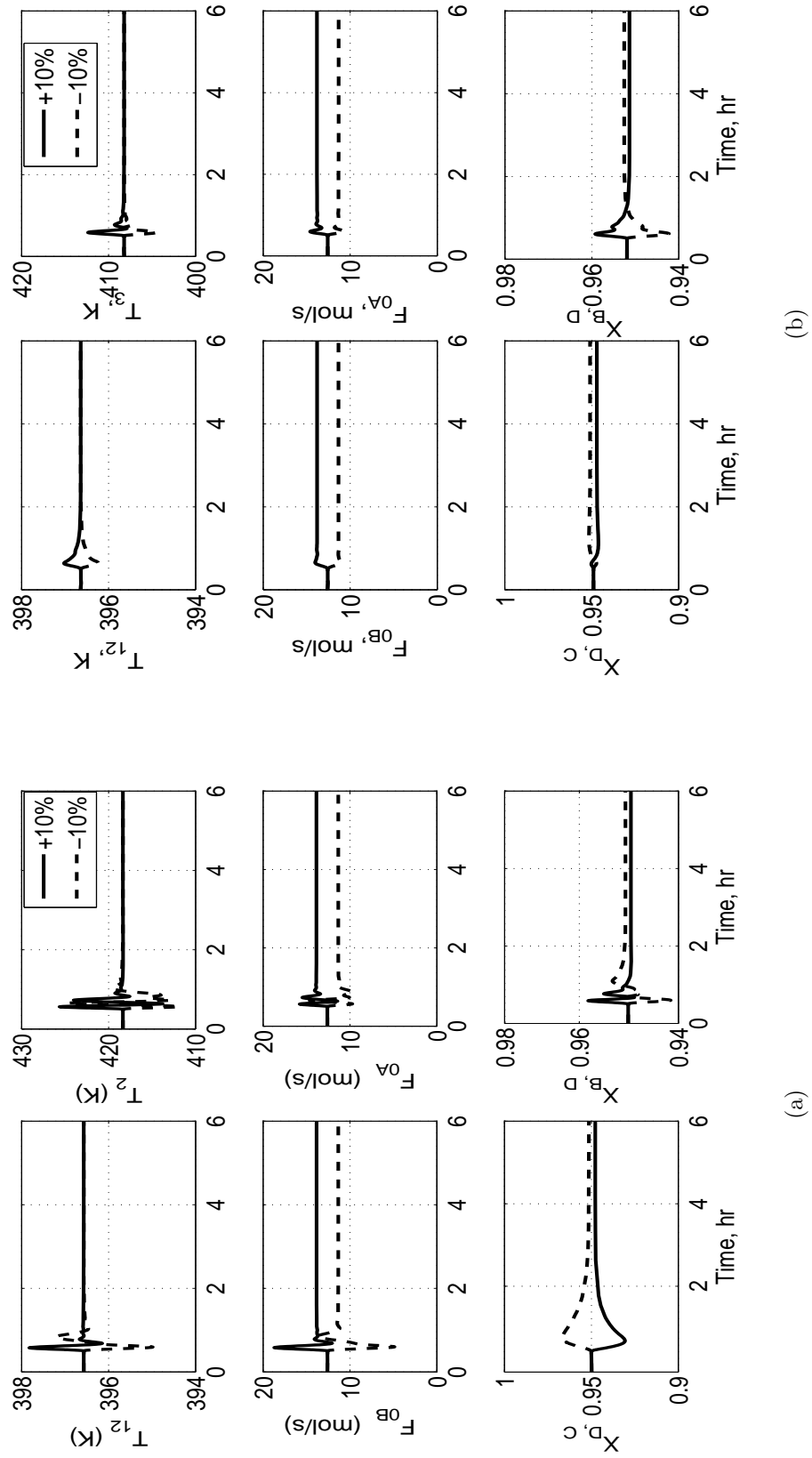


Figure 2.4: Closed loop response for a $\pm 10\%$ change in the vapor boil up VB - Ideal reactive distillation: (a) Heuristic method; (b) MIDO results (Formulation II)

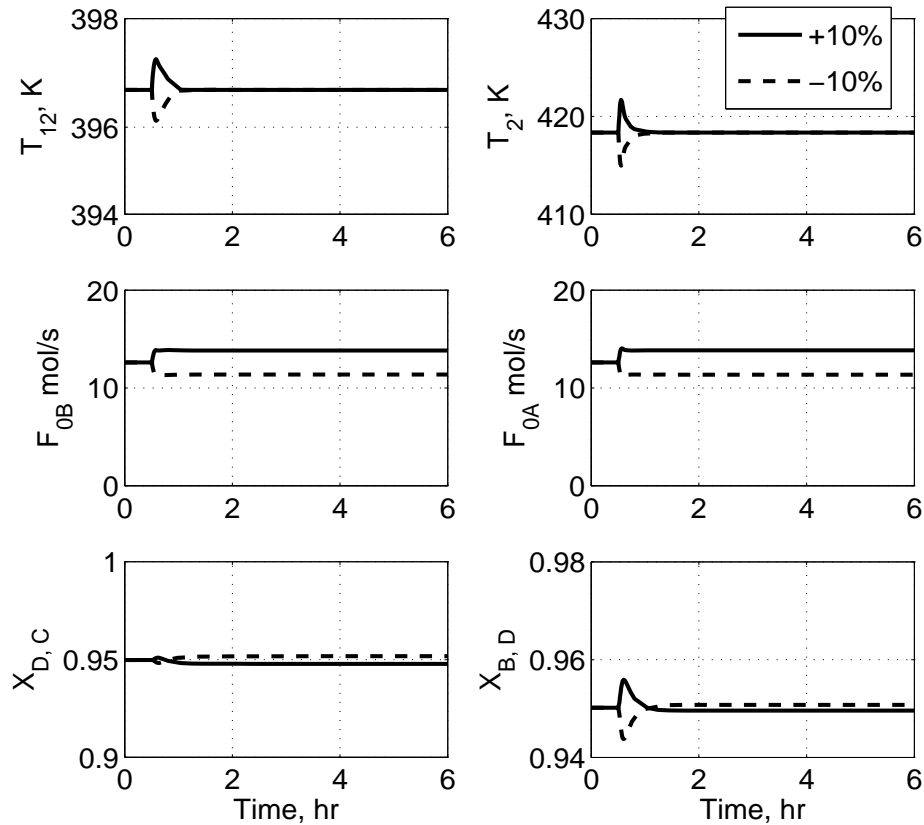


Figure 2.5: Closed loop response for a $\pm 10\%$ change in the vapor boil up VB, Formulation II - Multivariable controller (Ideal reactive distillation)

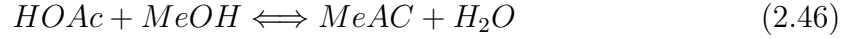
2.5.2 Case study 2: Methyl acetate system

Although the optimal solution of decentralized control system design performs better than heuristic approach in the previous case study, the difference between both approaches is relatively small. It is conjectured that this is also due to the ideal behavior postulated in this benchmark problem. Therefore in a second case study highly nonideal methyl acetate system is considered as a more challenging practical benchmark problem.

2.5.2.1 Process description

Methyl acetate reactive distillation column is used as an example of a real two-reactant/two-product system with a reversible reaction. Methyl acetate (MeAC) can be made by the liquid-phase reaction of acetic acid (HOAc) and methanol (MeOH)

in the presence of an acid catalyst (e.g. sulfuric acid) at a pressure of 1 atm. The reaction is



An activity based rate model for the reaction chemistry is given by,

$$r = k_f \left(a_{HOAc} a_{MeOH} - \frac{a_{MeAC} a_{H_2O}}{K_{eq}} \right) \quad (2.47)$$

where the reaction equilibrium constant and the forward rate constant are given by,

$$K_{eq} = 2.32 \exp \left(\frac{782.98}{T} \right) \quad (2.48)$$

$$k_f = 9.732 \times 10^8 \exp \left(-\frac{6287.7}{T} \right) h^{-1} \quad (2.49)$$

where T is in K. The reaction equilibrium constant was taken from Song et al., [51]. The pseudo-homogeneous rate equation and design parameters are taken from Huss et al., [52]. For modeling the vapor-liquid equilibrium (VLE), the vapor-phase is assumed to be ideal and the Wilson equation is used for the liquid-phase activity coefficients. Further, parameters for dimerization constant are taken from Huss et al., [52] in order to correct for the effect of vapor-phase acetic acid dimerization on the VLE. For this system, the heavy reactant is acetic acid (HOAc) and the light reactant is methanol (MeOH). Water (H_2O), the heavy product of the reaction is taken from the bottom, while the light product methyl acetate (MeAC) is removed from the top. The purity of both products is above 98 mol%. The fresh feed-rates of acetic acid and methanol are 280 kmol/hr. The total number of stages are 44, and stages are counted from top to bottom including the reboiler and condenser. The reactive zone runs from the stages 11 to 43. The light reactant is fed to the stage 40, which is near to the bottom of the column. The heavy reactant is introduced on stage 4, which is near the top of the reactive zone. The model is based on material balances only [53], heat effects are neglected like in the previous case study. The reactive distillation column details are illustrated in Fig 2.6. The steady state composition and temperature profiles are shown in Fig 2.7. In contrast to the previous section, focus is only on formulation II to find the optimal control structure and controller parameters. Further, the disturbance scenario considered is a ± 10 step change in one of the feed (F_{MeOH}). The selection of two-temperature control loops from 42 tray

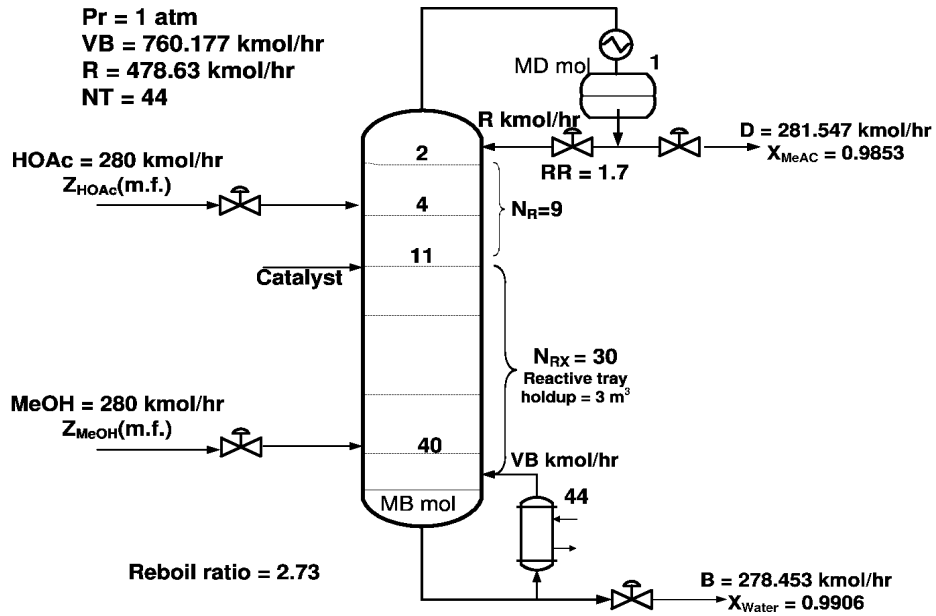


Figure 2.6: Methyl acetate reactive distillation column

measurements with a combination of 2 manipulated variables has 1722 numbers of possible combinations. Hence, the problem turns out to be more complex.

2.5.2.2 Heuristic method

First, the decentralized control system is designed using an heuristic approach. In the recent version of control structures for this reactive distillation [32, 54, 55], the light-reactant fresh feed stream is flow controlled and serves as the production rate handle. The ratio of the heavy reactant to the light reactant feed is controlled. The ratio is set by one of the tray temperature controllers. Further, the base level is controlled by manipulating the bottoms flow rate. The reflux drum level is controlled by the reflux flow rate, and the distillate flow rate is adjusted to give a constant reflux ratio. In summary, we have two manipulated variables associated with the MeAC system. One is the feed ratio FR, which is used to maintain the stoichiometric balance, and the other is the vapor boil up rate VB. In order to design an inferential control structure, the trays for temperature control have to be selected. The non-square relative gain (NRG) [55] is used here for this purpose, more details of the NRG based heuristic approach for control structure selection for reactive distillation can be found in the paper by Hung et al., [55]. The next step is to find the variable pairing for the controlled and manipulated variables. The relative gain array (RGA) is used for the pairings. From the RGA value, the vapor boil up rate VB is used

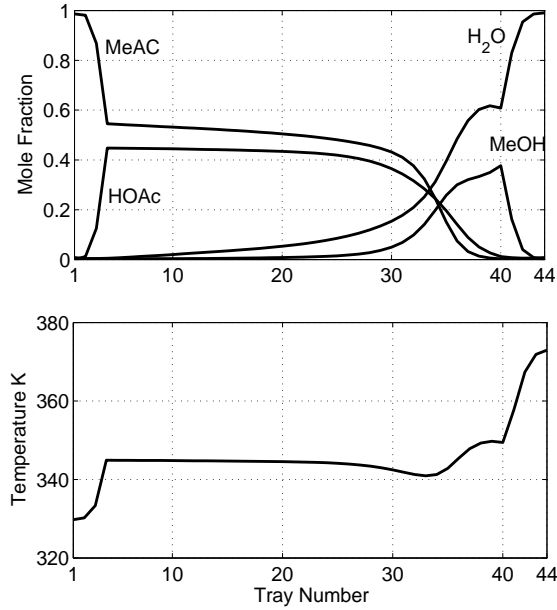
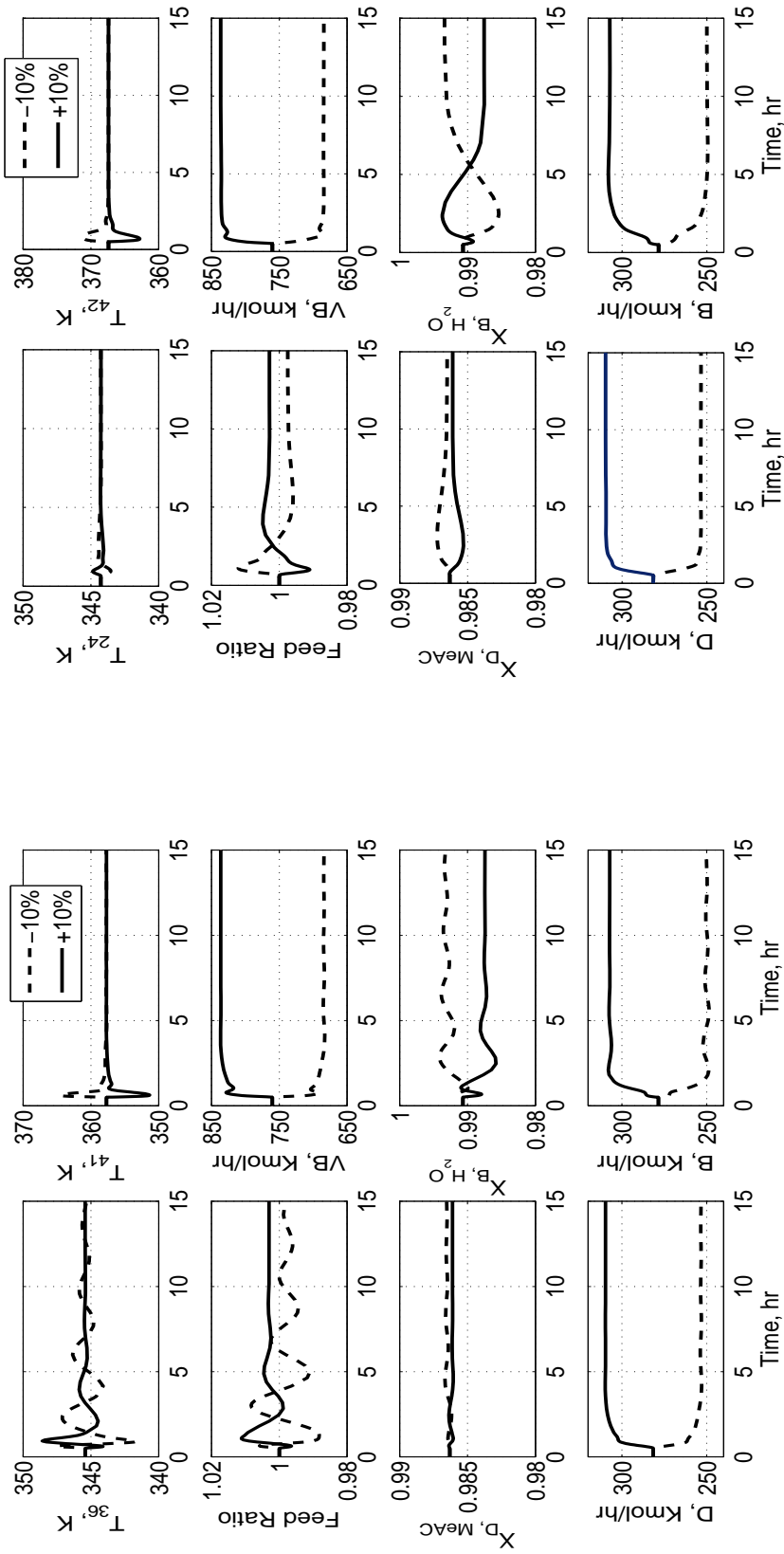


Figure 2.7: Steady state composition and temperature profile of Methyl acetate system

Table 2.3: Control structure and PI controller parameters - Methyl acetate system

	Control structure	kp	τ_I (min)
Heuristic method	$FR - T_{36}$	0.101	35.0
	$VB - T_{41}$	8.0	19.0
Formulation II	$FR - T_{24}$	0.209	28.0
Optimization method	$VB - T_{42}$	8.5	17.0

to control T_{41} and T_{36} is controlled by manipulating the feed ratio (i.e., $VB - T_{41}$ and $FR - T_{36}$). The sequential relay feedback test is used to find the ultimate gain K_u and the ultimate period P_u followed by the Tyreus-Luyben PI tuning rule [56]. The closed loop response for a $\pm 10\%$ change in the MeOH feed flow rate is shown in Fig 2.8(a). It is noticed in the closed loop response that the $FR - T_{36}$ control loop has larger overshoot and the oscillatory behavior. Therefore, similar oscillatory behavior is noticed in both product purities also. Further, the important point is that the control structure achieves the steady state value in 10 hour for the positive step change in the disturbance. But at the same time, the control structure provides oscillatory behavior and the controlled and manipulated variables are settling to the steady state values in 25 hour for the negative step change in the disturbance.



(a)

(b)

Figure 2.8: Closed loop response for a $\pm 10\%$ change in MeOH feed rate - Methyl acetate system: (a) Heuristic method; (b) MIDO results (Formulation II)

2.5.2.3 Decentralized PI controller from Formulation II

Formulation II (i.e., maximize the overall performance) is considered here to determine the optimal control structure and controller parameters simultaneously for the MeAC system. The sequential solution approach based on the GBD is considered to solve the complex MIDO problem of formulation II. Further, Q and R weighting matrices are calculated based on the inverse of the square of steady state values. With the sequential solution approach, we solved formulation II successfully for optimal control structure and controller parameters which are shown in Table 2.3. The optimal inferential control structure is $T_{24} - FR$ and $T_{42} - VB$ which is different from the heuristic method. This is because of the optimal control structure is designed by considering the rigorous nonlinear closed loop dynamics. The closed loop performance of the optimal control structure is shown in Fig 2.8(b) for a 10% change in the MeOH feed (F_{MeOH}). The overall response is well behaved and both temperature loops are fast, less oscillatory and achieved their set-point less than 5 hour. By comparing the optimal control loop performance with Fig 2.8(a), it is clearly shown that the closed loop performance is better than the heuristic method. Further, the sequential approach requires only 35 minutes of computational time to solve the problem.

2.6 Summary

A systematic procedure for simultaneous selection of a decentralized control structure and controller parameters was developed in view of (1) minimizing the effort to achieve a specified performance or (2) maximizing the overall performance in terms of quadratic cost functions. Both formulations were constructed as a MIDO problem. It was shown that the resulting MIDO problems can be solved with standard hard and software with reasonable effort using a Generalized Benders Decomposition. Application was demonstrated for two different reactive distillation processes: (1) Ideal quaternary system (2) Non-ideal methyl acetate process. It was shown that the resulting control systems have superior performance compared to standard heuristic design approaches

It is worth noting that the same methodology can be applied for the design of multivariable PI controllers by relaxing the corresponding structural constraints for the controllers. This was also done for the ideal reactive distillation benchmark problem presented in this chapter. However, only little improvement was observed compared to the decentralized controllers.

The design procedure presented in this chapter is based on a specific disturbance

scenario. However, since the systems are highly nonlinear the optimal controllers may differ for different scenarios. This will be addressed by an extended problem formulation accounting for different disturbance scenarios in the next chapter.

Chapter 3

Decentralized control system design under uncertainty

In the previous chapter, mixed integer optimization is used to determine the optimal control structure and controller parameters simultaneously. This will lead to a mixed-integer dynamic optimization (MIDO) problem if the nonlinear plant dynamics is explicitly taken into account. However, due to nonlinearity the optimal control structure and the optimal controller parameters will differ for different disturbance scenarios. Therefore, the deterministic approach described in the previous chapter is extended in this chapter, to account for various stochastic disturbances and to find an optimal compromise for the control structure and controller parameters in view of this class of disturbances. This leads to a MIDO problem under uncertainty in which the performance index of the control system is a stochastic quantity depending on random disturbances. The problem is solved by minimizing a convex combination of the expectation and the variance of this performance index. This requires the evaluation of multidimensional integrals for the computation of the expectation and the variance, which can be a challenging task [57]. Available methods fall into two categories: sample averaging and numerical integration. However, both are computationally expensive when the dimension of the uncertainty space is large.

To overcome this problem, the sigma point method suggested by Julier, and Uhlmann [58] is adopted here. This method allows a cheap approximation of a nonlinear transformation of a probability distribution. It has been developed originally for nonlinear state estimation and has been recently extended to optimal experimental design [59, 60]. With the help of the sigma point method, the stochastic MIDO problem is converted into a deterministic one, which can be solved by existing deterministic algorithms as described in the previous chapter. The benchmark problem of an ideal

reactive distillation column which was illustrated in the previous chapter is considered here to demonstrate the design of the control system under disturbance uncertainty.

3.1 Mathematical formulation

We consider the following stochastic MIDO problem for control system design:

$$\min_{p, \delta} \Phi(x(t), x_a(t), u(t), y(t), \theta, p, t) \quad (3.1)$$

s.t.,

$$h_a(\dot{x}(t), x(t), x_a(t), u(t), y(t), \theta, p) = 0, \quad \forall t \in [t_0, t_f] \quad (3.2)$$

$$h_a(x(t), x_a(t), u(t), y(t), \theta, p) = 0, \quad \forall t \in [t_0, t_f] \quad (3.3)$$

$$g_p(x(t_n), x_a(t_n), u(t_n), y(t_n), \theta, p, t_n) \leq 0, \quad \forall t_n \in [t_0, t_f] \quad (3.4)$$

$$h_c(\dot{x}(t), x(t), u(t), y(t), \theta, p) = 0, \quad \forall t \in [t_0, t_f] \quad (3.5)$$

$$h_\delta(p, \delta) = 0 \quad (3.6)$$

$$g_\delta(p, \delta) \leq 0 \quad (3.7)$$

$$\delta \in \{0, 1\} \quad (3.8)$$

$$\theta \in \Theta \quad (3.9)$$

where Eqs. (3.2) and (3.3) represent a system of differential-algebraic equations (DAEs) modeling the process dynamics; $g_p \leq 0$ from Eq. (2.4) represents a set of inequality point constraints, that must be satisfied at specific time instances; h_c represents the dynamic equations for the controllers; $h_\delta = 0$ and $g_\delta \leq 0$ are the time-invariant equality and inequality constraints for the controller parameters and control structure; $x(t)$ and $x_a(t)$ are the vectors of differential state and algebraic variables; $u(t)$ is the vector of manipulated variables; $y(t)$ is the vector of output variables which are measured and to be controlled at their setpoint; p is the vector of time-invariant continuous PID controller parameters and δ is the vector of time-variance binary variables which defines the control structure; θ are the uncertain disturbances. In particular, step disturbances are considered, the magnitude of which will vary randomly. For illustration purposes, we consider a Gaussian distribution of the magnitude of the disturbances: $\theta \sim N(\mu, \Sigma)$ where μ denotes the mean of θ and Σ is the covariance matrix. However, it should be noted that the methodology presented

here is neither limited to step disturbances nor limited to a Gaussian distribution of their magnitude. Finally, the objective function Φ is some suitable statistical measure of the control system performance. The objective of this MIDO formulation is to find the optimal control structure and controller parameters under uncertainty.

3.2 Objective function

In the objective function of the above stochastic MIDO problem, usually the expected value of the performance index is minimized. If the uncertain variables have a large variance, the variance of the performance index should also be taken into account. Therefore, the statistical objective function has the following form [61]:

$$\Phi = E [J(p, \delta, \theta, t)] + \omega \sqrt{V [J(p, \delta, \theta, t)]} \quad (3.10)$$

where E and V are the operators of expectation and variance, respectively, ω is a weighting factor between the two terms which can be adjusted to vary the degree of robustness. For illustration purposes, a value of ω of 0.5 is considered in the present study. Here, the performance index is the integral value of a weighted sum of the quadratic control error and quadratic control action and is given by:

$$J = \int_0^{t_f} [(y_{sp} - y)^T Q (y_{sp} - y) + (u_{ss} - u)^T R (u_{ss} - u)] dt \quad (3.11)$$

Q and R are positive definite weighting matrices, which are used here for scaling purposes. These weighting matrices are diagonal matrices, in which each diagonal entry is the inverse of the square of the steady state values.

In order to evaluate the statistical objective function, the calculation of the expectation and the variance of the performance index J is required. Since we assume that the uncertain disturbances θ follow a continuous probability density function (PDF) φ over the domain Θ , the expectation of J is given by the multidimensional integral:

$$E[J] = \int_{\Theta} J(\theta) \varphi(\theta) d\theta \quad (3.12)$$

Generally, the calculation of the expectation and the variance is numerically quite expensive for practically relevant cases with multiple correlated or uncorrelated uncertain variables. For example, using the sample average approach, the expectation

Table 3.1: Comparison of the sigma point method with other integration methods

No of parameters	Monte-Carlo	Specialized product Gauss	Specialized cubature $n \geq 3$	Sigma points
Formula :	1000 -10000	3^n	$2^n + 2n$	$2n + 1$
n = 2	5000	9	–	5
n = 3	5000	27	14	7
n = 5	10000	243	42	11
n = 10	10000	59049	1044	21

of the performance index for a fixed control structure is estimated by:

$$E[J] = \frac{1}{N} \sum_{i=1}^N J(p, \theta_i) \quad (3.13)$$

where θ_i is the i -th sample of the random variables. According to the central limit theorem, the accuracy of this approximation cannot be improved faster than $1/\sqrt{N}$. This implies that one order of magnitude increase in accuracy requires two order of magnitude increase in the sample size. It is, therefore, intractable to ask for an expected performance of high accuracy, unless the problem is small. Alternatively, numerical integration methods such as Gaussian Quadratures or Cubatures [62] can be used to evaluate the multidimensional integrals. However, this approach is only feasible for moderate numbers of uncertain parameters. This is due to the fact that total number of grid points increases exponentially with the number of uncertain parameters. For example, the total number of grid points required for the specialized product Gauss formula and specialized cubature formula [57] is shown in Table 3.1. To overcome this problem, the sigma point method proposed by Julier, and Uhlmann [58] is used here.

3.3 Sigma-point method

Sigma points (SP) are used to describe the statistical properties of a probability distribution through a nonlinear mapping. In this method, the sigma points are used in order to determine the mean and covariance of a random variable $\eta \in \mathfrak{R}^f$ from the mean (μ) and covariance (Σ) of a random variable $\theta \in \mathfrak{R}^n$, where η is related to θ by the nonlinear transformation:

$$\eta = g(\theta) \quad (3.14)$$

Table 3.2: Sigma point method

Set of sigma points	$\theta_0 = \mu$ $\theta_i = \mu + (\sqrt{(n + \lambda)\Sigma})_i \quad i = 1, \dots, n$ $\theta_i = \mu - (\sqrt{(n + \lambda)\Sigma})_i \quad i = n + 1, \dots, 2n$ $\lambda = \alpha^2(n + \kappa) - n$
Weights	$w_0 = \frac{\lambda}{n + \lambda}$ $w_i = \frac{1}{2(n + \lambda)} \quad i = 1, \dots, 2n$
No of points	$2n + 1$

Julier, and Uhlmann [58] showed that an accurate estimation of mean $E[\eta]$ and variance $V[\eta]$ can be obtained from $(2n + 1)$ evaluations of $\eta(\cdot)$ for the $(2n + 1)$ deliberately chosen samples of θ . The details of the sigma point method are shown in Table 3.2 in which λ is a scaling parameter and $(\sqrt{(n + \lambda)\Sigma})_i$ is the i th column of the matrix square root. The numerically efficient Cholesky factorization method is typically used to calculate the matrix square root. The meaning and the influence of other scaling parameters α , κ are explained by Julier, and Uhlmann [58]. The detailed description of the sigma point approach is given in the thesis by van der Merwe [63]. Here, each sigma point is propagated through nonlinear transformation:

$$\eta_i = g(\theta_i) \quad \forall i = 0, \dots, 2n \quad (3.15)$$

and approximated mean and variance of η are computed as follows:

$$E[\eta] = \sum_{i=0}^{2n} w_i \eta_i \quad (3.16)$$

$$V[\eta] = \sum_{i=0}^{2n} w_i (E[\eta] - \eta_i)(E[\eta] - \eta_i)^T \quad (3.17)$$

These estimates of the mean and covariance are accurate to the second order (third order for true Gaussian priors) of the Taylor series expansion of $g(\theta_i)$ for any nonlinear transformation [63]. The comparison of the sigma point method with other methods like Monte Carlo integration, specialized product Gauss rule and specialized cubature formula are summarized in terms of the number of points required for the evaluation of the expectation in Table 3.1. The above sigma point method is used in the present study to approximate the expectation and the variance of the performance index for

the optimal control system design problem and is given by:

$$E[J] \approx \sum_{i=0}^{2n} w_i J(\theta_i) \quad (3.18)$$

where, n is the number of uncertain disturbances. This will convert the stochastic MIDO problem into a deterministic one, which can be solved by existing deterministic algorithms using a sequential approach. The description of the GBD based sequential solution approach adopted here is provided in Chapter 2.

3.4 Case study : Ideal reactive distillation - Quaternary system

An ideal reactive distillation column with two products and two feeds presented by Al-Arjaj and Luyben [30] is considered here as a benchmark problem. The same benchmark problem was used in the previous chapter for a deterministic disturbance of $\pm 10\%$ step change in VB.

It has already been pointed out in the previous chapter that focus is on inferential control, i.e. product composition is controlled indirectly by controlling suitable tray temperatures, instead, since temperature measurement is usually much cheaper, faster and more reliable than concentration measurement. Key issue is the selection of suitable tray temperatures and their pairing with the available handles. For comparison with previous work [31] and the deterministic approach, the level control loops are assumed to be the same as given in Kaymak and Luyben [31]. Handles for inferential composition control are the two feed flows. Uncertain disturbances to be considered are the vapor boilup, feed composition and reflux ratio. For illustration purposes, disturbances are assumed to be step function, whose magnitude is described by normal PDFs $N(\mu_j, \sigma_j)$, $j = 1, \dots, n$, where n is the number of random disturbances acting on the column. Further, the joint normal PDF is denoted by $N(\mu, \Sigma)$, where μ is the vector of means and Σ is the covariance matrix. Assuming that all the uncertain disturbances are independent, then matrix Σ becomes equal to the diagonal matrix with variances as diagonal elements.

The problem is solved for an increasing number of uncertain disturbances for $n=1$, $n=2$ and $n=4$, according to the sequence of disturbances listed in Table 3.3. This will lead to three different cases to study the stochastic nature of the disturbances on the control system design.

- Case 1: Only VB vapor boil-up rate is considered to be uncertain with normal distribution of mean and variance as indicated in Table 3.3.
- Case 2: VB vapor boil-up rate and reflux ratio set-point (RR) are two uncertain disturbances with joint-normal distribution according to Table 3.3.
- Case 3: VB vapor boil-up rate, reflux ratio set-point (RR) and purity of the fresh feeds (Z_{0A} , Z_{0B} , i.e., presence of other reactant in the fresh feeds) are four uncertain disturbances with joint-normal distributions according to Table 3.3.

In all the cases, the expectation and the variance at the optimal solution are verified with 10000 random samples. Then the performance of the optimal control system design based on the stochastic MIDO problem is compared with the decentralized control system based on the nominal case for a deterministic disturbance of $\pm 10\%$ step change in VB described in the previous chapter and with the control system based on the heuristic approach described in Kaymak and Luyben [31].

Table 3.3: Uncertainty model - Ideal reactive distillation

Disturbance	Description	Normal Distribution (mean μ , standard deviation σ)
VB	Vapor boil-up rate	N(29.34, 8)
RR	Reflux ratio set-point	N(2.7, 0.05)
Z_{0A}	Feed concentration (F_{0A})	N(0.985, 0.005)
Z_{0B}	Feed concentration (F_{0B})	N(0.96, 0.015)

Case 1

First, we investigate the case in which the vapor boil up rate VB is considered as a step function whose magnitude follows the normal distribution with mean and variance according to Table 3.3. The GBD based sequential solution approach demands 10 minutes computation time to solve the resulting MIDO problem using the sigma point method. The expectation and the variance of the performance index for the optimal decentralized control system is compared with the specialized product Gauss formula [57] and verified with Monte Carlo random samples which are given in Table 3.4. It should be noted that the sigma point method requires only three points to estimate the expectation within 0.3% error around the random samples with 10000 observations which is shown in Fig 3.1. The optimal control structure and controller parameters are given in Table 3.5. Table 3.5 also summarizes the control structure

and the controller parameters of the heuristic approach [31] and the deterministic case for a nominal disturbance scenario of $\pm 10\%$ step change in VB (Chapter 2). The performance comparison of different control system is summarized in Table 3.6 through the statistical objective function values. For the evaluation of the statistical objective function, the sigma point method is used in all the three cases. We observe that only little improvement in the statistical objective function is noticed for the optimal control system obtained via the stochastic approach compared to the nominal case. However, the improvement in the overall performance is 50% higher than the heuristic approach. Furthermore, the performance of the optimal decentralized control system based on the stochastic approach is compared with a multivariable controller, which is given in Table 3.6. It is worth noting that not much improvement was found for a multivariable controller.

Table 3.4: The expectation and the variance of the performance index for the optimal decentralized control system for case 1

Method	No.of points	$E[J]$	$\sqrt{V[J]}$
Sigma point	3	3142	4275
Specialized product Gauss Formula [57]	3	3142	4275
Random samples (MC)	10000	3150	4290

Table 3.5: Decentralized control structure and controller parameters

Design method	Control Structure	Controller parameters (kp, τ_I)
Heuristic method	$F_{0A} - T_2$	0.95, 12.8 min
	$F_{0B} - T_{12}$	8.78, 16.8 min
Nominal case	$F_{0A} - T_3$	0.6, 10.6 min
	$F_{0B} - T_{12}$	4.5, 14.0 min
Stochastic approach (Case 1)	$F_{0A} - T_3$	0.8, 14 min
	$F_{0B} - T_{13}$	4.14, 12 min
Stochastic approach (Case 2)	$F_{0A} - T_1$	0.8, 24 min
	$F_{0B} - T_{14}$	3.5, 27 min
Stochastic approach (Case 3)	$F_{0A} - T_1$	0.92, 12 min
	$F_{0B} - T_{13}$	4.8, 13 min

Table 3.6: Performance comparison of different control system for case 1

Controller Type	Expectation $E[J]$	Statistical objective function $\Phi = E[J] + \omega\sqrt{V[J]}$
Multivariable controller (Stochastic approach)	3035	4916
Decentralized controller (Stochastic approach)	3142	5279
Decentralized controller (Nominal case)	3271	5859
Decentralized controller (Heuristic approach)	4201	6845

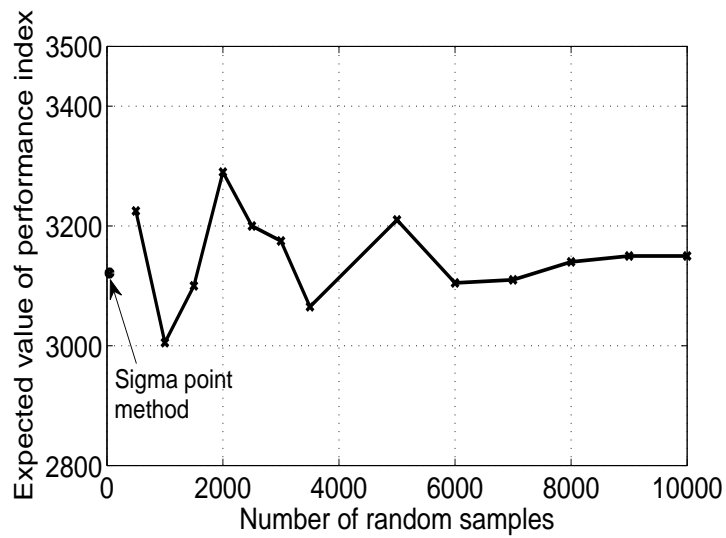


Figure 3.1: Expected value of the performance index: MC samples vs Sigma Point method - Case 1

Case 2

In case 2, the vapor boil-up rate VB and the reflux ratio set-point RR are two uncertain disturbances acting on the column. Since, we consider these two uncertain disturbances as independent, the covariance matrix is the diagonal matrix with variances as diagonal elements. Further, the location of the sigma points and random samples are shown in Fig 3.2 for the corresponding mean and covariance. The resulting MIDO problem using the sigma point method demands 30 minutes of computation time to find the optimal control structure and controller parameters using the GBD based sequential solution approach. Table 3.5 shows the optimal temperature control loops and controller parameters. The expectation and the variance of the performance index for the optimal decentralized control system is compared with the specialized product Gauss formula [57] and verified with random samples which are given in Table 3.7. It is worthwhile to mention that the sigma point method requires a minimum number of 5 points compared to 9 grid points of the specialized product Gauss formula to estimate the expectation within 0.7% error around the random samples with 10000 observations which is shown in Fig 3.3.

Table 3.8 gives a comparison of the stochastic approach, the heuristic approach and the deterministic approach for a nominal disturbance of VB of $\pm 10\%$ in terms of the statistical objective function value. In the stochastic approach, it is shown that the optimal control systems have superior performance compared to the nominal case and the heuristic method. Further, the closed loop performance of the different decentralized control system is compared qualitatively by giving the disturbances such as $\pm 20\%$ step change in the vapor boil up VB and $\pm 4\%$ step change in the reflux ratio set-point (RR). The performance of the decentralized control system from the stochastic MIDO problem is shown for a $\pm 20\%$ step change in VB in Fig 3.4(a) and for a $\pm 4\%$ step change in the reflux ratio RR in Fig 3.4(b). The system is stable, and the distillate and bottoms purities are well controlled within the specification limit of 94%. For the control system obtained via the nominal case and the heuristic method, the response to a $\pm 20\%$ change in VB is shown in Fig 3.5(a) and 3.6(a) respectively. The system is stable, however we observed some oscillatory behavior in the manipulated variable movement and the behavior is even worse in terms of the overshoot for the heuristic method. Furthermore, the response to a $\pm 4\%$ change in the reflux ratio set-point RR is shown in Fig 3.5(b) and Fig 3.6(b) for the nominal case and the heuristic method, respectively. Here, we observed that the distillate purity is not well controlled and falls below the specification limit of 94%. By comparing these different control system we conclude that the closed loop dynamics is improved by considering

Table 3.7: The expectation and the variance of the performance index for the optimal decentralized control system for case 2

Method	No.of points	$E[J]$	$\sqrt{V[J]}$
Sigma point	5	7808	5558
Specialized product Gauss Formula	9	7812	7221
Random samples (MC)	10000	7879	6250

Table 3.8: Performance comparison of different control system for case 2

Controller Type	Expectation $E[J]$	Statistical objective function $\Phi = E[J] + \omega\sqrt{V[J]}$
Multivariable controller (Stochastic approach)	7460	10205
Decentralized controller (Stochastic approach)	7808	10587
Decentralized controller (Nominal case)	14509	20290
Decentralized controller (Heuristic approach)	15948	24540

the disturbance uncertainty in the optimal control system design compared to the nominal case and the heuristic method.

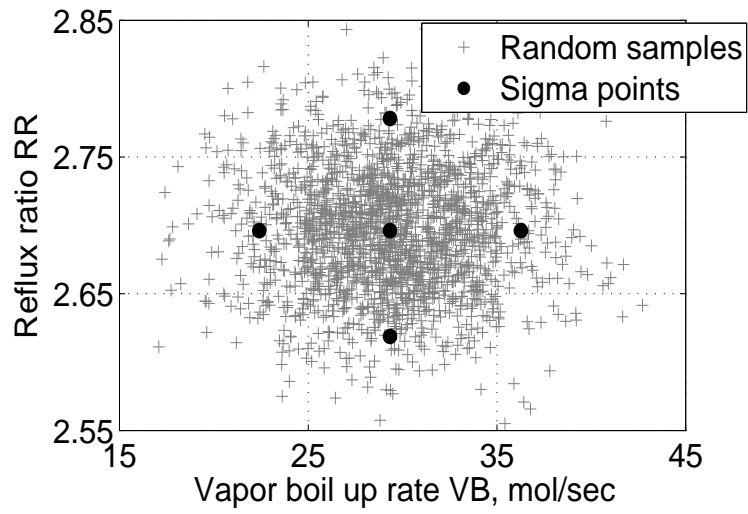


Figure 3.2: Location of the sigma points and random samples for calculating the mean and variance of the performance index - Case 2

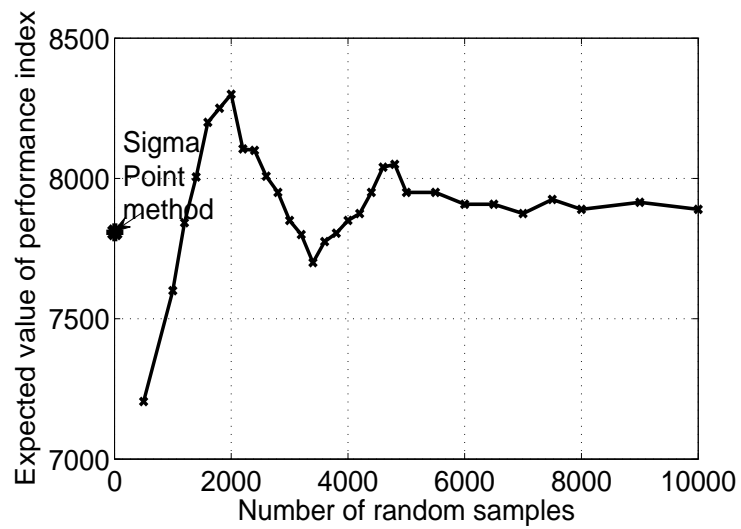


Figure 3.3: Expected value of the performance index: random samples vs sigma point method - case 2

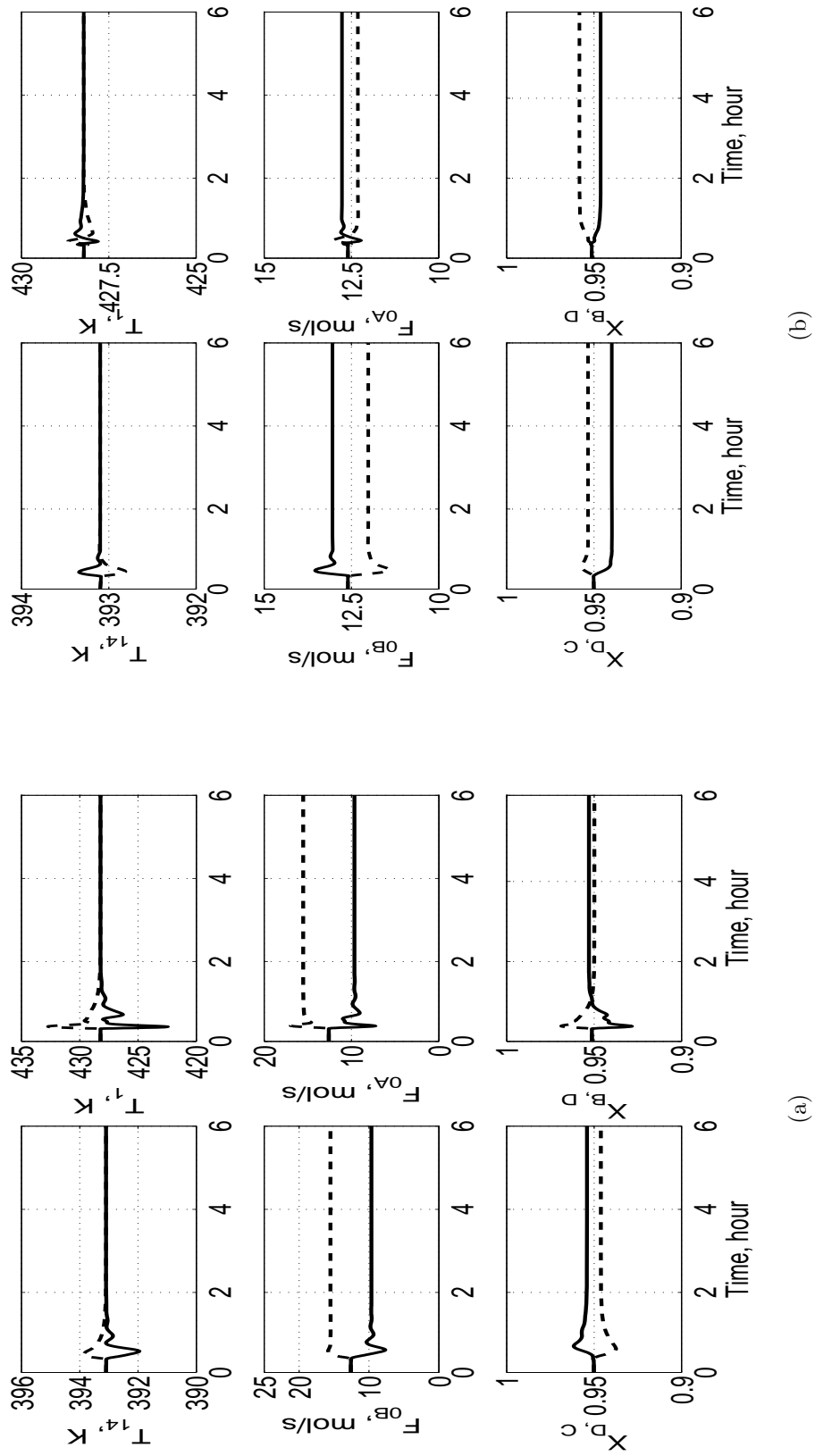


Figure 3.4: Closed loop response of the optimal decentralized control system - case 2 (stochastic approach): (a) $\pm 20\%$ step change in VB (solid line, -20% of VB; dashed line, $+20\%$ of VB); (b) $\pm 4\%$ step change in the reflux ratio (solid line, $+4\%$ of RR; dashed line, -4% of RR)

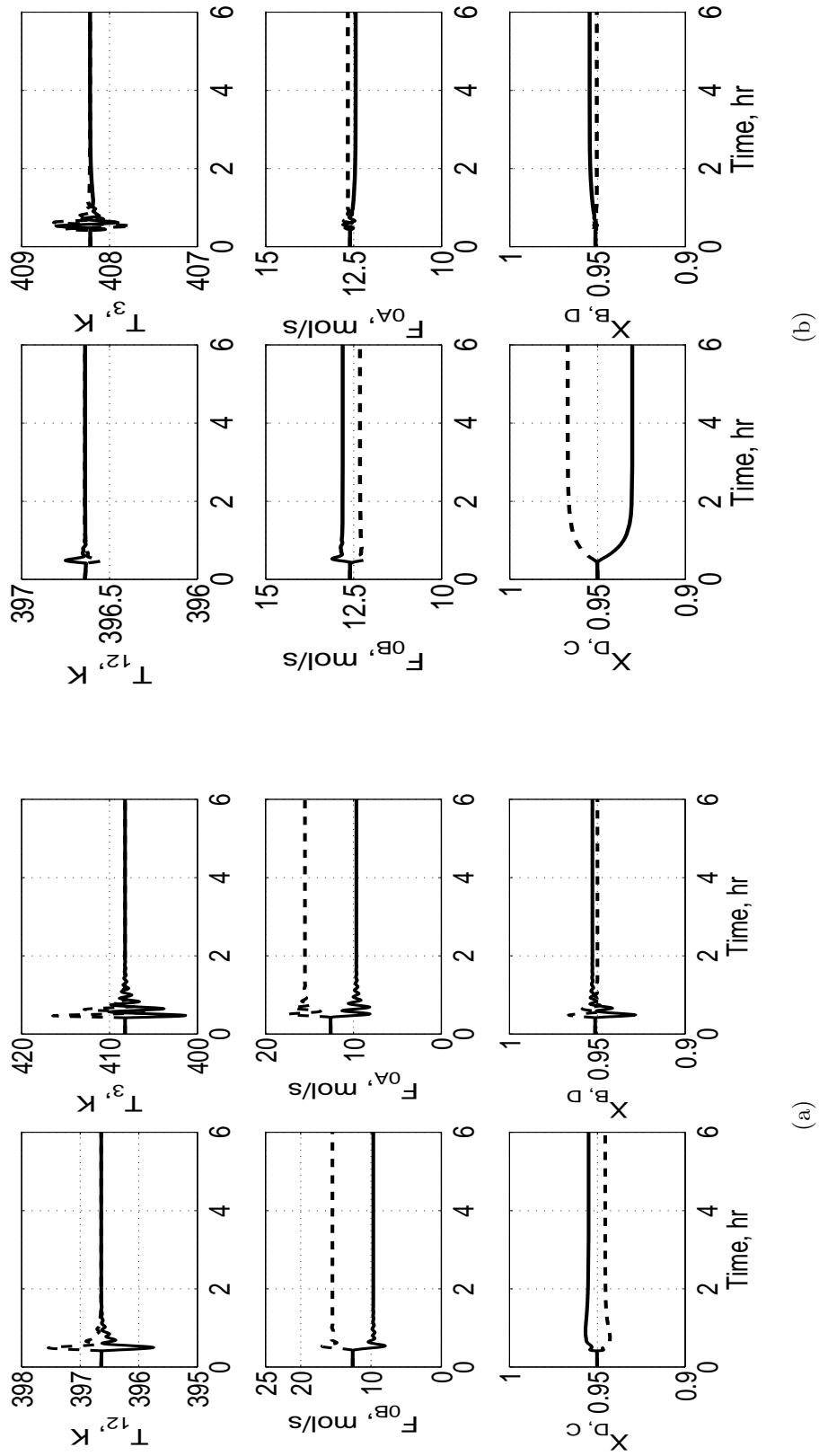


Figure 3.5: Closed loop response of the decentralized control system (nominal case): (a) $\pm 20\%$ step change in VB (solid line, -20% of VB; dashed line, $+20\%$ of VB); (b) $\pm 4\%$ step change in the reflux ratio (solid line, $+4\%$ of RR; dashed line, -4% of RR)

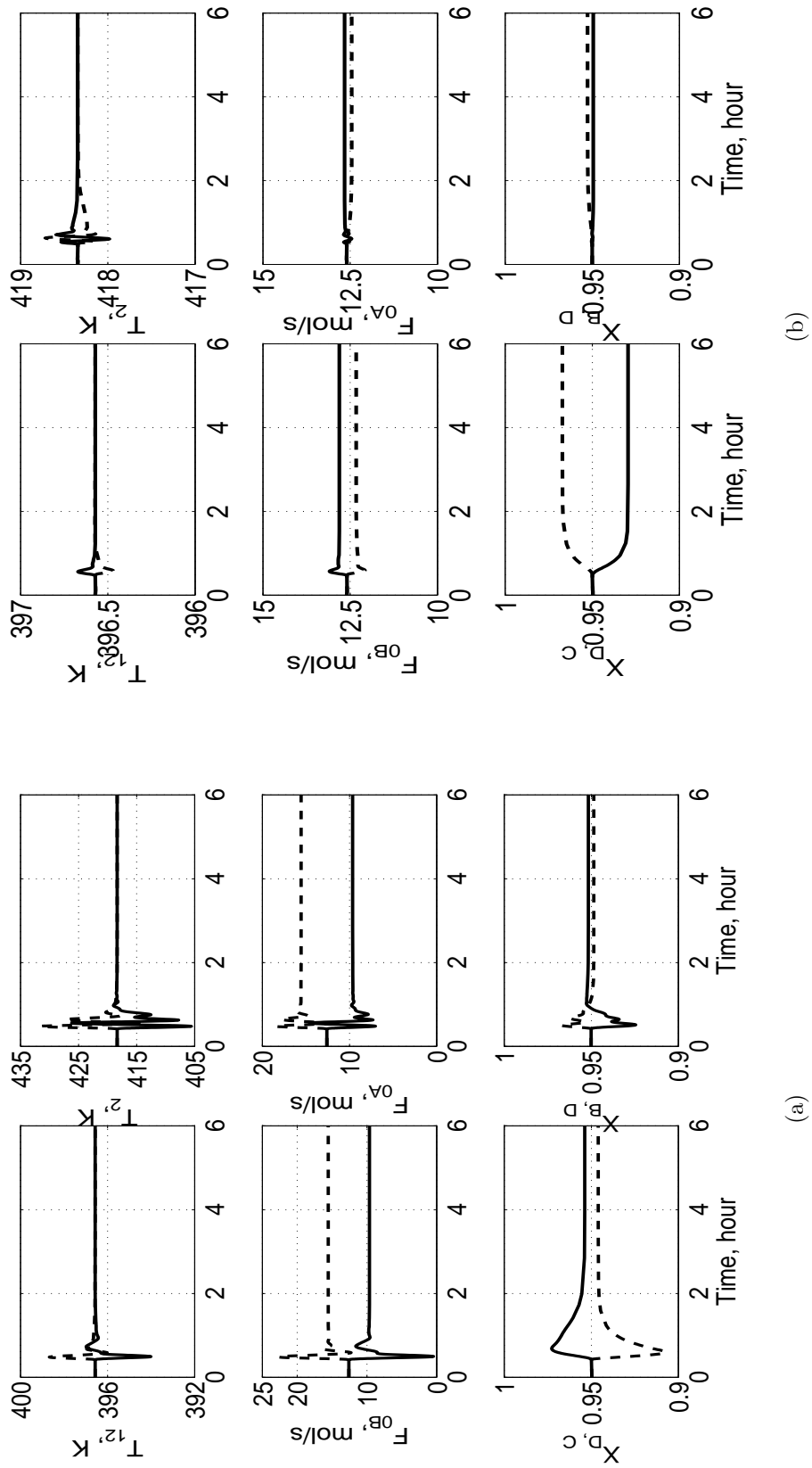


Figure 3.6: Closed loop response of the decentralized control system (heuristic method): (a) $\pm 20\%$ step change in VB (solid line, -20% of VB; dashed line, +4% of RR); (b) $\pm 4\%$ step change in the reflux ratio (solid line, +4% of RR; dashed line, -4% of RR)

Case 3

In case 3, the vapor boil-up rate VB, the reflux ratio set-point RR and purity of the fresh feeds (i.e., presence of other reactant in the fresh feed) are four uncertain disturbances acting on the column. The magnitude of these step disturbances follows the joint normal PDF with mean and covariance according to Table 3.3. The GBD based sequential solution approach demands 75 minutes of computation time using the sigma point method, since the complexity of the resulting MIDO problem is increased with the number of uncertain disturbances. The optimal control structure and controller parameters are summarized in Table 3.5 which are different from the other two cases as well as the heuristic method and the nominal case. The expectation and the variance of the performance index at the optimal decentralized control system is compared with specialized cubature formula [57] and verified with random samples which are given in Table 3.9. Here, we use the specialized cubature formula for comparison purpose in stead of the specialized product Gauss formula due to the fact that it is the choice of a suitable numerical integration method for $3 \leq n \leq 7$ [57]. However, it requires 24 number of grid points which is higher than that of the sigma point method. Further, the sigma point method estimates the expectation within 0.8% error around the random samples with 10000 observations which is shown in Fig 3.7. Like the previous cases, the optimal decentralized control system from the stochastic approach has superior performance compared to the heuristic method and the nominal case which is shown in Table 3.10 through the statistical objective function value. Further, we observed in this case also that not much improvement was found for a multivariable controller compared to the decentralized control system.

Table 3.9: The expectation and the variance of the performance index for the optimal decentralized control system for case 3

Method	No.of points	$E[J]$	$\sqrt{V[J]}$
Sigma point	9	16302	13506
Specialized cubature Formula	24	17884	16580
Random samples (MC)	10000	16030	12517

Table 3.10: Performance comparison of different control system for case 3

Controller Type	Expectation $E[J]$	Statistical objective function $\Phi = E[J] + \omega\sqrt{V[J]}$
Multivariable controller (Stochastic approach)	15278	21563
Decentralized controller (Stochastic approach)	16302	23055
Decentralized controller (Nominal case)	24895	34240
Decentralized controller (Heuristic approach)	26302	48629

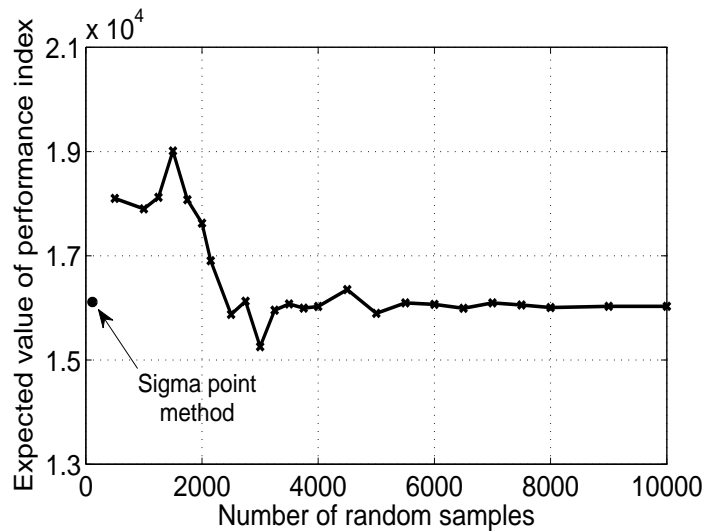


Figure 3.7: Expected value of the performance index: random samples vs sigma point method - case 3

3.5 Summary

A systematic framework for simultaneous selection of a decentralized control structure and controller parameters under uncertainty has been presented in this chapter. This leads to a MIDO problem under uncertainty. Application of the sigma point

method is proposed in order to approximate the expectation and the variance of the performance index to solve the MIDO problem under uncertainty. Successful application of the proposed methodology was demonstrated for the inferential control of an ideal reactive distillation column. Further, it was illustrated that the resulting control systems have superior performance compared to the standard heuristic method and the deterministic optimization. Furthermore, the sigma point method requires more computational effort than the deterministic optimization. However, it yields better results in the control system design for the collection of disturbance scenarios, in particular, when the spectrum of disturbances is broad or multidimensional.

In the present study, focus was on step disturbances with a normal probability distribution of the magnitudes. However, it is worth mentioning that any other kind of disturbances also with non-normal probability distributions can be handled with the sigma point method. In practice, realistic disturbance scenarios can be obtained from a statistical analysis of the recorded data. Further, in the present work focus was an uncertainty in the disturbance scenarios. It is worth noting, that parametric model uncertainty in the present problem formulation can be treated in a completely analogous way.

Chapter 4

Control of a ternary reactive distillation with inert

4.1 Introduction

Control studies of reactive distillation columns have explored a variety of chemical reactions, flowsheets, and control structures (Chapter 10 in Sundmacher and Kienle [1], book by Luyben and Yu [2] and references therein). Main focus was on quaternary reaction systems such as esterifications. Despite its practical importance relatively little attention was given to ternary reaction systems of type:



Typical examples are etherification systems [1] like methyl *tert*-butyl ether (MTBE), ethyl *tert*-butyl ether (ETBE) or *tert*-amyl methyl ether (TAME), where an alcohol reacts with an *iso*-olefin to the corresponding tertiary ether, which is obtained as the desired product at one end of the column. Often, in addition other nonreactive olefins are present, which are separated simultaneously and obtained with high purity in the other product stream.

Recently, Luyben [34] provided a systematic control study of such a ternary system with inert. To alleviate the analysis, focus was on an idealized benchmark problem and established heuristic procedures for decentralized control system design were applied. In this approach, first, a suitable control structure is selected using steady state sensitivities and singular value decomposition (SVD) analysis. Afterwards, relay feedback testing is applied for the determination of the control parameters. Using this approach it was concluded, that tight control of product purities is not possible

with inferential control using only temperature measurements. Large deviations of the product purities were observed during a $\pm 20\%$ change of the vapor flow rate which was used as a production rate handle. It was concluded that additional composition measurement is required to achieve good control of the product purities.

More recently, Kaymak et al [64] have provided an extended control study for this system using the same methodology in control system design, considering however an optimized process design. For the modified design, a modified inferential control system was presented, which could handle a $\pm 20\%$ change of the vapor flow rate and a $\pm 3\%$ change of the reactant feed concentration reasonably well. Disturbances of the inert concentration in the feed, which are usually more challenging for this process were not presented.

In this chapter, the original problem formulation and design as introduced by Luyben [34] is considered. Control system design is done more rigorously using mixed integer dynamic optimization. In a first step, a deterministic MIDO formulation is applied for a nominal disturbance of $\pm 20\%$ change of the vapor flow rate. It is shown, that for nominal disturbances in contrast to the heuristic approach inferential control with good performance of the product concentrations can be achieved in a systematic way with this approach. However, it is found that robustness of the proposed control system is poor in view of critical inert feed disturbances. To also account for robustness, an extended stochastic problem formulation is introduced and is further extended step by step. Through this significant improvements of robustness are observed and it is concluded that inferential control of ternary reactive distillation with inert is feasible.

4.2 Benchmark problem: Ternary RD column with inert

Focus is on a ternary reaction system with inert of type Eq. 4.1. Chemical kinetics, physical properties and steady state operating conditions are taken from Table 4 of the paper by Luyben [34]. The fresh feed stream F_{0A} is a mixture of reactant A and an inert component I, which is not involved in the reaction. The volatility of I is assumed to be identical to that of A, so both of these components are lighter than the other reactant B and the product C. The composition of this feed stream $Z_{0A(j)}$ is a 50/50 mixture of reactant A and chemically inert I.

The heavy product C is removed from the bottom with some impurities of the other components (mostly B). Because the inert component I has the same volatility as the low-boiling component A, it is removed from the column in the distillate stream.

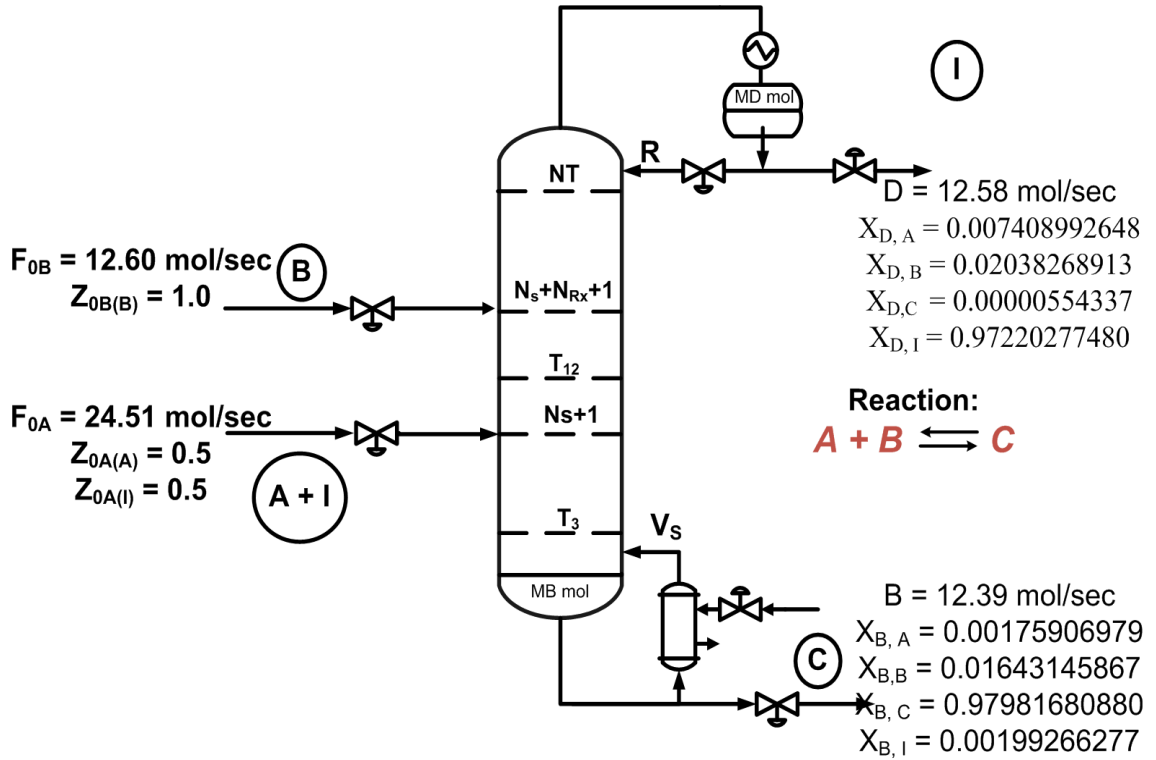


Figure 4.1: Flowsheet for a ternary reactive distillation column with inerts

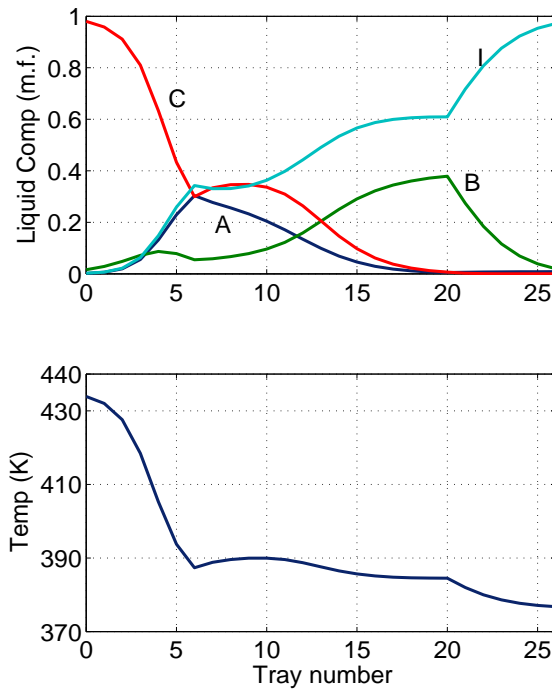


Figure 4.2: Steady state composition and temperature profile

Table 4.1: Control structure and PI controller parameters - nominal case

	Control structure	kp	τ_I (min)
Heuristic method	$F_{0A} - T_5$	1.6	6.6
	$F_{0B} - T_{13}$	2.8	100.0
Algorithmic approach (MIDO)	$F_{0A} - T_4$	0.65	6.0
	$F_{0B} - T_{19}$	2.0	24.0

Column configuration and steady state profiles are shown in Figure 4.1 and 4.2 respectively¹. The reactive distillation column has three zones. There are 5 stripping trays, 15 reactive trays, and 5 rectifying trays. The liquid holdup on the reactive trays is 2000 mol. The holdups in the column base and reflux drum are 23.2 kmol and 24.8 kmol respectively.

For comparison, the control system proposed by Luyben [34] is briefly introduced. First, the following control loops are assumed:

1. V_s - vapor boil up rate is used as the production rate control (flow control)
2. Reflux ratio is maintained by manipulating the reflux flow rate (ratio control)
3. Reflux drum level is controlled by manipulating the distillate flow (level control)
4. Column base level is controlled by manipulating the bottom flow (level control)

Since focus is on inferential control, i.e. temperature instead of composition measurements are used for product composition control; the selection of trays for temperature control loops is a key issue. Luyben [34] used the steady state gain and SVD analysis to choose the trays for temperature control and then proportional-integral (PI) controllers are designed based on the Tyreus-Luyben tuning rules [56]. The control structure and the PI controller parameters considered by Luyben [34] are given in Table 4.1. This control structure was tested with a specific disturbance scenario i.e., a $\pm 20\%$ step change in the vapor boil up rate V_s . The closed loop performance of this control system is given in Figure 4.3 for a $+20\%$ step change in V_s and in Figure 4.4 for a -20% step change in V_s . Here, this control system provides a stable control

¹For simplicity, slightly different values of the volatilities of 4, 2, 1 and 4 for components A, B, C and I respectively were used instead of 3.9749, 1.9937, 1.0 and 3.9749 in Luyben's paper [34] leading to slightly different values of V_s of 64.55 instead of 65.1 in Luyben's paper [34] and the reflux flow of 69.45 instead of 70.0 in Luyben's paper [34]. However, concentration and temperature profiles are similar to the paper by Luyben [34].

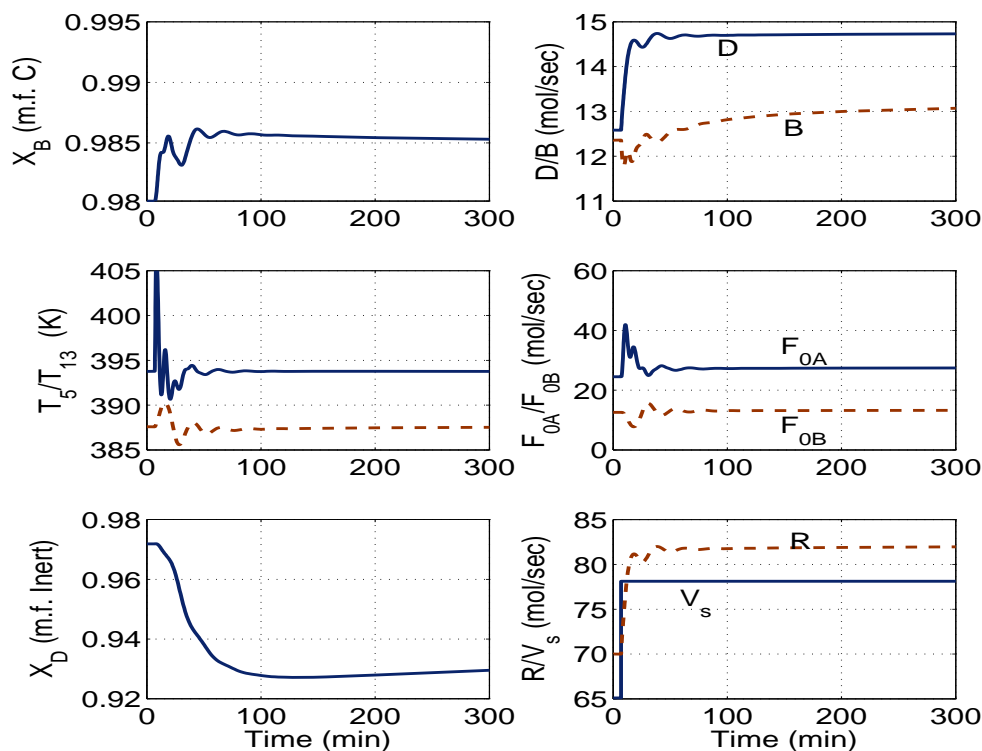


Figure 4.3: Closed loop response for a +20% change in the vapor boil up V_s - Heuristic method

for both positive and negative 20% step change in V_s . Although, the selected tray temperatures are settling quickly to their setpoints, large deviations in the bottoms purity and distillate purity from the desired specifications are observed. For a +20% change in V_s , the distillate composition decreases to 92 mol% of inert. For a -20% change in V_s , the bottoms composition decreases to 76 mol % of C and the distillate composition decreases to 96 mol% of inert. Therefore, it was concluded by Luyben [34] that the inferential control scheme is not feasible for a ternary system with inert.

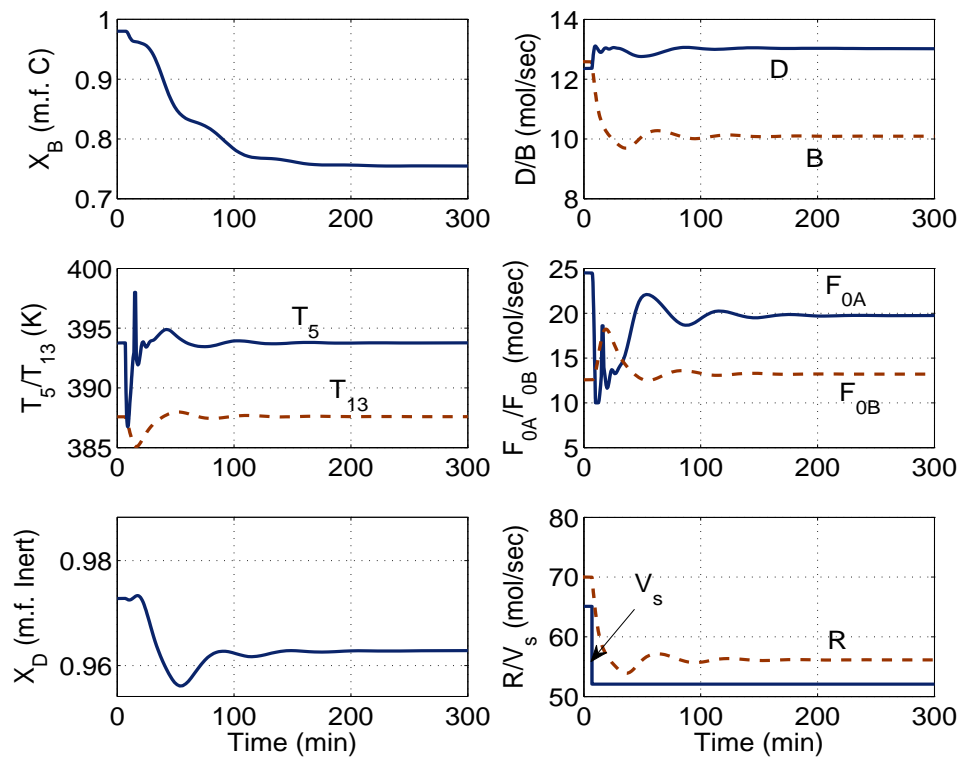


Figure 4.4: Closed loop response for a -20% change in the vapor boil up V_s - Heuristic method

4.3 Control system design : Deterministic MIDO approach

Formulation II (i.e. maximize the overall performance) is considered here to find the optimal control structure and controller parameters simultaneously. The sequential solution approach based on the GBD is considered to solve the complex MIDO problem of formulation II. Further, Q and R weighting matrices are calculated based on the inverse of the square of steady state values in order to calculate the objective function (Eq. 2.21). Further, the control error in the distillate and bottoms purities from their desired specifications is also included in the objective function along with the tray temperatures as the output variables. Since, we noticed that the offset in the distillate and bottoms purities from the desired setpoint is very large in the heuristic method, the corresponding weights are multiplied by the factor of 100. This will lead to an optimal control structure and controller parameters with only small offset in the product purities.

The selection of two-temperature control loops from 25 tray temperature measurements and their combination with 2 manipulated variables has 600 numbers of possible combinations. Due to the underlying assumptions of the control loops mentioned in the previous section, the problem has still moderate complexity but manual enumeration is not feasible. Further, the disturbance scenario which is considered in the heuristic method is adopted as a specific disturbance in the MIDO problem, i.e., a $\pm 20\%$ step change in the vapor boil up rate V_s . The optimal control structure and controller parameters are reported in Table 4.1, which are different from the heuristic method. The closed loop performance of this control system is given in Figure 4.5 for a $+20\%$ step change in V_s and in Figure 4.6 for a -20% step change in V_s . The system is stable, further the bottoms and distillate purities are well controlled. Further, the selected tray temperatures as controlled variables are maintained at their set-points by smooth manipulation of the inputs. These results demonstrate that a feasible inferential control scheme is found using the deterministic MIDO approach for rejecting the disturbance in V_s as a production rate control.

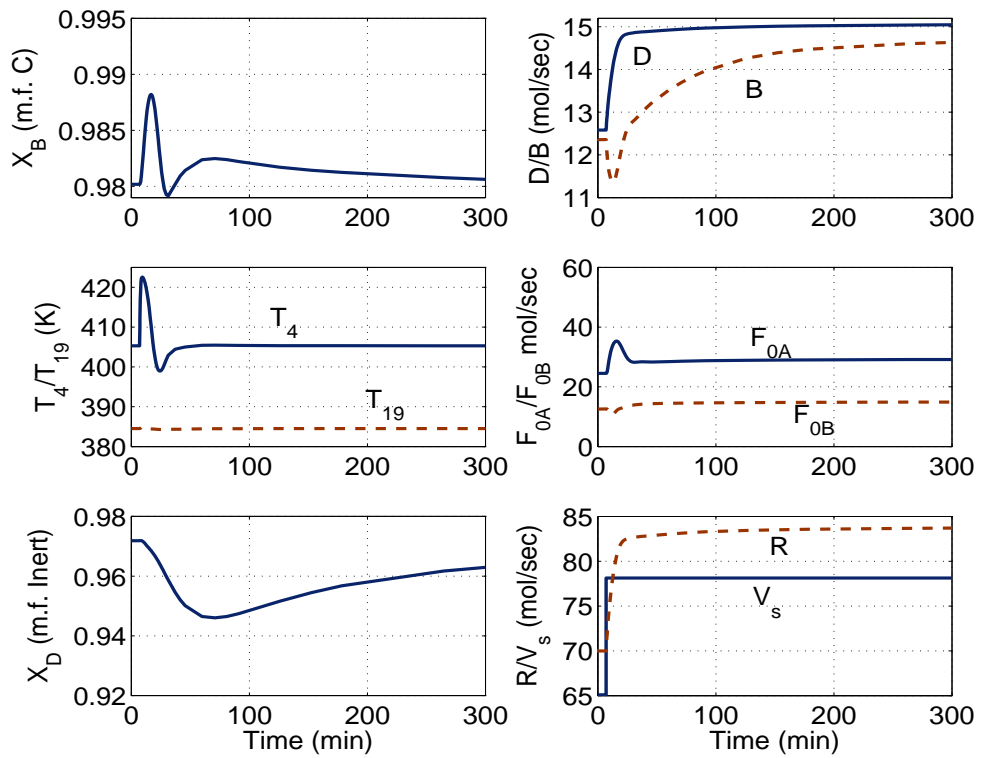


Figure 4.5: Closed loop response for a +20% step change of the vapor boil up V_s - Deterministic MIDO approach

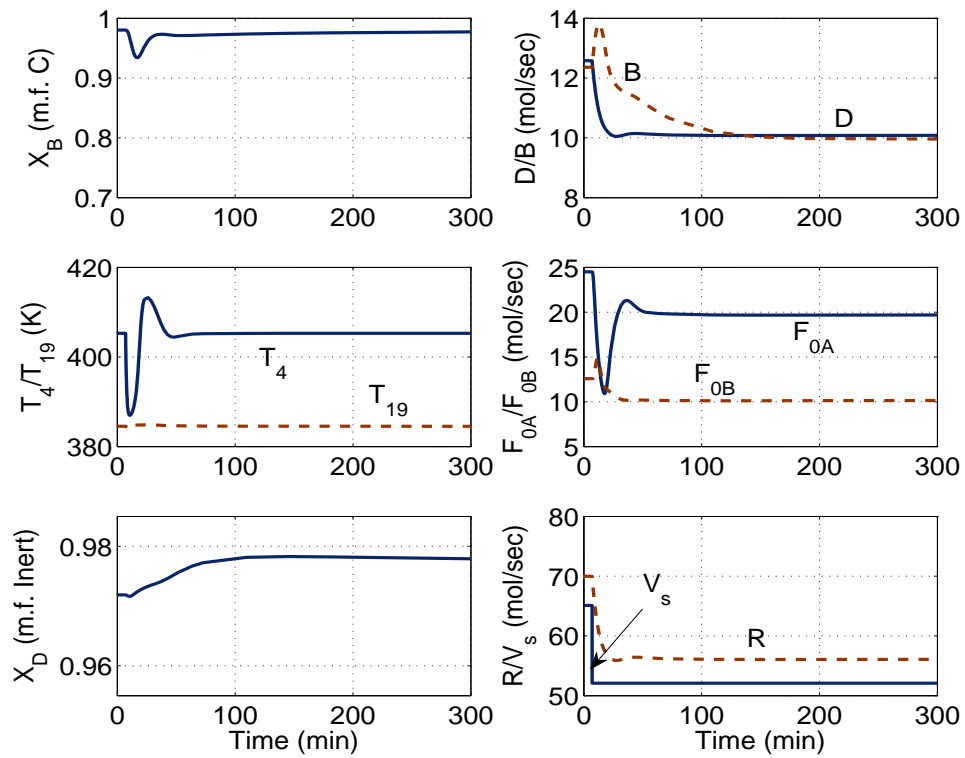


Figure 4.6: Closed loop response for a -20% step change of the vapor boil up V_s - Deterministic MIDO approach

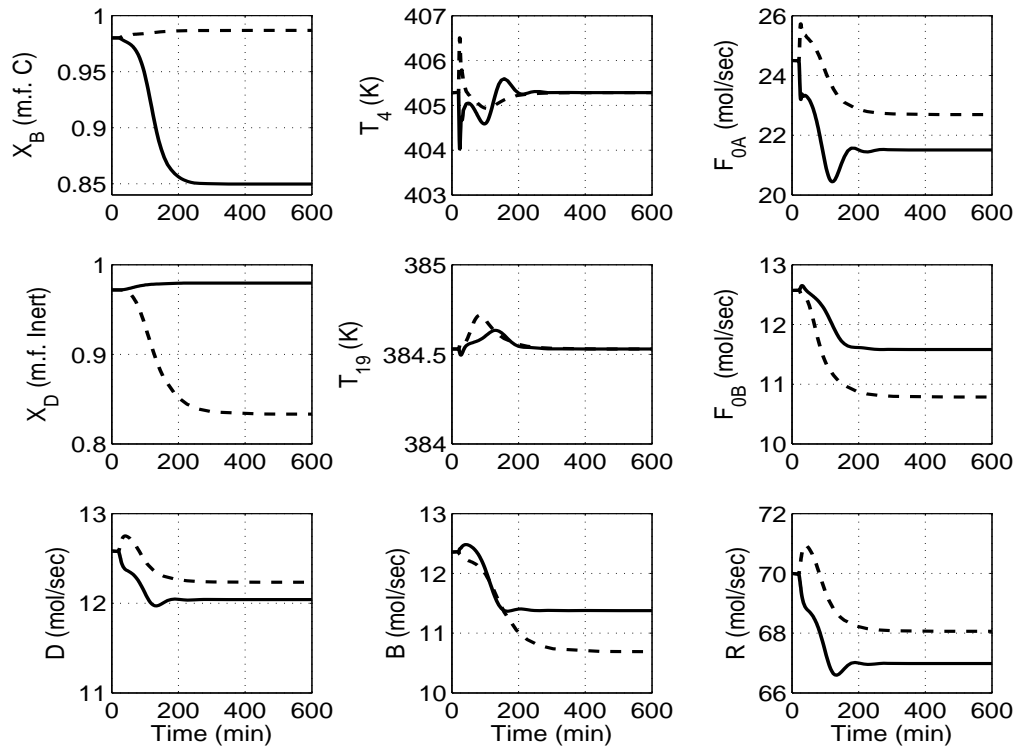


Figure 4.7: Closed loop response for a $\pm 10\%$ step change of the inert concentration $Z_{0A(I)}$ in the feed F_{0A} - Deterministic MIDO approach (solid line, $Z_{0A(I)} = 0.55$; dashed line, $Z_{0A(I)} = 0.45$)

Further, the optimal control system is achieved for a reference test scenario, i.e., a $\pm 20\%$ step change in V_s . However, the resulting optimal control system may not perform well for the other kind of disturbances. For example, Figure 4.7 shows the performance of this optimal control system for a $\pm 10\%$ step change in the inert concentration of the feed F_{0A} . The system is stable, however large offsets in the bottoms and distillate purities are observed. To overcome this problem, disturbance of the inert concentration should be explicitly taken into account when designing the control system. This is done using a stochastic approach which is following in the next section.

4.4 Control system design: Stochastic MIDO approach

In the previous section, the optimal control structure and controller parameters are achieved for a specific disturbance scenario, i.e., a $\pm 20\%$ step change in V_s . However, due to nonlinearity the optimal control structure and the optimal controller parameters will differ for different disturbance scenarios. To find an optimal compromise, a stochastic approach is applied where the disturbances are modeled using multivariate probability distributions. For illustration purposes, disturbances are assumed to be step functions, whose magnitude is described by normal probability distribution function. Consequently, the performance index considered in the deterministic MIDO approach becomes a stochastic quantity. Therefore, the statistical objective function which is formulated in the previous chapter by its mean and variance is given by:

$$\Phi = E[J] + \omega \sqrt{V[J]} \quad (4.2)$$

It has been shown in the previous chapter that the sigma point method gives a good approximation for the mean and variance with reasonable effort. With the help of the sigma point method, the stochastic MIDO problem is converted into a deterministic one, which can be solved using the GBD based sequential solution approach (see Chapter 3).

In the present benchmark problem, uncertain disturbances to be considered are the setpoint for the production rate control loop and the inert concentration of the feed F_{0A} . Here, three different cases are presented in order to improve the controllability with respect to the offset in the product purities.

4.4.1 Case 1

In this case, the vapor boil-up rate V_s and the inert concentration of the feed F_{0A} are two uncertain disturbances acting on the column. Hence, handles for inferential composition control are the two reactant feed flows F_{0A} and F_{0B} . The uncertain disturbances follow a joint normal distribution with mean and covariance:

$$\mu = \begin{bmatrix} V_s \\ Z_{0A(I)} \end{bmatrix} = \begin{bmatrix} 64.55 \\ 0.5 \end{bmatrix} \quad (4.3)$$

$$\Sigma = \begin{bmatrix} 64.0 & 0.0 \\ 0.0 & 0.001 \end{bmatrix} \quad (4.4)$$

Table 4.2: Control structure and PI controller parameters - Stochastic MIDO approach

	Control structure		PI parameters	Statistical objective function
Case 1	Production rate control Temperature control loops	V_s $F_{0A} - T_4$ $F_{0B} - T_{19}$	$k_p = 1.1; \tau_I = 15.0 \text{ min}$ $k_p = 2.8; \tau_I = 35.0 \text{ min}$	49668
Case 2	Production rate control Temperature control loops	F_{0B} $F_{0A} - T_7$ $V_s - T_2$	$k_p = 1.1; \tau_I = 11.5 \text{ min}$ $k_p = 0.46; \tau_I = 13.0 \text{ min}$	22088
Case 3	Production rate control Temperature control loops	F_{0B} $F_{0A} - T_7$ $V_s - T_3$ $R - T_{14}$	$k_p = 1.0; \tau_I = 12.5 \text{ min}$ $k_p = 0.6; \tau_I = 15.0 \text{ min}$ $k_p = 1.5; \tau_I = 20.0 \text{ min}$	3325

Then, the resulting stochastic MIDO problem is converted to the deterministic problem using the sigma point method and solved for the optimal control structure and controller parameters. The optimal control structure and controller parameters are given in Table 4.2. It should be noted that the optimal control structure is the same as in the deterministic MIDO approach, however the controller parameters are different. This control system is tested with $\pm 20\%$ step change in the vapor boil up rate V_s and $\pm 10\%$ step change in the inert concentration of the feed F_{0A} . Although, this control system provides effective control for the disturbance of V_s , it does not provide the effective control for the change in the inert concentration. Hence, large offsets in the bottoms and distillate purities are still observed for the change in the inert concentration.

These results illustrate that robust control may not be feasible with the underlying assumption of the handles for the temperature control loops. In this case, handles for inferential composition control are the two reactant feed flows. Therefore, we consider two different cases in order to design an optimal compromise for the control structure and controller parameters by means of relaxing the assumption on the control loops. These cases will be discussed subsequently.

4.4.2 Case 2

In the control of RD columns, one of the input streams F_{0A} , F_{0B} and V_s can be used as a production rate control and the remaining two input streams can be used as the manipulated variables for a two-temperature control. In the previous case and the deterministic MIDO approach, we assumed V_s as the production rate control in order to compare the results with previous studies. In the present case, this assumption will be relaxed. Therefore, additional binary variables are considered to select one of the input stream for the production rate control loop along with the binary variables for selecting the temperature control loops. Further, the setpoint for the production rate control and the inert concentration of the F_{0A} feed stream are considered as a step function whose magnitude follows the normal distribution with the mean and the covariance as:

$$\mu = \begin{bmatrix} \Delta PR_{sp} \\ Z_{0A(I)} \end{bmatrix} = \begin{bmatrix} 0.0 \\ 0.5 \end{bmatrix} \quad (4.5)$$

$$\Sigma = \begin{bmatrix} 0.015 & 0.0 \\ 0.0 & 0.001 \end{bmatrix} \quad (4.6)$$

ΔPR_{sp} is the change of the set-point for the production rate. Here, the set-point for the production rate control is modeled as the percentage of deviation from the normal operating conditions. For example, if one of the reactant feed F_{0A} is selected for the production rate control loop, then the step function in the F_{0A} is given by $F_{0A}(t) = (1 + \Delta PR_{sp})F_{0A,steady}$. The resulting MIDO problem using the sigma point method is successfully solved for the optimal control structure and controller parameters which are given in Table 4.2.

The optimal control system in this case is different from the previous case. Here, one of the reactant feed stream F_{0B} is selected for the production rate control. Further, the feed F_{0A} and the vapor boil up rate V_s are used as the manipulated variables for controlling two tray temperatures T_7 and T_2 respectively. The performance of this control system is better than in the previous case which can be seen from the statistical objective function values. Further, the closed loop performance of this control system is investigated with $\pm 20\%$ step change in the feed F_{0B} and $\pm 10\%$ step change in the inert concentration of the feed F_{0A} .

Figure 4.8 shows the performance of this control system for the step change in the feed F_{0B} . The system is stable and both tray temperatures are controlled at their

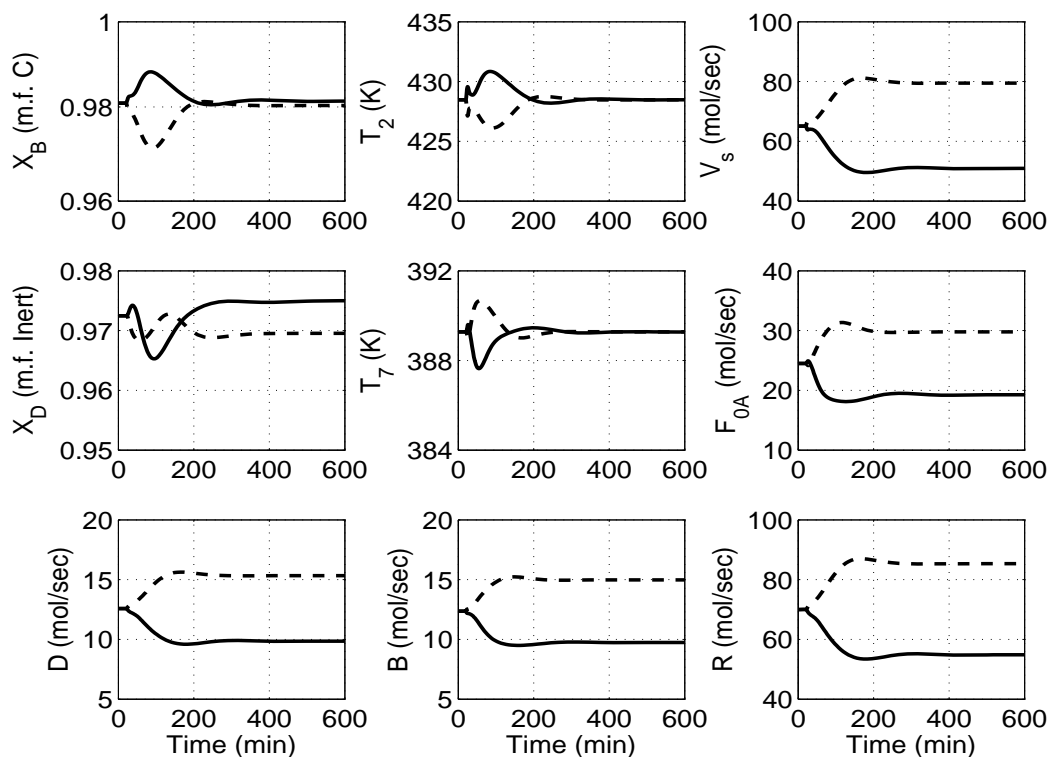


Figure 4.8: Closed loop response for a $\pm 20\%$ step change of the feed F_{0B} - Stochastic MIDO approach (case 2)
(solid line, -20% ; dashed line, $+20\%$)

setpoints. Further, the bottoms and distillate purities are well controlled. Figure 4.9 shows the performance of this control system for the step change in the inert concentration of the feed F_{0A} . Here, the bottoms and distillate compositions are well controlled for a 10% increase in the inert concentration, and at the same time distillate purity is decreased to 87% for a 10% decrease in the inert concentration of the feed F_{0A} . This indicates a change in conversion and loss of reactants. However, the bottoms purity is well maintained around the required specification.

It is worthwhile to mention about this control system that the handles for the temperature control loops are the feed F_{0A} and the vapor boil up rate V_s which are similar to the control structure studied by Kaymak et al.[64] In the present study, this control system provides a stable regulatory control, but the offset in the distillate purity is still existing for decreasing the inert concentration of the feed F_{0A} .

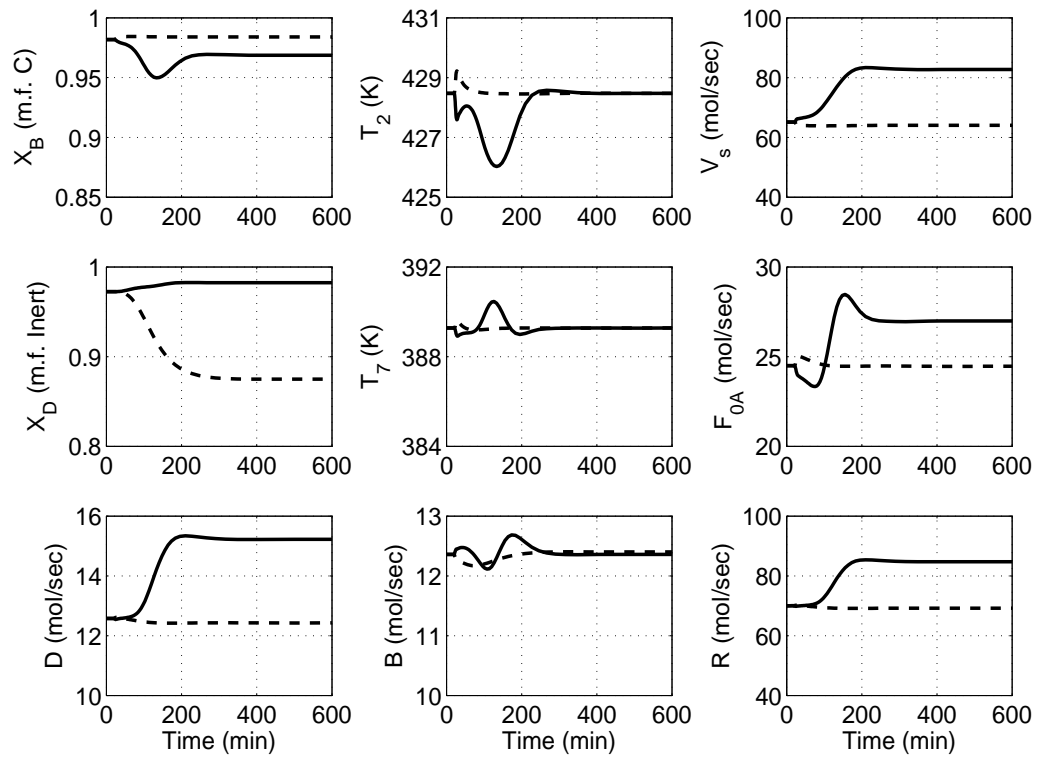


Figure 4.9: Closed loop response for a $\pm 10\%$ step change of the inert concentration $Z_{0A(I)}$ in the feed F_{0A} - Stochastic MIDO approach (case 2) (solid line, $Z_{0A(I)} = 0.55$; dashed line, $Z_{0A(I)} = 0.45$)

4.4.3 Case 3

In the previous case, a two-temperature control structure is considered. Further, it is observed that the resulting optimal control system provides the offset in the distillate purity for the disturbance of a decrease in the inert concentration. However, this offset can further be reduced by using an additional tray temperature control loop. This leads to a three-point temperature control structure which had been demonstrated in the quaternary system in the literature [65]. However, the selection of tray temperature measurements and pairing with available handles will be a more complex task due to the combinatorial complexity.

In this case, only level controllers are assumed to be the same as in the heuristic method. Therefore, the reflux flow rate can be used either to maintain the reflux ratio or can be used as a manipulated variable for a three-point temperature control structure. The corresponding binary variables with suitable constraints are added into the MIDO formulation in order to account for a three-point temperature control. Further, the mean and the covariance of the random disturbances are the same as the previous case. The resulting MIDO problem using the sigma point method is successfully solved for the optimal control structure and controller parameters which are given in Table 4.2.

Here, one of the reactant feed stream F_{0B} is selected for the production rate control. The feed F_{0A} , the vapor boil up rate V_s and the reflux flow rate R are used as the manipulated variables for controlling three tray temperatures T_7 , T_3 and T_{14} respectively. The performance of this control system is improved significantly compared to earlier cases, which can be seen through the statistical objective function value. The closed loop response for a $\pm 20\%$ step change in the feed F_{0B} and $\pm 10\%$ step change in the inert concentration is shown in Figure 4.10 and Figure 4.11 respectively. The system is stable and all the selected tray temperatures are controlled at their setpoints. The bottoms and distillate purities are tightly controlled. Further, the performance of this control system is better for the change in the inert composition of the feed F_{0A} compared to the previous cases. Furthermore, it is interesting to observe in the closed loop response that the movement of the vapor-boil up rate V_s is much smaller to maintain the product purities compared to the previous case and deterministic results.

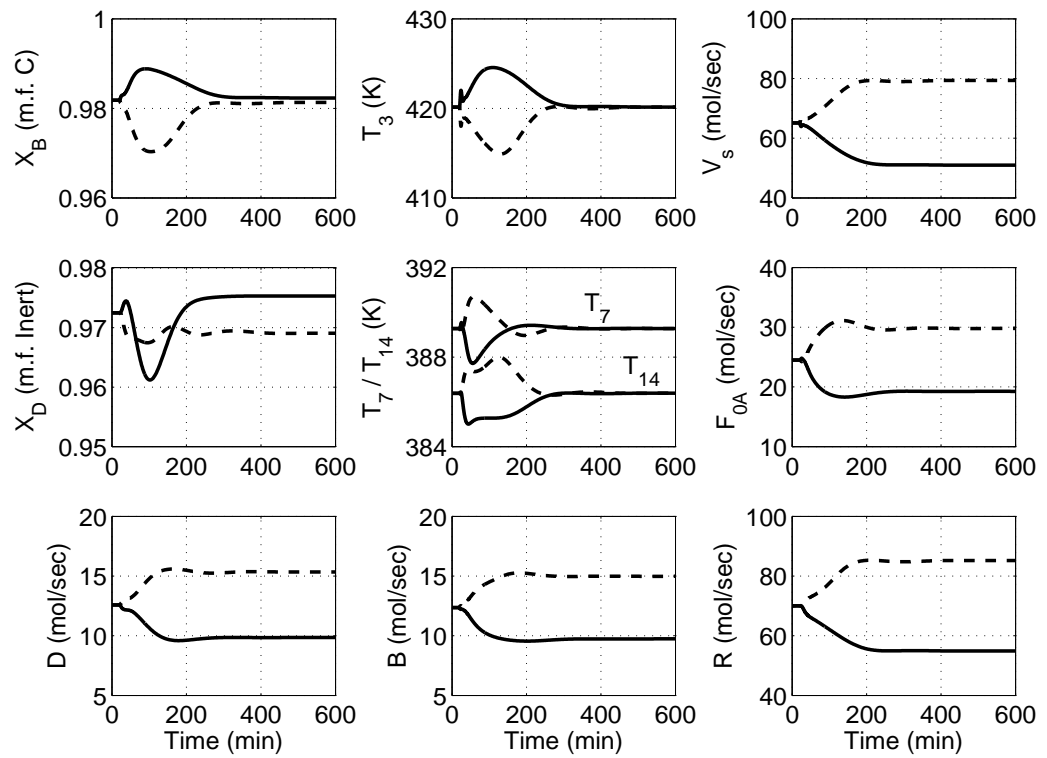


Figure 4.10: Closed loop response for a $\pm 20\%$ step change of the feed F_{0B} - Stochastic MIDO approach (case 3)
(solid line, -20%; dashed line, +20%)

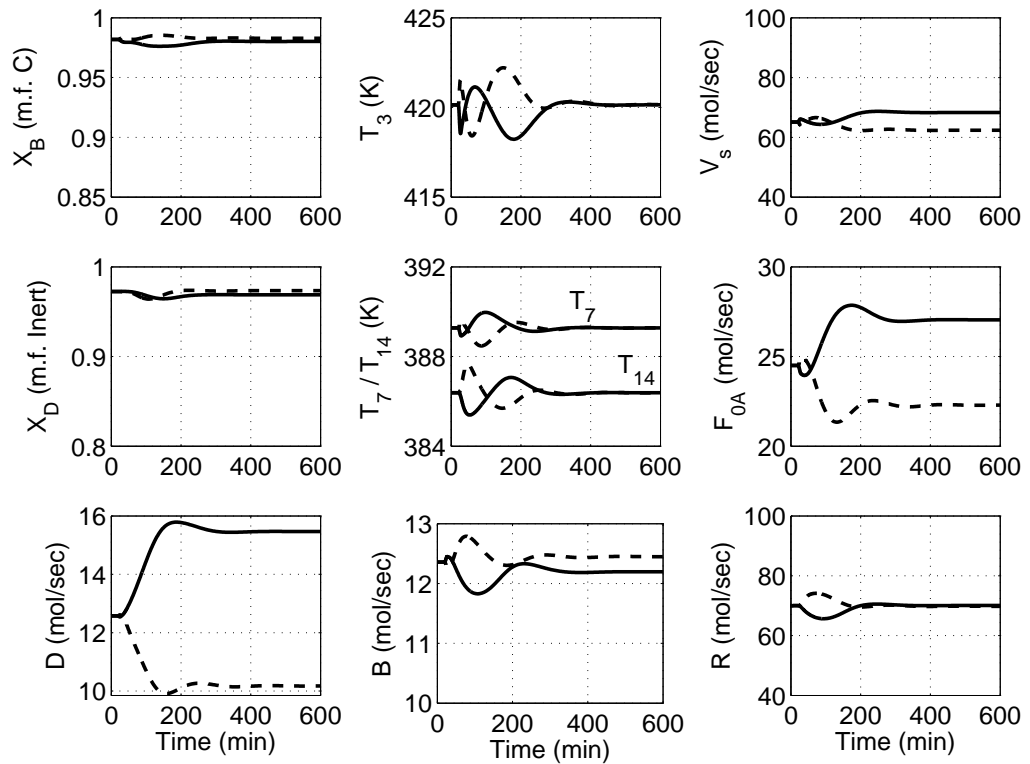


Figure 4.11: Closed loop response for a $\pm 10\%$ step change of the inert concentration $Z_{0A(I)}$ in the feed F_{0A} - Stochastic MIDO approach (case 3) (solid line, $Z_{0A(I)} = 0.55$; dashed line, $Z_{0A(I)} = 0.45$)

4.5 Summary

Application of the proposed MIDO framework for simultaneous selection of a decentralized control structure and controller parameters is presented for a ternary reactive distillation with inert. First, the MIDO problem is successfully solved using the sequential solution strategy for the nominal case i.e., a specific disturbance scenario ($\pm 20\%$ step change in vapor boil up rate V_s). It was shown that the resulting inferential control system has superior performance compared to earlier studies on this system, but still lacks robustness.

Therefore in a second step, a stochastic approach is applied accounting explicitly for various disturbances, which are modeled by multivariate probability distributions. This leads to a MIDO problem under uncertainty which can be translated into a deterministic problem by using the sigma point method. The methodology was applied to different cases where restrictions on the control structure were relaxed step by step and significant improvements could be achieved.

Chapter 5

Application to plantwide control problem

To discuss the feasibility of the proposed MIDO framework for plantwide control problems, focus of this chapter is on a multi unit process with material and energy recycles. As a challenging, highly integrated and highly nonlinear process for the production of dimethyl carbonate (DMC) is considered, which has been proposed recently in the literature [35].

5.1 DMC process

Dimethyl carbonate is an environmentally benign chemical because of its negligible ecotoxicity and low bioaccumulation and persistence [36]. It has been used as a substitute to replace dimethyl sulfate and methyl halides in methylation reactions and as a carbonylation agent to substitute phosgene for the production of polycarbonates and urethane polymers. Other applications of DMC have been evaluated, for example, as nonaqueous electrolyte component in lithium rechargeable batteries and as an oxygenate for internal combustion engine fuels.

In the recent literature [35], the transesterification reaction of methanol (MeOH) and propylene carbonate or ethylene carbonate (EC) is used to produce DMC and to co-produce useful propylene glycol or ethylene glycol (EG). In the later case, the chemical reaction is presented as follows:



A reactive distillation column can be utilized for the complete conversion of EC with methanol in excess. However, the top product of the reactive distillation column is the azeotrope of methanol and DMC because the azeotropic temperature is the

lowest of the system. An extractive distillation is employed to separate the azeotrope. The steady-state flowsheet for the entire process, reactive distillation + extractive distillation is shown in Fig 5.1. The distillate from the RD column is fed to an extractive distillation column. In this process, aniline is used as a solvent in the column to remove DMC. The solvent is fed to the column on a stage above the feed stage of MeOH/DMC mixture from the distillate of RD Column and below the column top. The extractive distillation column (ED) can be divided into three sections. They are: rectifying section (stages above the aniline feed), extractive section (stages between the feeds), and stripping section (stages below the feed of MeOH/DMC mixture). The relative volatility between MeOH and DMC is changed in the presence of aniline. High-purity methanol is produced in the column distillate and recycled back to the RD. In the stripping section, methanol is stripped toward the extractive section and only very small amount of methanol exists in the column base. A distillation column for solvent recovery is added to separate the DMC/aniline mixture coming from the base of the extractive distillation column. DMC is obtained from the column overhead and aniline recovered from the column base is recycled back to the extractive column. Extractive and solvent recovery columns are operated at 1 atm. To compensate for the loss of aniline from the distillate of the solvent recovery column, a small makeup stream of aniline should be added. The steady state operating conditions are given in Fig 5.1.

5.2 Process modeling

In the reactive distillation column, the reversible transesterification reaction of EC and MeOH is presented in Eq.5.1. The kinetic equation for the reaction catalyzed by a homogeneous catalyst, sodium methylate with its concentration between 0.2 and 0.3 wt % [66], is expressed as:

$$r_{EC} = k_+ C_{EC} C_{MeOH} - k_- \frac{C_{EG} C_{DMC}}{C_{MeOH}} \quad (5.2)$$

$$k_+ = 1.3246 \exp\left(\frac{-13060}{RT}\right) \quad (5.3)$$

$$k_- = 15022 \exp\left(\frac{-28600}{RT}\right) \quad (5.4)$$

here r_{EC} is the reaction rate of EC in moles per liter per minute and C_i is the concentration of i th component in moles per liter.

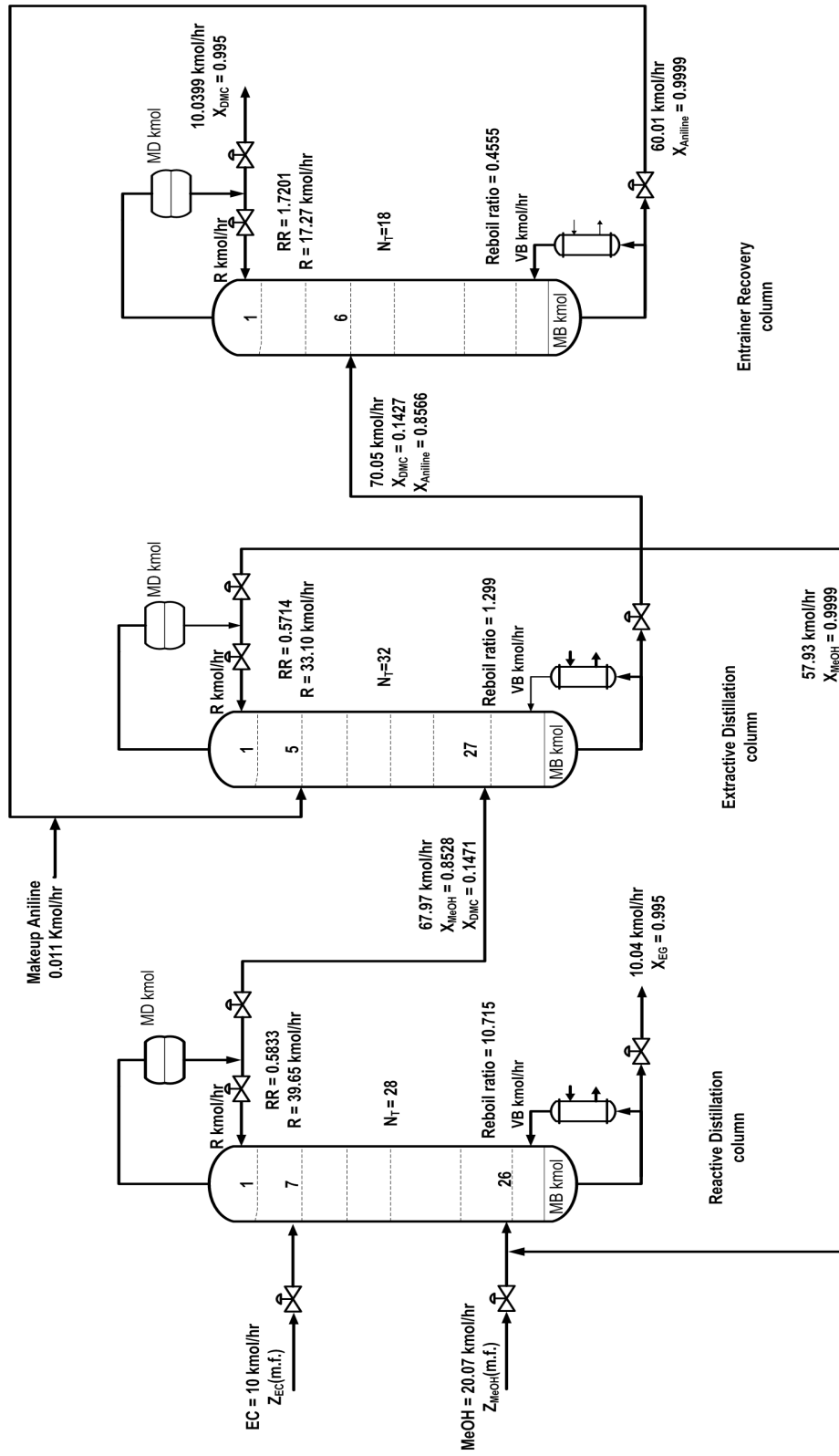


Figure 5.1: Flowsheet of the complete process for Dimethyl Carbonate (DMC) synthesis [35]

In the process modeling, the catalyst concentration is assumed to be constant and is therefore not explicitly appearing in the model equations. The plant model considered by Hsu et.al., [35] is based on material and energy balances. The vapor-liquid equilibrium is described with UNIQUAC model for the liquid phase and an RK model for the vapor phase. In the present work, very similar steady state conditions are achieved with simplification of the original model. The simplifications are that the plant model is based on the material balance only, heat effects are neglected; UNIQUAC model for the liquid phase and the vapor-phase is assumed to be ideal in the vapor-liquid equilibrium. The UNIQUAC parameters for this system are taken from the paper by Hsu et.al., [35] and Aspen Plus [67]; the model equations are reported in Appendix A. The extended Antoine equation is used for vapor pressure calculation (see Appendix A). However, it is worth noting that these simplifications do not reduce the combinatorial complexity of the decentralized control system design.

5.3 Control strategy - Heuristic method

In this section, the control strategy based on the heuristic method is presented. The recent literature [35] provides the detailed description of this control strategy. There are two recycle streams in the overall process. One is to recycle the excess reactant, methanol, back to the reactive distillation column. The other one is to recycle the entrainer to the extractive distillation column. There are four product compositions (MeOH at the distillate of the extractive column, aniline at the bottom of the entrainer recovery column, DMC at the distillate of the entrainer recovery column and EG at the bottom of the RD column) to be maintained in this process. The overall process flow sheet is implemented in DIVA [42] and 10 minutes of residence time with 50% liquid level is used to calculate the volume of each column base and reflux drum of each column. All the columns are operated at atmospheric pressure. The overall control strategy according to Hsu et.al., [35] is displayed in Fig 5.2 and the important control loops are listed below:

1. EC feed is flow controlled. (used as a throughput manipulator)
2. Total MeOH feed is flow-controlled by manipulating a control valve at fresh feed stream. The total MeOH feed set point is changed to maintain MeOH/EC feed ratio into the RD column. This feed ratio can be reset by a tray temperature control loop.

3. RD column base level is controlled by manipulating the bottom flow (EG product flow).
4. RD column reflux drum level is controlled by manipulating the distillate flow
5. RD column reflux is a ratio to EC feed flow
6. RD column vapor boil up rate is a ratio to EC feed flow
7. Base level of the extractive distillation column is controlled by manipulating the bottom flow.
8. Reflux drum level of the extractive distillation column is controlled by manipulating the distillate flow (MeOH recycle flow).
9. Reflux flow of the extractive distillation column is ratio to distillate of RD column.
10. Base level of the entrainer recovery column is controlled by manipulating the aniline makeup flow.
11. The entrainer feed flow to the extractive distillation column is flow-controlled and ratio to distillate of RD column
12. Reflux flow of the entrainer recovery column is a ratio to distillate of the RD column.
13. Extractive distillation column vapor boil up rate is used to control the tray temperature of T_{30} in the extractive column.
14. Entrainer recovery column vapor boil up rate is used to control the tray temperature of T_4 in the entrainer column.

In the closed-loop simulation runs, P controllers are used in all level loops. The reason for using P controllers are that maintaining the liquid levels at the set-points is not necessary. For the two bottom level loops in the extractive distillation system, $kp = 10$ is used so that faster dynamics of the internal flow of the overall process can be achieved and also for faster increase or decrease of entrainer makeup into the system. For the remaining level control loops, $kp = 2$ as suggested in Luyben [10] is used. In each temperature loop, an additional 1-min dead time is included for modeling the other neglected dynamics in the system. The tuning constants are determined via relay feedback test with Tyreus and Luyben tuning rule [56]. The resulting PI

tuning constants for the tray 27 temperature loop of the reactive distillation column are $kp = 0.71$ and $\tau_I = 10.5$ min; the tuning constants for the tray 30 temperature loop of the extractive distillation column are $kp = 1.2$ and $\tau_I = 3.0$ min; and the tuning constants for the tray 4 temperature loop of the entrainer recovery column are $kp = 1.3$ and $\tau_I = 5.5$ min. Further, a specific disturbance scenario which is adopted to test the control strategy is a $\pm 20\%$ step change in the F_{EC} .

5.3.1 Remarks on the control strategy by heuristic method

Fig 5.3 shows the closed-loop performance for the control strategy with heuristic method. The overall control strategy is stable for a specific disturbance scenario of a $\pm 20\%$ step change in F_{EC} . It should be noted that all three controlled temperatures are returned back to their set point values with smooth manipulated variable changes. The compositions of two products (DMC and EG) as well as the compositions of the two recycle streams (MeOH and aniline) all display only small deviations from their specifications. It should be noted in this control strategy that the disturbances are measured. Based on the measured disturbance, the overall control strategy behaves accordingly, since most of the control loops are feed-forward with the measured disturbance. Therefore, it is possible to adjust the temperature set points to make the compositions closer to their specifications. However, there is no guarantee that the control strategy will perform well for unknown disturbances which happen frequently in real chemical plants (e.g., feed temperature, feed composition changes etc.). For example, the closed loop response for the step change in the feed composition of F_{MeOH} , i.e., MeOH feed contains 2% and 5% of DMC is shown in Fig 5.4 for this control strategy. Here, the product purity X_{EG} is not well maintained at the desired level. This is due to the fact that the control system from the heuristic method has the ratio controllers with the measured feed disturbance F_{EC} , it leads to the constant flow rate in the reflux and vapor boil up rate in the reactive distillation column. Therefore, the bottom purity is decreasing from the steady state value. Further, there are 22 control loops with 17 measurements in the overall control strategy, because of many ratio control loops. Furthermore, the DMC process requires theoretically 15 control loops by performing the degree of freedom analysis for the closed loop control. In the next section, the proposed MIDO framework is applied to this complex process to explore whether a suitable control strategy and also for unmeasured disturbances, is even possible with a smaller number of control loops. Later, the same methodology is extended to account for a collection of disturbance scenarios.

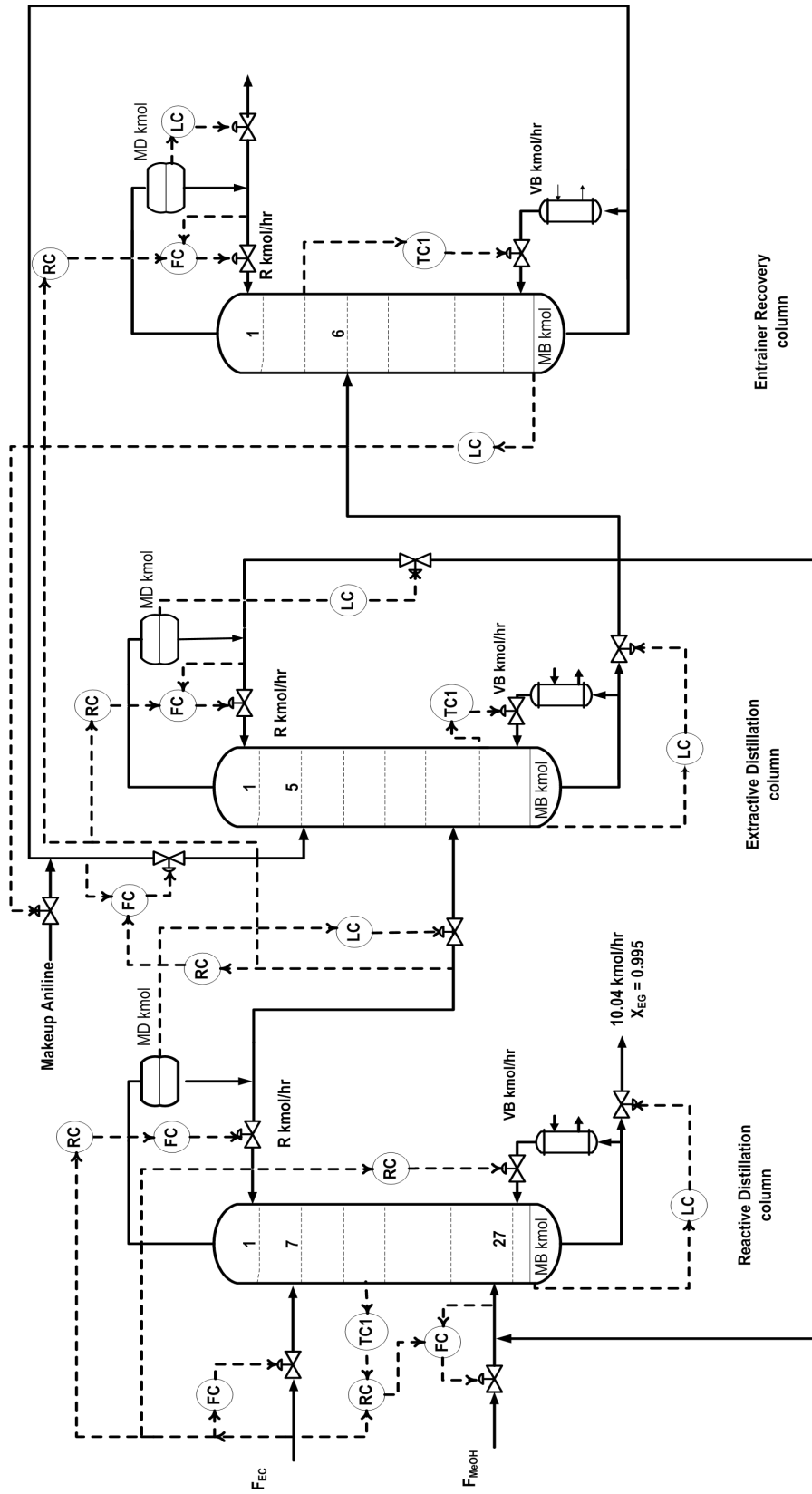


Figure 5.2: Overall control strategy - Heuristic method [35]

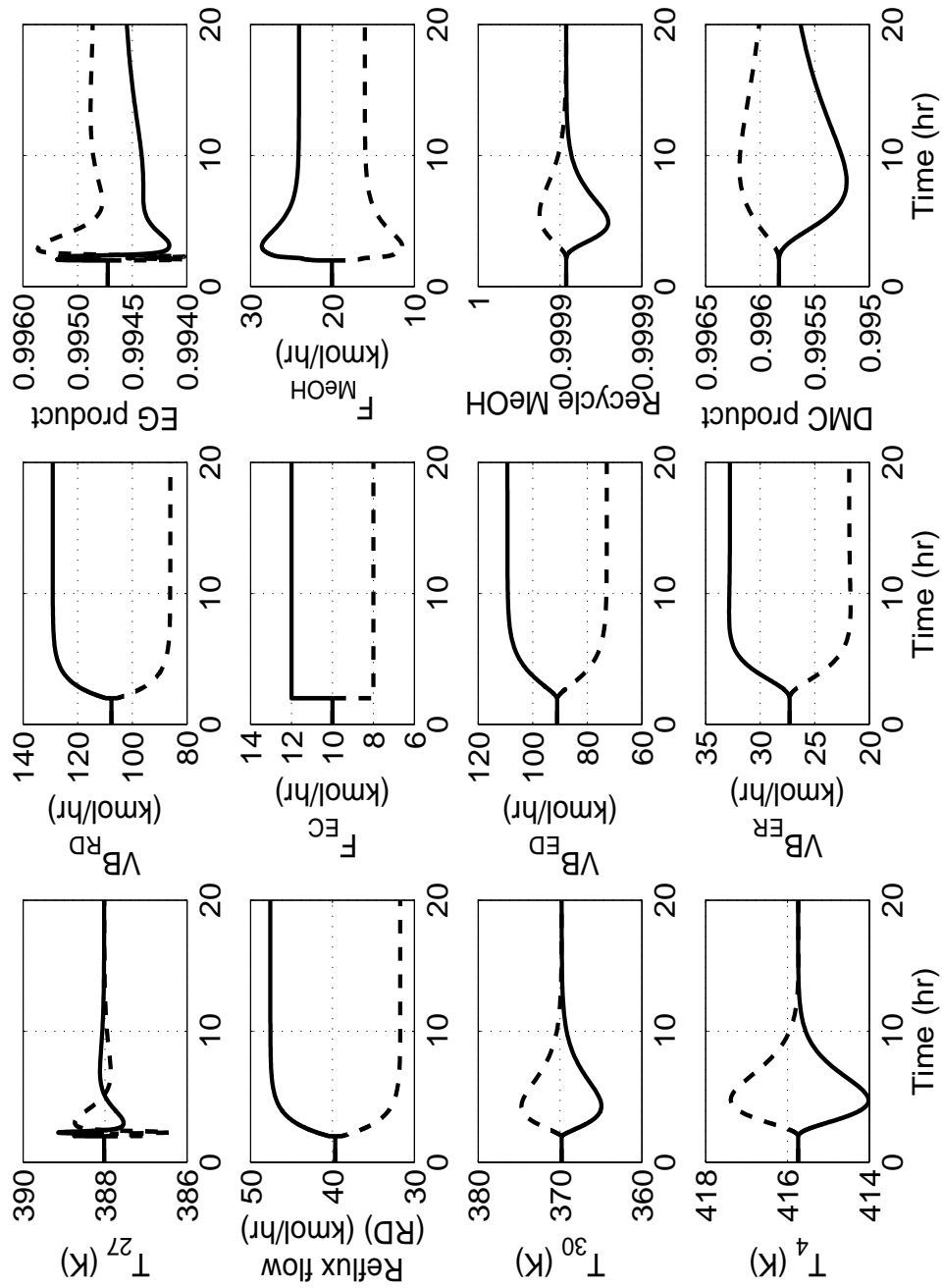


Figure 5.3: Closed loop results with $\pm 20\%$ change in F_{EC} - Heuristic method (solid line, +20% of F_{EC} ; dashed line, -20% of F_{EC})

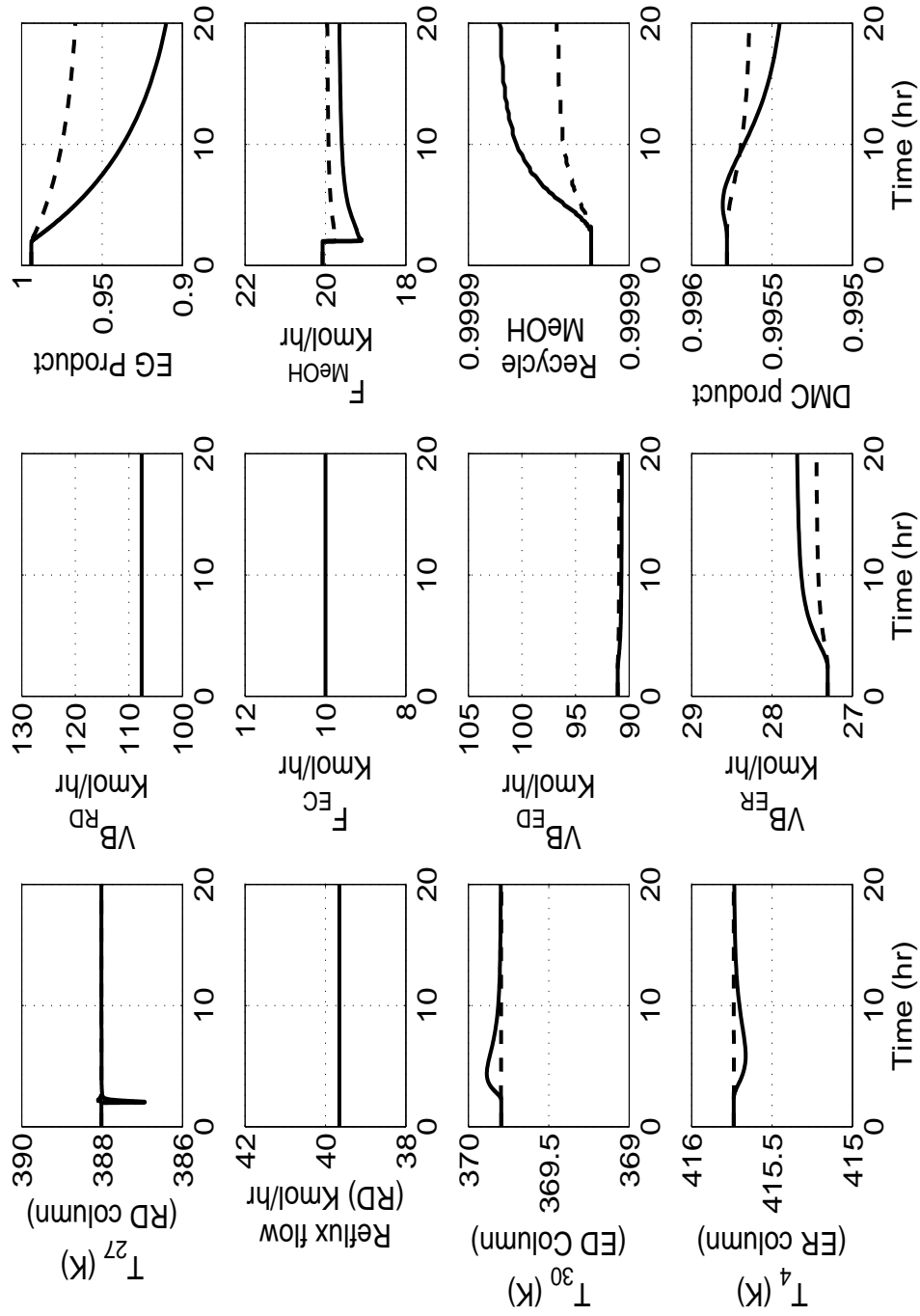


Figure 5.4: Closed loop response for change in MeOH feed composition (heuristic method) (solid line, $Z_{MeOH} = 0.95$, $Z_{DMC} = 0.05$; dashed line, $Z_{MeOH} = 0.98$, $Z_{DMC} = 0.02$)

5.4 Optimal control strategy - MIDO formulation

Due to the combinatorial complexity, decomposition of the problem is required in order to achieve the optimal solution with an acceptable computational effort.

5.4.1 Complexity of the plantwide control problem

This plant has 15 potential manipulated variables i.e., available valves. Since, focus is on inferential control, i.e., tray temperatures are used to control product composition. This will lead to a large number of potential controlled variables including the base and reflux drum level in all the three columns. This turns out to be 81 potential controlled variables.

Since, one of the input stream is used to fix the production rate, there are 14 manipulated variables. As a result, there are 1.5×10^{26} alternative choices for these 14 control loops. First, the problem will be decomposed step by step in order to reduce the combinatorial complexity before addressing the solution with the MIDO formulation. There are three steps in the present application to reduce the complexity of a combinatorial problem.

5.4.1.1 Step 1: Design of the level controllers

In the DMC process, there are six liquid levels that must be controlled. These are the base and reflux drum levels in the reactive, extractive and entrainer recovery columns, respectively. In the present study, these level control loops are assumed to be the same as in the heuristic method. The assumed level controllers are listed below:

1. RD column base level is controlled by manipulating the bottom flow (EG product flow).
2. RD column reflux drum level is controlled by manipulating the distillate flow
3. Base level of the extractive distillation column is controlled by manipulating the bottom flow.
4. Reflux drum level of the extractive distillation column is controlled by manipulating the distillate flow (MeOH recycle flow).
5. Base level of the entrainer recovery column is controlled by manipulating the aniline makeup flow.

6. Reflux drum level of the entrainer recovery column is controlled by manipulating the corresponding column's distillate flow (DMC product flow).

This will reduce the number of potential manipulated variables to 8, and number of potential controlled variables to 75. As a result there are 6.8×10^{14} alternative choices for the remaining control loops.

5.4.1.2 Step 2: Account of the operational requirement

In this stage, the operational requirement of a chemical plant will be taken into account to reduce the complexity further. It is reasonable to assume that the respective input streams to the column are used as manipulated variables in order to control the tray temperatures of the column. This will be helpful in the case of controller failure, start-up and shutdown etc.,. Further, the reflux ratios in all the columns are maintained by manipulating the reflux flow rate in the respective columns. Operating the columns by maintaining a constant reflux ratio is a standard practice in distillation. This will give further reduction in the complexity of the problem, as a result there are 4.8×10^8 possible alternative choices for the remaining control loops.

5.4.1.3 Step 3: Restriction on the selection of controlled tray temperatures

The “sign reversal” is an important issue which is noticed in the reactive and extractive distillation columns. The “sign reversal” indicates that the steady-state gain of a specific tray temperature changes sign as the magnitude of the same manipulated variables varies. In the recent literature [55], it was pointed out that the temperatures with the “sign reversal” cannot be used as controlled variables. Therefore, the “sign reversal” of the tray temperatures can be used to reduce the set of possible controlled variables. First, the “sign reversal” test is applied to reactive and extractive distillation columns where the nonlinearity plays a significant role. The following procedure is adopted to identify the “sign reversal”:

The tray temperatures are treated as the state variables. The manipulated variables are the vapor boil up VB_{RD} , the two reactant flow F_{EC} and F_{MeOH} in the reactive distillation column. In the extractive distillation column, the manipulated variable is the vapor boil up VB_{ED} . First, the upper and lower bounds of the steady-state gains between the tray temperatures and the manipulated variables are obtained for a range of input variations. In this work, -10% to +10% changes in the manipulated variables are used to find the upper and lower bounds of the steady state gain. Note

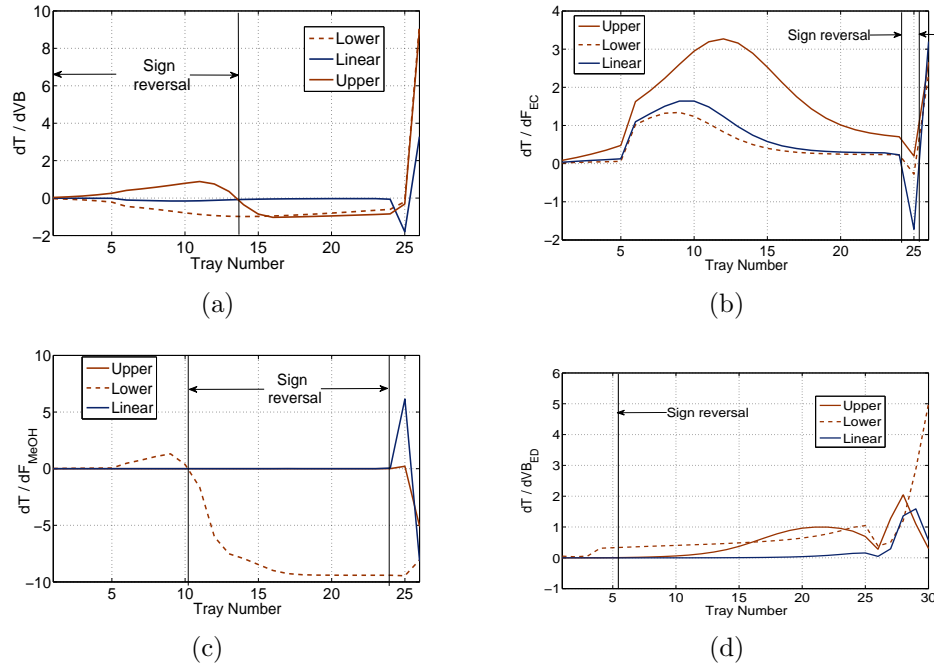


Figure 5.5: Upper and lower bounds of steady-state gains of all tray temperatures with “sign reversal”: (a) For vapor boil up VB_{RD} in RD column; (b) For EC feed F_{EC} in RD column; (c) For MeOH feed F_{MeOH} in RD column; and, (d) For vapor boil up VB_{ED} in ED column.

that, for a linear system, the upper and lower bounds should coincide with each other.

The steady state gains of the tray temperatures in the reactive distillation column are shown in Fig 5.5(a), 5.5(b), 5.5(c) for the available manipulated variables. It shows that the reactive distillation column exhibits strong nonlinearity, and almost 2/3 of the tray temperatures exhibit the “sign reversal”. A similar kind of behavior is observed for the extractive column, which is shown in Fig 5.5(d) for the vapor boil up rate. It should be noted that the tray temperatures with the “sign reversal” cannot be used as controlled variable [55]. Thus, the number of potential controlled variables can be reduced significantly. As a result, there are 387072 possible alternative choices for the decentralized control loops which is by far too much for enumeration. The optimal solution can be achieved with the proposed MIDO framework.

5.4.2 MIDO formulation

The mathematical formulation which is outlined in Chapter 2 is adopted in this plantwide control example problem. Formulation II, i.e., maximize the overall per-

Table 5.1: Measurements and control loops requirement for DMC process

	Heuristic method	Optimal control strategy - nominal case
Measurements	17	15
Control loops	22	18

formance is considered, in which the objective function is given by:

$$J = \int_0^{t_f} [(y_{sp} - y)^T Q (y_{sp} - y) + (u_{ss} - u)^T R (u_{ss} - u)] dt \quad (5.5)$$

In this example, these weighting matrices are calculated using the steady state sensitivities. Then, the Q and R matrices can be calculated according to (see Chapter 2):

$$Q = \text{diag} \{q_i\} = \text{diag} \left\{ \frac{1}{(y_{i,U})^2} \right\} \quad (5.6)$$

$$R = \text{diag} \{r_i\} = \text{diag} \left\{ \frac{1}{(u_{j,U})^2} \right\} \quad (5.7)$$

Again, decentralized PI controllers are considered in all the temperature control loops. The specific disturbance which is adopted in the heuristic method i.e., a $\pm 20\%$ change in the F_{EC} is considered first to design the optimal control loops in order to compare the results. The GBD based sequential approach is used to solve for optimality.

5.4.2.1 Performance of the optimal control strategy

With the GBD based sequential solution approach formulation II is solved successfully for the optimal control structure and controller parameters. Since, the level controllers are already discussed, only temperature and other control loops are reported in Table 5.2. The problem demands 16 hours of computational effort to achieve the optimal solution. The overall control strategy is shown in Fig 5.6. Table 5.1 also summarizes the number of control loops and measurements for this process. This optimal control strategy has 18 control loops compared to the heuristic method which has 22 control loops, and the number of measurements is 15 compared to the heuristic method which has 17. The closed loop performance of the optimal control strategy is shown in Fig 5.7 which is better than the heuristic method (Fig 5.3). Further, the

selected tray temperatures as controlled variables are maintained at their set-points by smooth manipulation of the inputs.

5.4.2.2 Reduction of computational effort using integer cuts

The computational effort can be further reduced by using integer cuts which are used in order to reduce the number of feasible alternative solutions at this variable pairing and tuning step. The following constraints are also used:

$$\lambda_{i,j} \left(\sum \delta_{i,j} \right) \geq 0 \quad (5.8)$$

where $\lambda_{i,j}$ is the $i - j$ element of the relative gain array defined as:

$$\Lambda = [\lambda_{i,j}] = G(0) \otimes [G^T(0)]^{-1} \quad (5.9)$$

and $G(0)$ is the steady state gain matrix. Eq (5.8) imposes the well-known necessary condition for integral controllability with integrity (ICI). Furthermore, systems that are not integral stabilizable (IS), that is, structures that do not satisfy the (necessary) condition for IS [68]

$$\det [G(0)] \neq 0 \quad (5.10)$$

never enter the variable pairing and tuning step, and are excluded from further consideration by using the integer cuts. This decomposition has proven to be efficient in practice due to the fact that the MIDO problem can be solved easily to first integer solution even for large-scale problems, while the conditions given by Eqs. (5.8) and (5.10) eliminate a substantial number of alternatives that do not satisfy the IS or ICI conditions. It should be noted that the same optimal solution is achieved with and without adding the integer cuts (see Table 5.2). However, it is worth noting that the computational effort is reduced to 7 hours compared to a rigorous approach with 16 hours.

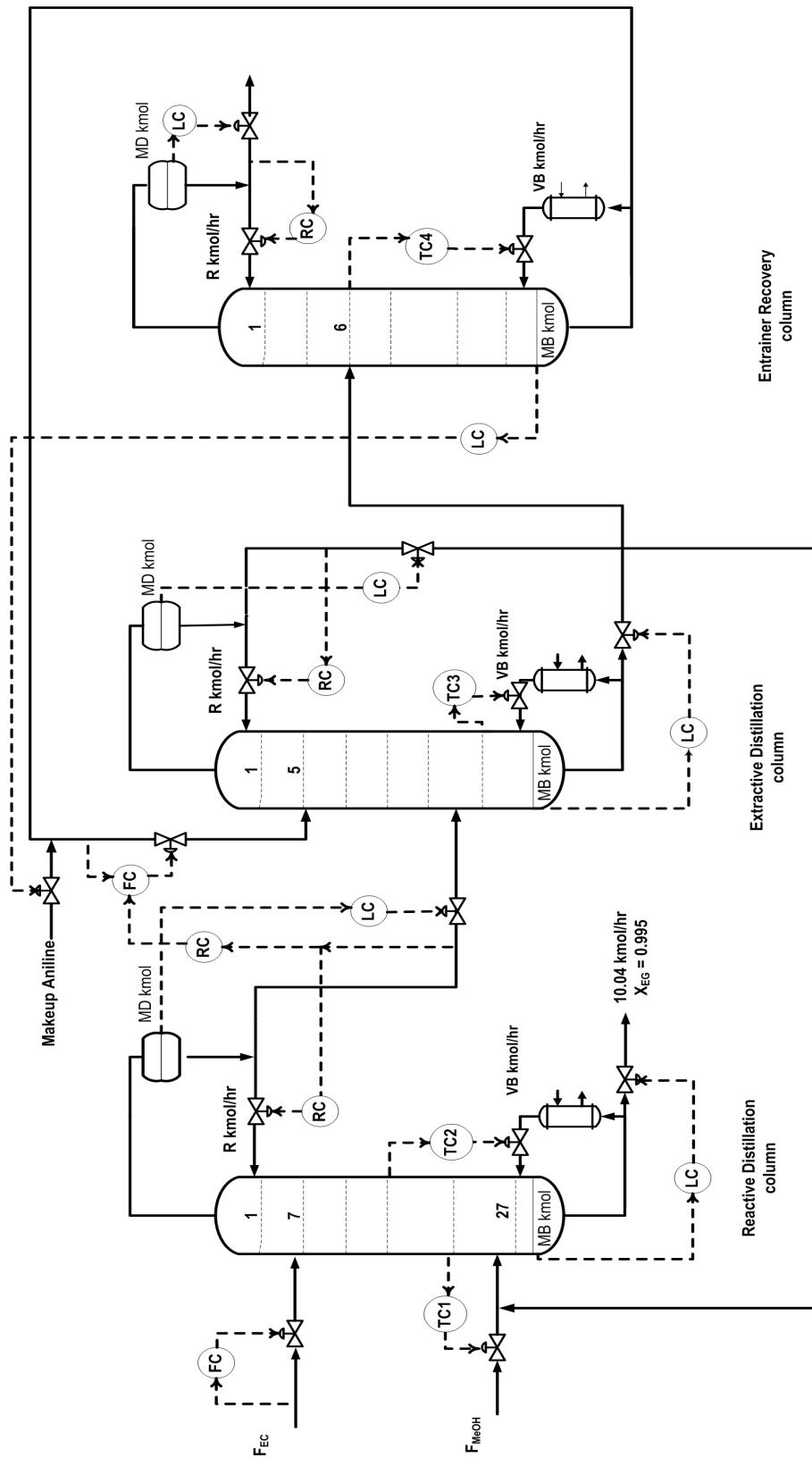


Figure 5.6: Optimal control strategy - Formulation II

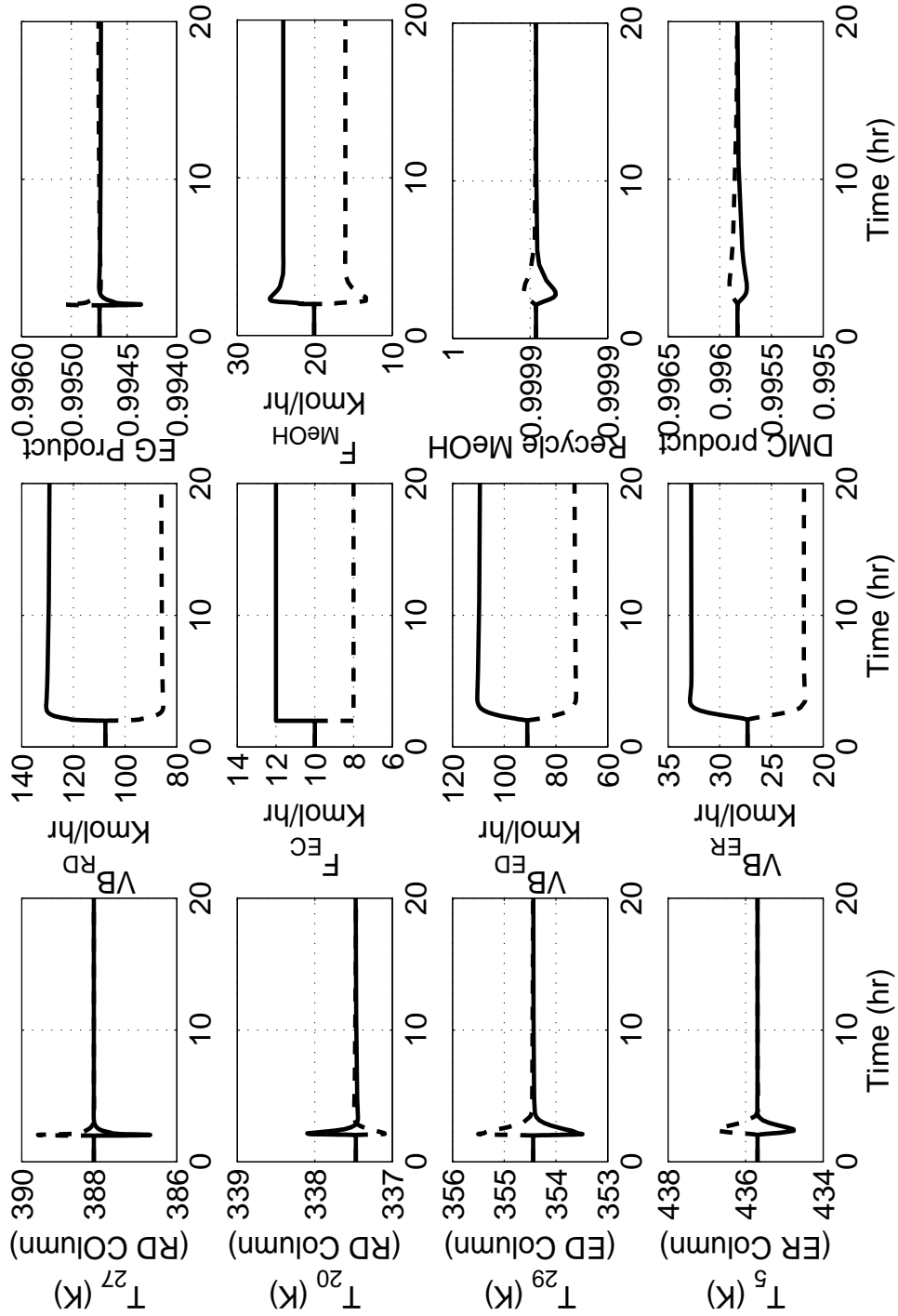


Figure 5.7: Closed loop results with $\pm 20\%$ change in F_{EC} - Optimal solution (Formulation II) (solid line, +20% of F_{EC} ; dashed line, -20% of F_{EC})

Table 5.2: Optimal control loops and PI controller parameters for DMC process

Sequential solution approach	GBD	GBD
Integer cuts (Eqs. (5.8) and (5.10))	NO	YES
No of Iterations	14	8
CPU time	16 hours	7 hours
Initial Guess	Heuristic Method	Heuristic Method
Objective function value	5113.0	5113.0
Optimal solution	$VB_{RD} - T_{20}$ $(k_p = 0.7; \tau_I = 10\text{min})$ $F_{MeOH} - T_{27}$ $(k_p = 0.5; \tau_I = 8\text{min})$ $VB_{ED} - T_{29}$ (ED column) $(k_p = 1.4; \tau_I = 6\text{min})$ $VB_{ER} - T_5$ (ER column) $(k_p = 1.2; \tau_I = 8\text{min})$ F_{EC} - Production rate control	$VB_{RD} - T_{20}$ $F_{MeOH} - T_{27}$ $VB_{ED} - T_{29}$ $VB_{ER} - T_5$ Identical controller parameters
Objective function	2376.0	2376.0

5.5 Optimal control strategy under uncertainty

In the previous section, the optimal control system is achieved for a specific disturbance scenario, i.e. a $\pm 20\%$ step change in the feed F_{EC} . However, due to nonlinearity the optimal control system will differ for different disturbance scenarios. Therefore, in this section, the optimal control system design under disturbance uncertainty which was explained in the previous chapter is extended to the DMC process.

In the DMC process, the disturbances are the fresh feeds either F_{EC} or F_{MeOH} as a production rate control, feed compositions. These disturbances are random, i.e. they can not be defined in advance, but the stochastic nature of these disturbances can be incorporated. However, the resulting MIDO problem using the sigma point method will become more complex if all the disturbances are considered as random quantity. Instead, the influence of these disturbances on the output variables have to be determined, which can be detected using first order sensitivity indices e.g. Sobol's indices (S_i) [69]. The steady state model is used to calculate the Sobol's indices. The following procedure is adopted to detect the influence of uncertain disturbances on the output variables:

Treating disturbances θ and the output variables (here, the products X_{EG} and X_{DMC})

Table 5.3: Uncertainty model for the DMC process

Disturbance	Description	Normal Distribution (mean μ , standard deviation σ)
F_{EC}	Fresh feed flow of EC	N(10, 2)
F_{MeOH}	Fresh feed flow of MeOH	N(20.07, 4)
Z_{EC}	Feed concentration (F_{EC})	N(0.96, 0.015)
Z_{MeOH}	Feed concentration (F_{MeOH})	N(0.96, 0.015)

y as random variables, it is required to quantify the amount of variance that each disturbance θ_i contributes to the variance of the output $\sigma^2(y)$. The ranking of a disturbance θ_i is done by the amount of output variance that would vanish, if this disturbance θ_i is assumed to be known. Formally, this can be done using the first order sensitivity index i.e., Sobol's indices [70], and is used in the following disturbance sensitivity analysis.

$$S_i = \frac{\sigma_i^2(E_{-i}[y | \theta_i])}{\sigma^2(y)} \quad (5.11)$$

where, $\sigma_i(E_{-i}[y | \theta_i])$ is the variance of the conditional expectation which represents the contribution of disturbance θ_i to the variance $\sigma^2(y)$ indicating the importance of this disturbance. The detailed procedure can be found in the paper by Schenkendorf and Mangold [71].

Usually, the multidimensional integrals, i.e., determining $\sigma^2(y)$ or $\sigma^2(y | \theta_i)$, are evaluated by Monte Carlo methods. However, this is a high computational effort. To reduce the computation cost, the sigma point method which was described in Chapter 3 is adopted. In the present problem of the DMC process, the disturbances are considered as a step function whose magnitude is described by the normal distribution. The uncertain model of the DMC process disturbances are given in Table 5.3. Here, $Z_{EC} \sim N(0.96, 0.015)$ means that the EC feed is not pure, but contains the product EG as the impurity in the feed stream. Also, $Z_{MeOH} \sim N(0.96, 0.015)$ means that the MeOH feed is not pure, but contains the product DMC as the impurity in the feed stream. The output variables are the two product composition i.e., X_{EG} and X_{DMC} . The Sobol's indices are calculated using the sigma point method and shown in Fig 5.8. It is clear from Fig 5.8 that the most important disturbances are F_{EC} , F_{MeOH} and Z_{MeOH} . An optimal compromise for the control structure and the controller parameters has to be determined for rejecting these disturbances, whereas the disturbance Z_{EC} can be fixed at the nominal values.

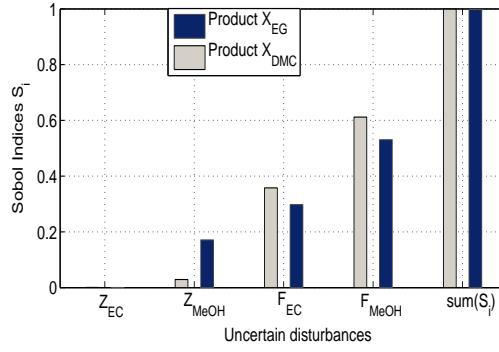


Figure 5.8: First order sensitivity indices of the output variables

5.5.1 MIDO problem under uncertainty

The statistical objective function which involves the expectation and the variance of a chosen performance index is given by:

$$\min_{p, \delta} \Phi = E \left\{ \int_0^{t_f} [(y_{sp} - y)^T Q (y_{sp} - y) + (u_{ss} - u)^T R (u_{ss} - u)] dt \right\} \quad (5.12)$$

$$+ \omega V \left\{ \int_0^{t_f} [(y_{sp} - y)^T Q (y_{sp} - y) + (u_{ss} - u)^T R (u_{ss} - u)] dt \right\}$$

The expectation and the variance are approximated with the sigma point method, and converted to a deterministic problem. This leads to a large-scale MIDO problem which can be however solved with reasonable effort of 14 hours with integer cuts. The optimal control structure and controller parameters are shown in Table 5.4. Here, the feed F_{MeOH} is used for the production rate control and F_{EC} is used for the handles of the temperature control loop. The closed loop response for the step change in the feed composition of F_{MeOH} , i.e., MeOH feed contains 2% and 5% of DMC is shown in Fig 5.9 for this robust control strategy obtained via the stochastic approach. The performance is better than the heuristic method (see Fig 5.4). Here, the bottom product from the RD column is controlled within the specification limit i.e., 95%. The smooth manipulation in the vapor boil up rate is also noticed, since it is paired with one of the tray temperatures in the respective columns.

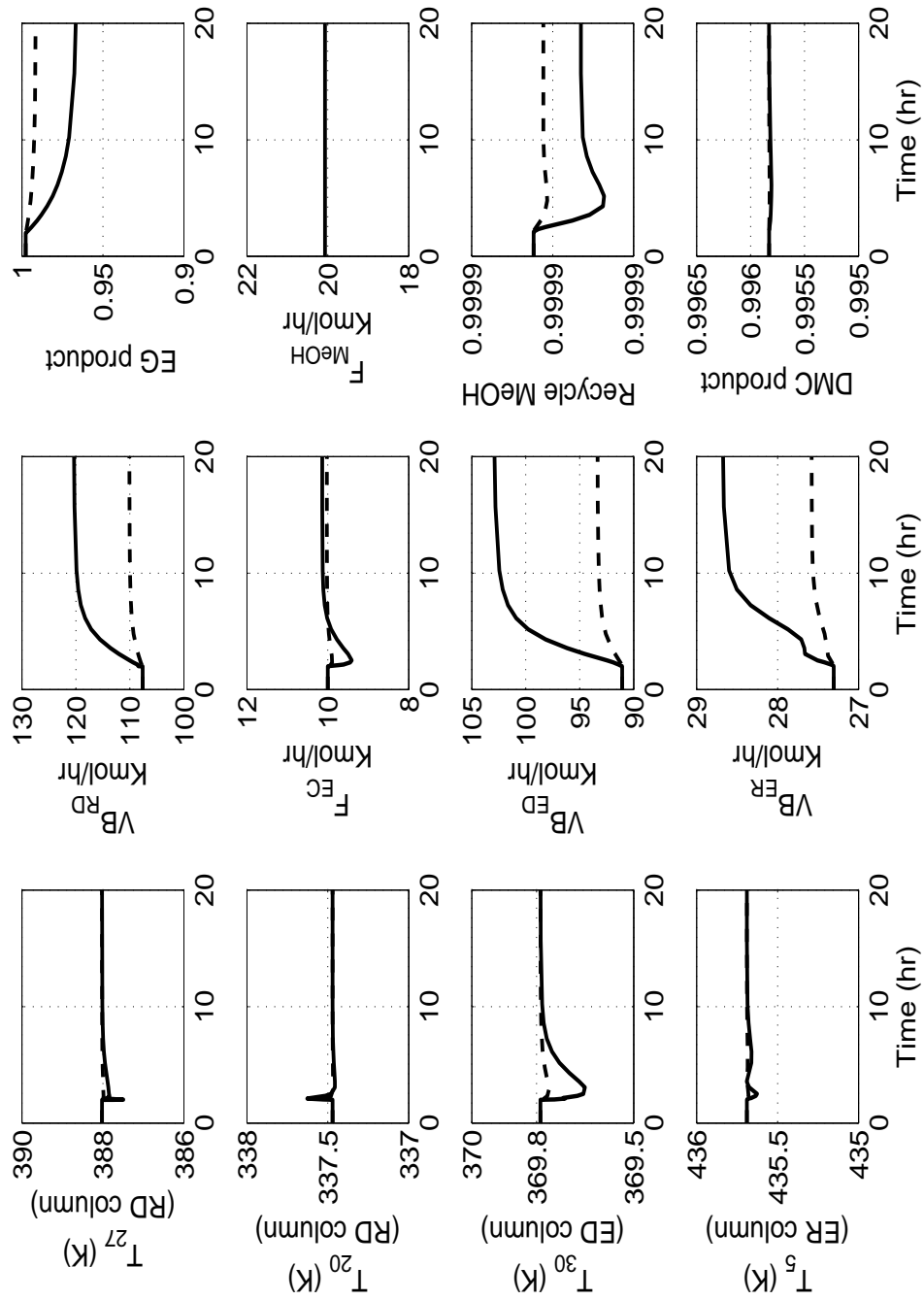


Figure 5.9: Closed loop response for change in MeOH feed composition (Stochastic approach) (solid line, $Z_{MeOH} = 0.95$, $Z_{DMC} = 0.05$; dashed line, $Z_{MeOH} = 0.98$, $Z_{DMC} = 0.02$)

Table 5.4: Optimal control loops and PI controller parameters under disturbance uncertainty

Sequential solution approach	GBD	
No of Iterations	12	
CPU time	19 hours	
Optimal solution	$VB_{RD} - T_{27}$ ($kp = 0.9; \tau_I = 8\text{min}$)	$F_{EC} - T_{20}$ ($kp = 0.65; \tau_I = 8\text{min}$)
	$VB_{ED} - T_{30}$ (ED column) ($kp = 1.5; \tau_I = 5\text{min}$)	
	$VB_{ER} - T_5$ (ER column) ($kp = 1.2; \tau_I = 8\text{min}$)	
	F_{MeOH} - Production rate control	

5.6 Summary

Application of the proposed MIDO framework for a large-scale DMC plant is presented, and the use of some decomposition strategies is also discussed. It is shown that these decomposition strategies are more efficient to reduce the computational effort. The optimal decentralized control structure and controller parameters are achieved for a large-scale DMC plant. Although, the control strategy via the heuristic method fulfills the main process objectives and possesses an acceptable dynamic behavior for a specific disturbance scenario, the solution with fewer hardware requirements (sensors, actuators and controllers) is preferred. This results from a control strategy obtained via the MIDO framework that has the lowest hardware requirement compared with the heuristic method.

It was shown that the resulting optimal control strategy has superior closed loop performance compared to standard heuristic design approaches. Further, the control strategy via the heuristic method will not provide the acceptable performance for other kind of unforeseen disturbances, since most of the control loops are feed-forward with the measured disturbance. Therefore, the optimal control structure and controller parameters under disturbance uncertainty is further investigated. The resulting MIDO problem under uncertainty is solved more efficiently using the sigma point method. These promising results obtained in a large-scale DMC plant supports the proposed MIDO framework for establishing the effective control system even for a more complex system.

Chapter 6

Conclusions

Plantwide control is arguably the most important problem in chemical process control. In recent years, research devoted to find a suitable plantwide control strategy for an integrated chemical process has been receiving a tremendous increase in attention from people in both academia and industry. This is primarily attributed to the importance that a large-scale chemical plant with material and energy recycles crucially depends on its control system to run safely, to maintain the production rate and quality, and to keep the process variance low.

However, the plantwide control problem is complicated by its large-scale nature and complex dynamic behavior. There are numerous combinations of controlled variables, manipulated variables, control structures, controller designs and even tunings which have to be evaluated for optimality. For the process engineer confronted with this challenging problem of deriving an optimal control strategy for a large-scale plant, this task possesses a **challenge for creativity** [9].

In this work, the algorithmic approach is considered to design the optimal plantwide control strategy. A systematic framework for simultaneous selection of the optimal control structure and controller parameters has been developed in view of (1) minimizing the effort to achieve a specified performance and (2) maximize the overall performance in terms of quadratic cost functions. Both formulations are constructed as a mixed-integer dynamic optimization (MIDO) problem by explicitly incorporating the nonlinear plant dynamics. It has been shown that the resulting MIDO problems can be solved with a sequential approach using Generalized Benders Decomposition with standard hard and software with reasonable computational effort.

First, focus was on a deterministic problem formulation for a specific disturbance scenario. Application of the proposed formulations was demonstrated in decentralized control system design for two different reactive distillation processes: (1) Ideal reactive distillation (2) Non-ideal methyl acetate process. It was demonstrated that the resulting control systems have superior performance compared to standard heuristic design approaches for a specific disturbance scenario.

In a second step, the approach was extended to explicitly account for various disturbances modeled by multivariate probability distributions. This leads to a complex MIDO problem under uncertainty. The sigma point method was used to approximate the expectation and the variance of the performance index to solve the MIDO problem under uncertainty. The proposed framework was successfully demonstrated for inferential control of an ideal reactive distillation column. Further, it was illustrated that the resulting control systems have superior performance compared to the standard heuristic method and the deterministic optimization. It was shown that the approach is particularly useful when the spectrum of disturbances is broad or multidimensional and therefore justifies the additional computational effort compared to the deterministic approach. It is worth noting that parametric model uncertainty of formulation II can be handled in an analogous way.

The practical advantages of the proposed MIDO formulation were further illustrated with a very promising benchmark problem which was discussed controversially in the recent literature [34, 64] i.e., ternary reactive distillation with inert. In this case, the heuristic method fails to find a suitable inferential control scheme. However, the optimal inferential control structure and controller parameters were determined using the proposed MIDO framework with formulation II. It was illustrated that the resulting optimal control system is providing an effective control fulfilling the operational requirements of the process.

Finally, also application to a large scale multi-unit chemical process with recycles was discussed. As an innovative application example dimethyl carbonate synthesis was considered. It was shown that the problem can be solved with reasonable effort if further decomposition strategies are applied giving superior performance of the resulting control system compared to standard heuristic methods.

Stability, which is an important issue in the control system design, was not addressed explicitly in this thesis. However, it is worth noting that “practical stability“ is included implicitly in the problem formulations. In formulation I, for example, the settling time requirements in the constraints imply that the control variables converge to some bounded neighborhood ($\pm 5\%$ in the present thesis) of the nominal operating point. Of course, this does not prove stability in the strict sense but turns out to be sufficient in all the cases we studied so far. In formulation II, we minimize the quadratic control error. Again, this does not imply stability in the strict sense but it seems unlikely that significant instabilities will come out as an optimal solution to such a formulation and in fact was not observed in the cases we studied so far.

Future work should include hard constraints on the design of an optimal control structure and controller parameters under uncertainty. For example, the stochastic MIDO approach presented in this thesis can be extended to handle the formulation I. Then, hard constraints like overshoot, settling time etc., can also become stochastic quantity along with the performance index. In this situation, chance constrained programming seems promising [72] to handle those hard constraints. This will lead to a new class of chance constrained MIDO problems for the future research.

In the present thesis, the control system design is conducted only after the steady state process design in order to focus in a first step on the challenging plantwide control problem. However in a next step, the process design and control should be performed simultaneously. More work is needed along these lines in order to improve the controllability of a complete chemical plant in the face of model uncertainties and disturbances.

Appendix A

VLE model for dimethyl carbonate (DMC) process

A.1 VLE model for dimethyl carbonate (DMC) process

Vapor pressure calculation

The extended Antoine equation is used for vapor pressure calculation which is given by:

$$\ln P_i = C_{1,i} + \frac{C_{2,i}}{T} + C_{3,i} \ln T + C_{4,i} T^{C_{5,i}} \quad (\text{A.1})$$

Molar density calculation

The Racket model/DIPPR equation is used for molar volume calculation, which is given by:

$$\rho_i = \frac{v_{1,i}}{v_{2,i}^{\rho L_i}} \quad (\text{A.2})$$

$$\rho L_i = [1 + (1 - T/v_{3,i})]^{v_{4,i}} \quad (\text{A.3})$$

where, ρ_i is the pure component molar density (mol/lit).

UNIQUAC VLE model

UNIQUAC model for the liquid phase activity co-efficient is used, and the vapor phase is assumed to be ideal. The liquid phase activity is given by:

$$\ln \gamma_i = \ln \frac{\phi_i}{x_i} + \frac{z}{2} q_i \ln \frac{\theta_i}{\phi_i} - q_i \ln t'_i - q_i \sum_j^{NC} \frac{\theta_j \tau_{i,j}}{t'_i} + l_i + q_i - \frac{\phi_i}{x_i} \sum_j^{NC} x_j l_j \quad (\text{A.4})$$

where,

$$\theta_i = \frac{q_i x_i}{q_T} \quad q_T = \sum_k^{NC} q_k x_k \quad (\text{A.5a})$$

$$\phi_i = \frac{r_i x_i}{r_T} \quad r_T = \sum_k^{NC} r_k x_k \quad (\text{A.5b})$$

$$l_i = \frac{z}{2} (r_i - q_i) + 1 - r_i \quad (\text{A.5c})$$

$$t'_i = \sum_k^{NC} \theta_k \tau_{k,i} \quad (\text{A.5d})$$

$$\tau_{i,j} = \exp \left(a_{i,j} + \frac{b_{i,j}}{T} + c_{i,j} \ln T \right) \quad (\text{A.5e})$$

$$z = 10 \quad (\text{A.5f})$$

The parameters for the extended Antoine equation, the Racket model for molar density and UNIQUAC model are taken from the paper by Hsu et.al., [35] and Aspen Plus [67].

Bibliography

- [1] K. Sundmacher and A. Kienle. *Reactive distillation: Status and Future Directions*. Wiley-Vch Verlag GmbH & Co., Germany, 2003.
- [2] W.L. Luyben and C.C. Yu. *Reactive Distillation Design and Control*. John Wiley & Sons., New Jersey, 2008.
- [3] W L. Luyben. Snowball effects in reactor/separator processes with recycle. *Ind. Eng. Chem. Res.*, 33:299–305, 1994.
- [4] S. Pushpavanam and A. Kienle. Nonlinear behavior of an ideal reactor separator network with mass recycle. *Chem. Eng. Sci.*, 56:2837–2849, 2001.
- [5] G. Stephanopoulos and C. Ng. Perspectives on the synthesis of plant-wide control structures. *J. Process Control*, 10:97–111, 2000.
- [6] T. Larsson and S. Skogestad. Plantwide control - a review and a new design procedure. *Modeling, Identification and Control*, 21:209–240, 2000.
- [7] S. Vasudevan, S N. Murthy Konda, and G P. Rangaiah. Plantwide control : Methodologies and applications. *Rev. Chem. Eng.*, 25:297–337, 2009.
- [8] P. Buckley. *Techniques of process control*. Wiley, New York, 1964.
- [9] G. Stephanopoulos. Synthesis of control systems for chemical plants - a challenge for creativity. *Comput. Chem. Eng.*, 7:331–365, 1983.
- [10] W L. Luyben, B D. Tyreus, and M L. Luyben. *Plantwide process control*. McGraw Hill Book Co., 1999.
- [11] N M. Konda, G P. Rangaiah, and P R. Krishnaswamy. Plantwide control of industrial processes: An integrated framework of simulation and heuristics. *Ind. Eng. Chem. Res.*, 44:8300–8313, 2005.
- [12] N L. Ricker. Decentralized control of the Tennessee eastman challenge problem. *J. Proc. Cont.*, 6:205–221, 1996.
- [13] R M. Price and C. Georgakis. Plant-wide regulatory control design procedure using a tiered framework. *Ind. Eng. Chem. Res.*, 32:2693–2705, 1993.

-
- [14] E H. Bristol. On a new measure of interactions for multivariable process control. *IEEE Trans. Autom. Control*, 11:133–134, 1966.
- [15] W L. Luyben and M L. Luyben. *Essentials of process control*. McGraw Hill Book Co., New York, 1996.
- [16] S H. Shen and C C. Yu. Use of relay-feedback test for automatic tuning of multivariable systems. *AIChE J.*, 40:627–646, 1994.
- [17] L. Narraway and J D. Perkins. Selection of process control structure based on linear dynamic economics. *Ind. Eng. Chem. Res.*, 32:2681–2692, 1993.
- [18] I K. Kookos and J D. Perkins. Heuristic-based mathematical programming framework for control structure selection. *Ind. Eng. Chem. Res.*, 40:2079–2088, 2001.
- [19] I K. Kookos and J D. Perkins. An algorithmic method for the selection of multivariable process control structures. *J. Process Control*, 12:85–89, 2002.
- [20] I K. Kookos and J D. Perkins. Regulatory control structure selection of linear systems. *Comput. Chem. Eng.*, 26:875–887, 2002.
- [21] L. Narraway and J D. Perkins. Selection of process control structure based on economics. *Comput. Chem. Eng.*, 18:S511–S515, 1994.
- [22] A. Flores-Tlacuahuac and L T. Biegler. Simultaneous mixed-integer dynamic optimization for integrated design and control. *Comput. Chem. Eng.*, 31:588–600, 2007.
- [23] M L. Luyben and C A. Floudas. Analyzing the interaction of design and control 1. a multiobjective framework and application to binary distillation synthesis. *Comput. Chem. Eng.*, 18:933–969, 1994.
- [24] M J. Mohideen, J D. Perkins, and E N. Pistikopoulos. Optimal design of dynamic systems under uncertainty. *AIChE J.*, 42:2251–2272, 1996.
- [25] V. Sakizlis, J D. Perkins, and E N. Pistikopoulos. Recent advances in optimization-based simultaneous process and control design. *Comput. Chem. Eng.*, 28:2069–2086, 2004.
- [26] Z. Yuan, B. Chen, and J. Zhao. An overview on controllability analysis of chemical processes. *AIChE J.*, 57:1185–1201, 2011.
- [27] S. Skogestad. Control structure design for complete chemical plants. *Comput. Chem. Eng.*, 28:219–234, 2004.
- [28] S. Skogestad. Plantwide control: The search for self-optimizing control structure. *J. Process Control*, 10:487–503, 2000.

-
- [29] L T. Biegler and I E. Grossmann. Retrospective on optimization. *Comput. Chem. Eng.*, 28(8):1169 – 1192, 2004.
- [30] M A. Al-Arfaj and W L. Luyben. Comparison of alternative control structures for an ideal two-product reactive distillation column. *Ind. Eng. Chem. Res.*, 39(9):3298–3307, 2000.
- [31] D B. Kaymak and W L. Luyben. Evaluation of a two-temperature control structure for a two-reactant/two-product type of reactive distillation column. *Chem. Eng. Sci.*, 61:4432–4450, 2006.
- [32] D B. Kaymak and W L. Luyben. Comparison of two type of two-temperature control structures for reactive distillation columns. *Ind. Eng. Chem. Res.*, 44(13):4625–4640, 2005.
- [33] N. Sharma and K. Singh. Control of reactive distillation column: A review. *International Journal of Chemical Reactor Engineering*, 8, 2010.
- [34] W L. Luyben. Control of ternary reactive distillation columns with and without chemically inert components. *Ind. Eng. Chem. Res.*, 46:5576–5590, 2007.
- [35] K Y. Hsu, Y C. Hsiao, and I L. Chien. Design and control of dimethyl carbonate - methanol separation via extractive distillation in the dimethyl carbonate reactive distillation process. *Ind. Eng. Chem. Res.*, 49:735–749, 2010.
- [36] S J. Wang, C C. Yu, and H P. Huang. Plantwide design and control of DMC synthesis process via reactive distillation and thermally coupled extractive distillation. *Comput. Chem. Eng.*, 34:361–373, 2010.
- [37] A.E. Bryson and Y.C. Ho. *Applied Optimal Control: Optimization, Estimation, and Control*. John Wiley & Sons, New York, 1975.
- [38] S. Kameswaran and L T. Biegler. Simultaneous dynamic optimization strategies: Recent advances and challenges. *Comput. Chem. Eng.*, 30:1560–1575, 2006.
- [39] V. Bansal, V. Sakizlis, R. Ross, J D. Perkins, and E N. Pistikopoulos. New algorithms for mixed-integer dynamic optimization. *Comput. Chem. Eng.*, 27:647–668, 2003.
- [40] R J. Allgor and P I. Barton. Mixed-integer dynamic optimization I: problem formulation. *Comput. Chem. Eng.*, 23:567–584, 1999.
- [41] C A. Schweiger and C A. Floudas. Interaction of design and control : Optimization with dynamic models. In W W. Hager and P M. Pardalos, editors, *Optimal Control: Theory, Algorithms, and Applications*. Kluwer Academic Publishers B.V., 1997.

-
- [42] M. Mangold, A. Kienle, E D. Gilles, and K D. Mohl. Non-linear computing in diva - methods and applications. *Chem. Eng. Sci.*, 55:441–454, 2000.
- [43] M. Caracotsios and W E. Stewart. Sensitivity analysis of initial value problems with mixed odes and algebraic equations. *Comput. Chem. Eng.*, 9(4):359 – 365, 1985.
- [44] NAG. Numerical algorithms group, nag fortran library manual, 2006.
- [45] A M. Geoffrion. Generalized Benders Decomposition. *J. Optimiz. Theory App.*, 10:237–260, 1972.
- [46] M A. Duran and I E. Grossmann. An outer-approximation algorithm for a class of mixed-integer nonlinear programs. *Math. Program.*, 36:307–339, 1986.
- [47] A. Brooke, D. Kendrick, and A. Meeraus. *GAMS: A user's guide*. GAMS Software GmbH, Germany, 1998.
- [48] C A. Floudas. *Nonlinear and mixed-integer optimization*. Oxford University Press, New York, 1995.
- [49] S.D. Roat, J.J. Downs, E.F. Vogel, and J.E. Doss. *Chemical Process Control; CPC III*, chapter Integration of rigorous dynamic modeling and control system synthesis for distillation columns. Elsevier, Amsterdam, The Netherlands, 1986.
- [50] GAMS. *The solver manuals*. GAMS Development Corporation, Washington, DC, 2006.
- [51] M F. Malone W. Song, G. Venimadhavan and M F. Doherty. Measurement of residue curve maps and heterogeneous kinetics in methyl acetate synthesis. *Ind. Eng. Chem. Res.*, 37:1917–1928, 1998.
- [52] F. Chen, R S. Huss, M F. Malone, and M F. Doherty. Simulation of kinetic effects in reactive distillation. *Comput. Chem. Eng.*, 24:2457–2472, 2000.
- [53] M F. Malone R S. Huss, F. Chen and M F. Doherty. Reactive distillation for methyl acetate production. *Comput. Chem. Eng.*, 27:1855–1866, 2003.
- [54] H P. Huang Y D. Lin and C C. Yu. Relay feedback tests for highly nonlinear processes: Reactive distillation. *Ind. Eng. Chem. Res.*, 45:4081–4092, 2006.
- [55] S B. Hung, M J. Lee, Y T. Tang, and C C. Yu. Control of different reactive distillation configurations. *AIChE J.*, 52 (4):1423–1440, 2006.
- [56] B D. Tyreus and W L. Luyben. Tuning PI controllers for integrator/dead time processes. *Ind. Eng. Chem. Res.*, 31:2625–2628, 1992.
- [57] F P. Bernardo, E N. Pistikopoulos, and P M. Saraiva. Integration and computational issues in stochastic design and planning optimization problems. *Ind. Eng. Chem. Res.*, 38:3056–3068, 1999.

-
- [58] S Julier and J K. Uhlmann. A general method for approximating nonlinear transformations of probability distributions. *Tech. Rep., Robotics Research Group, University of Oxford*, 1996.
- [59] R. Schenkendorf, A. Kremling, and M. Mangold. Optimal experimental design with the sigma point method. *IET Syst. Biol.*, 3(1):10–23, 2009.
- [60] R. Schenkendorf, A. Kremling, and M. Mangold. Optimal experimental design and model selection by a sigma point approach. *Proceedings MATHMOD 09 Vienna*, pages 2389–2395, 2009.
- [61] J Darlington, C C. Pantelides, and B A. Tanyi. An algorithm for constrained nonlinear optimization under uncertainty. *Automatics*, 35:217–228, 1999.
- [62] E N. Pistikopoulos and M G. Ierapetritou. Novel approach for optimal process design under uncertainty. *Comput. Chem. Eng.*, 19:1089–1110, 1995.
- [63] Rudolph van der Merwe. *Sigma-point kalman filters for probabilistic inference in Dynamic state-space models*. PhD thesis, OGI School of Science & Engineering at Oregon Health & Science University, 2004.
- [64] D. B. Kaymak, D. Yilmaz, and A. Z. Güreer. Inferential temperature control structures for different types of two-reactant reactive distillation systems. *Ind. Eng. Chem. Res.*, DOI:10.1021/ie102333q, 2011.
- [65] M V. Pavan Kumar and N. Kaistha. Decentralized control of a kinetically controlled ideal reactive distillation column *Chem. Eng. Sci.*, 63:228–243, 2008.
- [66] Y J. Fang and W D. Xiao. Experimental and modeling studies on a homogeneous reactive distillation system for dimethyl carbonate synthesis by transesterification. *Separation and Purification Technology*, 34:255–263, 2004.
- [67] Aspen Technology. Aspen plus users manual 10.2. Technical report, Aspen Technology, Inc., Cambridge, MA, 2000.
- [68] P J. Campo and M. Morari. Achievable closed-loop properties of systems under decentralized control: Conditions involving the steady-state gain. *IEEE Trans. Autom. Control.*, 39:932, 1994.
- [69] I M. Sobol'. Sensitivity analysis for nonlinear mathematical models. *Mathematical Modeling and Computational Experiment*, 1:407–414, 1993.
- [70] A. Saltelli, M. Ratto, S. Tarantola, and F. Campolongo. Sensitivity analysis for chemical models. *Chemical Reviews*, 105:2811–2828, 2005.
- [71] R. Schenkendorf, and M. Mangold. Challenges of parameter identification for nonlinear biological and chemical systems *SIAM Conference on Optimization*, Darmstadt, Germany, 2011.

- [72] P. Li, H. Arellano-Garcia, and G. Wozny. Chance constrained programming approach to process optimization under uncertainty. *Comput. Chem. Eng.*, 32:25–45, 2008.